Investigating Transcription Factors Involved in the Coordinated Regulation of Adherence and Motility in Uropathogenic *Escherichia coli*

by

Courtney L. Luterbach

A dissertation submitted in partial fulfillment
of the requirements for the degree of
Doctor of Philosophy
(Microbiology and Immunology)
in the University of Michigan
2018

Doctoral Committee:

Frederick G. Novy Professor Harry L. T. Mobley, Chair
Associate Professor Matthew Chapman
Rudolph Hugh Professor Victor DiRita, Michigan State University
Assistant Professor Nicole M. Koropatkin
Professor Michele Swanson

Courtney L. Luterbach

courtl@umich.edu

ORCID iD: 0000-0003-2509-0842

Acknowledgements

I would like to first thank my advisor Dr. Harry Mobley for being an inspiring and motivational mentor throughout my Ph.D. Working in your lab has been incredibly enjoyable, and with your guidance, I have learned how to approach each new challenge with confidence and a positive outlook. I would also like to thank all of the members of the Mobley lab who have made each day in lab a great place to work, and I am very honored to have been able to connect with so many wonderful people over the past six years. I would like to especially acknowledge Dr. Chris Alteri for being an excellent mentor and friend.

I would also like to thank my thesis committee members Dr. Vic DiRita, Dr. Michele Swanson, Dr. Matt Chapman, and Dr. Nicole Koropatkin for all of their guidance and thoughtful suggestions regarding my research. Also, I would like to acknowledge my collaborators Dr. Stephen Smith, Dr. Helen Miajlovic, Dr. Gary Moran, Dr. Eric Buckles, and Dr. Michael Donnenberg who have all greatly contributed to my thesis work, as well as the Molecular Microbial Mechanism of Pathogenesis training program for partially funding the work described in this thesis. From the School of Public Health, I would like to thank Dana Thomas, Brandie Epiken, and my advisor Dr. Carl Marrs who provided substantial mentorship in my pursuit of public health service. Finally, I would like to thank my parents, friends and family, especially Dr. Matt Foley, Kyle Luterbach, Dr. Hayley Warsinske, Danelle Weakland, Dr. Zack Abbott, Dr. Travis Kochan, Konrad Kalpen, Elisa Hughes, Elizabeth Stevens, and Jay Lubow, who have all greatly contributed to my happiness and success during my Ph.D. I would like to especially thank Matt Foley for all of his love, support and laughter during this scientific journey

Table of Contents

List of Tables

List of Figures

List of Appendices

Abstract

Uropathogenic *Escherichia coli* (UPEC) are the main cause of uncomplicated urinary tract infections (UTIs), one of the most common bacterial infections in humans. Both adherence and motility are critical for productive colonization of the urinary tract. However, the mechanisms involved in coordinating the transition between adherence and motility are not well characterized. Pyelonephritis-associated pili (Pap), or P-fimbriae, bind the P-blood group antigen located on human kidney epithelial cells and erythrocytes, and UPEC strains harboring the *pap* operon are more likely to cause pyelonephritis. In this dissertation, a signature-tagged mutagenesis screen identified a P-fimbrial gene (*papC*) and 18 other genes as being among those required for full fitness of the cystitis isolate *E. coli* F11. Additionally, P fimbriae were confirmed by Molecular Koch's postulates as a virulence factor for the pyelonephritis isolate *E. coli* CFT073 in the murine model of UTI.

The production of P fimbriae is coordinated with the repression of swimming motility. Unlike the majority of other fimbrial operons, the 3' end of the *pap* operon encodes a MarR-like transcription factor, PapX. Using SELEX and high-throughput sequencing, our lab has previously shown that PapX binds to a 29-bp palindromic DNA sequence located upstream of *flhDC*, the master regulator of flagellar gene expression, and thereby represses motility. However, the UPEC strain CFT073 carries both *papX* and a homolog *focX*, located in the *foc* operon encoding F1C fimbriae. In this dissertation, the dose-effects of these "X" genes on flagellar gene expression and cross-talk between *focX* and *papX* were investigated. Similar to PapX, the production of FocX was shown to repress *flhDC* transcription. Furthermore, the

deletion of PapX and FocX in CFT073 resulted in a subtle, but not statistically significant, decrease in kidney colonization in the ascending murine model of UTI. Using 5'RACE, a proximal promoter was located upstream of both *focX* and *papX*, suggesting that these genes are transcribed independently from their fimbrial operons and therefore may be regulated by different transcription factors. Indeed, the deletion of *focX* resulted in increased expression of *papX* but had no effect on *papA* expression. Thus, cross-talk between "X" genes may provide a mechanism to mediate fine-tune coordinated transitions between motility and adherence.

Similar to PapX and FocX, the transcription factor TosR is a critical component of the regulatory network linking adherence and motility in UPEC. TosR, encoded by the type one secretion (*tos*) operon, has previously been shown to function as a transcriptional repressor of the *pap* operon and as a dual regulator of the *tos* operon. The *tos* operon also encodes the non-fimbrial adhesin TosA, which is predominately expressed during murine UTI, binds to kidney epithelial cells, and promotes survival during invasive infections. In this dissertation, TosR was demonstrated to also regulate the expression of genes involved with adhesins, including P, F1C, and Auf; nitrate/nitrite transport; microcin secretion; and biofilm formation. Altogether, these studies provide an in-depth characterization of three transcription factors (PapX, FocX, and TosR) and their contribution to the coordinated regulation of motility and adherence in UPEC.

Chapter I: Introduction

Diversity of *Escherichia coli*

Escherichia coli strains reside in the intestinal tracts of mammals and are considered commensals alongside other microorganisms collectively referred to as the human gut microbiota (1, 2). However, *E. coli* is a highly versatile and diverse species, and various pathogenic *E. coli* strains are capable of also causing diarrhea or extraintestinal infections, including neonatal meningitis, surgical site infections, pneumonia, bacteremia, and urinary tract infections (UTIs) (3, 4). Accordingly, pathogenic *E. coli* strains are conventionally categorized into pathotypes based on their clinical source and virulence-associated factors: enteropathogenic (EPEC), enterohemorrhagic (EHEC), enterotoxigenic (ETEC), enteroaggregative (EAEC), enteroinvasive (EIEC), diffusely adherent (DAEC), adherent-invasive (AIEC), sepsis-associated (SePEC), neonatal meningitis (NMEC), and uropathogenic *E. coli* (UPEC) **(Table 1.1)** (5-7).

UPEC, NMEC, and SePEC strains represent a specialized subset of *E. coli* associated with infections outside of the gastrointestinal tract and are classified as extraintestinal pathogenic *E. coli* (ExPEC) (8). To overcome environmental restrictions and host defenses during extraintestinal infections, ExPEC strains are equipped with virulence and accessory genes, absent from the majority of fecal *E. coli* isolates, that aid in nutrient acquisition, colonization, injury and/or invasion of host cells, and evasion of the host immune responses (9-11). Many of these virulence factors, including adhesins, toxins, and iron acquisition systems, are encoded by multiple ExPEC strains regardless of pathotype. Therefore, diverse extraintestinal host sites can share similar environmental and nutritional restrictions (12-15).

For example, iron is vital for bacterial survival and plays a significant role in multiple cellular processes, including metabolism, DNA replication, resistance to oxidative stress, and cellular respiration (16-19). However, available iron is heavily restricted at extracellular host sites. Instead, the majority of host iron is located intracellularly incorporated into heme, which functions as a cofactor of hemoglobin or myoglobin, or sequestered by the iron storage protein ferritin (17). Thus, iron limitation serves as a form of host nutritional immunity and is an effective defense mechanism to limit bacterial infections (17). ExPEC strains encode multiple iron acquisition systems, including siderophores, iron transporters, and outer-membrane iron receptors to acquire host iron, and many of these iron acquisition systems contribute to virulence during UTI, bacteremia, and neonatal meningitis (20-24). Therefore, the characterization of a fitness or virulence factor in UPEC is not only important for expanding our understanding of uropathogenesis but may also provide insight to mechanisms of pathogenesis used by NMEC and SePEC.

Table 1.1. Description of virulence factors associated with pathogenic *E. coli*

***E. coli* Pathotype**	**Disease Syndrome**	**Subtype[a]**	**Virulence-associated factors or phenotypes[b]**
Enteropathogenic (EPEC)	Diarrhea	IPEC	Locus of enterocyte effacement (LEE) Pathogenicity Island, Bundle-forming pili (*bfpA*)
Enterohemorrhagic (EHEC)	Hemorrhagic colitis, hemolytic uremic syndrome	IPEC	Shiga toxin 1 and 2 Intimin (*eae*), Hemolysin (*ehxA*)
Enterotoxigenic (ETEC)	Diarrhea	IPEC	Heat-labile (LT) and heat-stable (ST) enterotoxins
Enteroaggregative (EAEC)	Diarrhea	IPEC	pAA virulence plasmid Cytotoxin (Pet); aggregative adhesion (AAF fimbriae),
Enteroinvasive (EIEC)	Bacillary dysentery	IPEC	pINV virulence plasmid, type 3-secreted effector protein (IpaH)
Diffusely Adherent (DAEC)	Diarrhea	IPEC	Diffuse adherence (AIDA-1), Afa/Dr adhesins
Adherent-invasive (AIEC)	Associated with Crohn's disease	IPEC	Adherent-invasive phenotype
Sepsis-associated (SePEC)	Bacteremia, Sepsis	ExPEC	Invasion of Vero kidney cells
Neonatal meningitis (NMEC)	Meningitis	ExPEC	K1 capsule, S fimbriae, OmpA adhesin
Uropathogenic (UPEC)	UTI, Urosepsis	ExPEC	Fimbriae (type 1, P, F1C, and S), Afa/Dr adhesins, Sat toxin

a: Intestinal pathogenic *E. coli* (IPEC), Extraintestinal pathogenic *E. coli* (ExPEC)
b: Common, but not all-inclusive or definitive list of virulence factors or phenotypes associated with individual *E. coli* pathotypes (adapted from Kaper, *et al* and Robins-Browne *et al.* (7, 25))

Uropathogenic *E. coli* are the primary cause of urinary tract infections

Urinary tract infections (UTIs) are one of the most pervasive bacterial infections, with over 150 million cases worldwide each year, and occur when bacteria infect sites within the lower (urethra and bladder) and upper (ureters and kidneys) urinary tract **(Figure 1.1)** (26, 27). Due to their high prevalence, UTIs impose a heavy burden on healthcare resources in the United States, accounting for 2-3 million emergency department visits in 2007 and an estimated $3.5 billion per year in direct and indirect health care costs (28, 29). Multiple bacterial species have been isolated from UTIs, including *Escherichia coli*, *Klebsiella spp*, *Proteus spp*, *Pseudomonas aeruginosa*, *Enterococcus spp*, *Staphylococcus saprophyticus*, *Streptococcus agalactiae*, *Enterobacter*, and *Serratia spp.*, and many of these species have exhibited increasing levels of resistance to antibiotics commonly used to treat UTIs (30). In 1995, the estimated annual cost of antimicrobial therapy for community-acquired UTIs was $1.6 billion. With the widespread emergence of antibiotic resistance, healthcare-associated costs are projected to remain high until there are advancements in therapeutic strategies or the development of an effective vaccine (31-34).

UTIs range in severity depending on the genetic attributes of the bacterial pathogen as well as predisposing conditions of the patient (35). For instance, UTIs are classified as complicated in individuals who are either immunocompromised, have disrupted genitourinary function (including urinary catheterization), or structural abnormalities (26). Additionally, UTIs in otherwise healthy adult men are rare and therefore are also classified as a complicated UTI when they occur (36). In general, individuals experiencing complicated UTIs have a higher risk of developing severe clinical outcomes including bacteremia, sepsis and death (37, 38). In contrast, uncomplicated UTIs occur in anatomically normal and otherwise healthy individuals.

Risk factors for developing an uncomplicated UTI include sexual activity, age, a history of prior UTIs, diabetes, contraceptive use, and female gender, with almost 50% of women experiencing at least one UTI during her lifetime (33, 39-41).

While a variety of bacterial species can infect the urinary tract, UPEC are the primary cause of approximately 70-90% of uncomplicated UTIs (29, 33, 42). Most uncomplicated UTIs occur when periurethral bacteria ascend the urethra and colonize the bladder causing inflammation known as cystitis, which can present clinically as increased urinary frequency and urgency, dysuria, suprapubic pressure, and malaise (43, 44). In general, uncomplicated UTIs are limited to the bladder, and symptoms typically resolve within 3-7 days without antibiotic treatment (45). However, 20-44% of women experience at least one recurrent UTI within six months of initial diagnosis, and approximately 3% of these women experience multiple recurrent UTIs requiring follow-up physician visits and in some cases long-term treatment with antibiotics to limit recurrence (46, 47).

In a small percentage of cystitis cases (< 3%), bacteria ascend the urinary tract via the ureters and cause a secondary infection in the kidneys known as pyelonephritis, which can result in flank pain, vomiting, fever, and renal scarring (48, 49). Additionally, during pyelonephritis there is an increased risk that bacteria will cross the renal epithelium and endothelium barriers to disseminate throughout the bloodstream, which may lead to severe outcomes such as urosepsis and death (50).

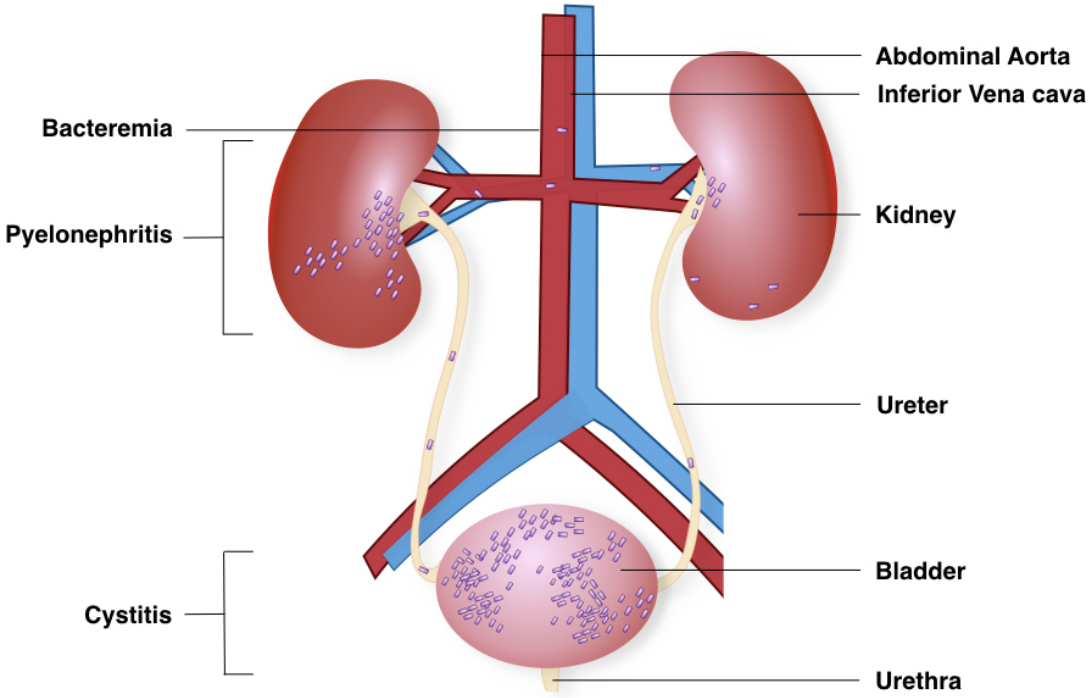

Figure 1.1 Schematic of an ascending uncomplicated urinary tract infection
The urinary tract consists of the urethra, bladder, ureter and kidneys. The kidneys filter approximately 1/3 of all blood leaving the heart, which is pumped into the kidneys through the abdominal aorta and drained via the inferior vena cava. An uncomplicated UTI begins when bacteria (shown as purple rods) colonize the bladder via the urethra, which can result in inflammation known as cystitis. Bacteria may also ascend from the bladder to the kidneys via the ureters, resulting in pyelonephritis. Bacteremia develops when bacteria residing in the kidneys cross the epithelial and endothelial barriers and enter the bloodstream.

Most bacteria are unable to thrive within the urinary tract environment due to it's high osmolarity, elevated urea concentrations, low pH, and limited iron availability (51, 52). Additionally, infecting bacteria must navigate a number of host immune defenses that function synergistically to remove bacteria from the urinary tract (53). For example, adherence of UPEC via the adhesin type 1 fimbriae to the bladder epithelium triggers exfoliation of host cells into the bladder lumen via an apoptosis-like mechanism that is an attempt to eliminate both infected cells and bacteria (54). Likewise, urination (also known as micturition) is a powerful host defense that can displace bacteria from attaching to the bladder epithelium and during voiding can flush bacteria from the urinary tract system (55). Individuals with dysfunctional voiding, including those with increased vesicoureteral reflux, experience more frequent UTIs and are more at risk for developing pyelonephritis during a UTI (56, 57). Lastly, bacterial colonization of the urinary tract can stimulate the induction of host innate and adaptive immune defenses. The early recruitment to the bladder of neutrophils can use the generation of reactive oxygen intermediates and antimicrobial peptides to eliminate invading bacteria (58-60)

To circumvent host defenses, UPEC strains encode multiple virulence and fitness factors that promote colonization of the urinary tract, including adherence factors (type 1, P, F1C, and S fimbriae), toxins, iron sequestration systems, flagella, lipopolysaccharide (LPS), and capsular polysaccharides **(Figure 1.2)** (10, 14, 21, 61). However, despite the ubiquity of UTIs, the UPEC virulence factors involved in colonization and persistence in the urinary tract are still not fully understood. As it has been difficult to identify a shared UPEC gene essential for UTI, there are likely variable or redundant combinations of virulence factors that mediate colonization of the urinary tract.

Many of the genes encoding virulence factors are located on large (>10 kb) mobile DNA regions termed pathogenicity-associated islands (PAIs) that have been acquired through horizontal gene transfer. Typically, UPEC genomes harbor multiple different PAIs (62, 63). For example, the UPEC strain CFT073, isolated from the blood and urine of a woman experiencing acute pyelonephritis, harbors 13 genomic islands with 7 being confirmed as PAIs (64). Thus, UPEC strains have high genomic plasticity and heterogeneity. Indeed, only 60-77% of the genes in the CFT073 genome are conserved among the UPEC strains 534, F11, UTI89, UMN026, and HM isolates (64, 65). Therefore, it is more clinically impactful to study the function of transcription factors regulating universal fitness factors, such as adherence and motility, than a strain-specific factor. During a UTI, extensive cross-talk regulates genes associated with adherence and motility to coordinate the transitions between attachment to host cells and ascension of the urinary tract. Thus, further investigation of the regulation between these two opposing states is essential for understanding the colonization and persistence of UPEC within the urinary tract.

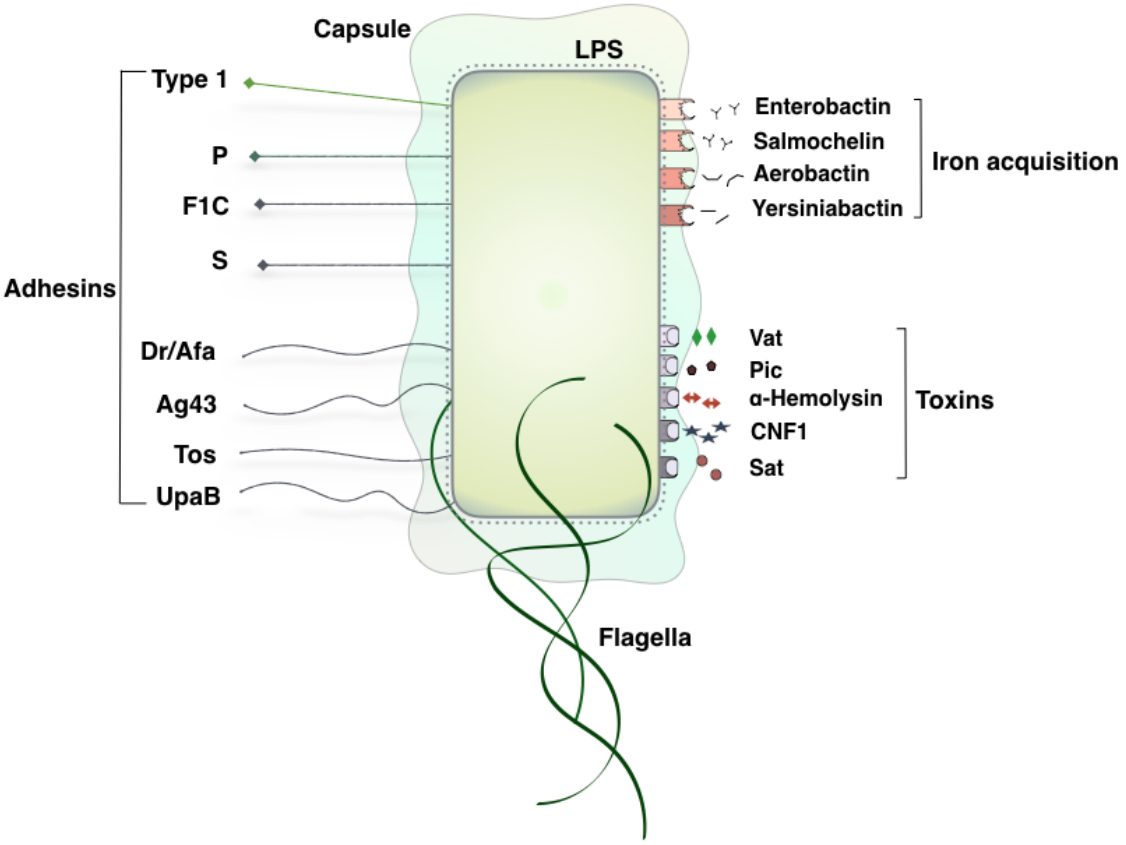

Figure 1.2 Virulence and fitness factors contributing to colonization of the urinary tract
A model UPEC bacterium is represented that harbors many of the commonly encoded virulence and fitness factors demonstrated to contribute to pathogenesis during a UTI. Virulence-associated categories include adhesins, capsule, lipopolysaccharide (LPS), iron acquisition, toxin production, and motility. The number of encoded factors varies within UPEC strains. Therefore, this model is a limited representation of the diversity of the UPEC-associated virulence and fitness factors.

Production and regulation of flagella

Motile bacteria can rapidly respond to changes within their environment and, if needed, localize to more favorable niches (66). Thus, motility frequently provides a competitive advantage for nutrient acquisition and survival during infection where harsh host environments can be resource-limited (67). In *E. coli*, swimming and swarming motility are the two main methods of motility. Both mechanisms share a reliance on filamentous extracellular polymers known as flagella for locomotion and chemotaxis systems to navigate towards favorable conditions (68-71). In response to growth on a semisolid surface, bacteria differentiate into hyperflagellated swarmer cells and migrate together as a collective movement (72). In contrast, bacteria can perform swimming motility during culture in liquid or a semi-liquid medium (73). Many of the genes associated with the regulatory, secretory and signaling pathways for swimming and swarming are different, and therefore, bacteria swim and swarm in response to different environmental conditions.

Flagellum construction is a complex process that requires the coordinated regulation of more than 50 genes. Flagellar genes are arranged in multiple operons and encode various regulatory and structural components needed for the assembly of the hook, membrane-spanning basal body and flagellum (74, 75). Thus, flagellar gene expression must be accurately timed to effectively assemble the multiprotein complex. To achieve this, flagellar genes are regulated in a transcriptional hierarchy divided into Class I, Class II, and Class III gene groups **(Figure 1.3)** (76).

The class I genes *flhDC* encode a heteromultimeric complex $FlhD_4C_2$ that functions as the master regulator of flagellar gene (77). $FlhD_4C_2$ interacts with the α-subunit of RNA polymerase to promote the transcription of numerous Class II genes, including the alternative sigma factor

FliA (σ^{28}) as well as genes needed for the assembly of the hook-basal apparatus that provides a structural platform for flagellum export, attachment, and rotation (78, 79). The σ^{28}-RNA polymerase induces the transcription of Class III genes encoding the remaining proteins needed for flagellum construction, including the motor torque generator subunits (MotA and MotB), flagellin (FliC), chemoreceptors (Tar, Tsr, Tap, and Trg), and the signaling Che proteins (80, 81). The flagellum structure is comprised of > 20,000 FliC proteins and is rotated by a motor switch complex within the basal apparatus powered by the protein motive force across the inner membrane **(Figure 1.4)** (82). In *E. coli*, flagella are assembled in a peritrichous arrangement on the cell surface, and the synchronized counter-clockwise rotation of these flagella propel a bacterium forward (83, 84).

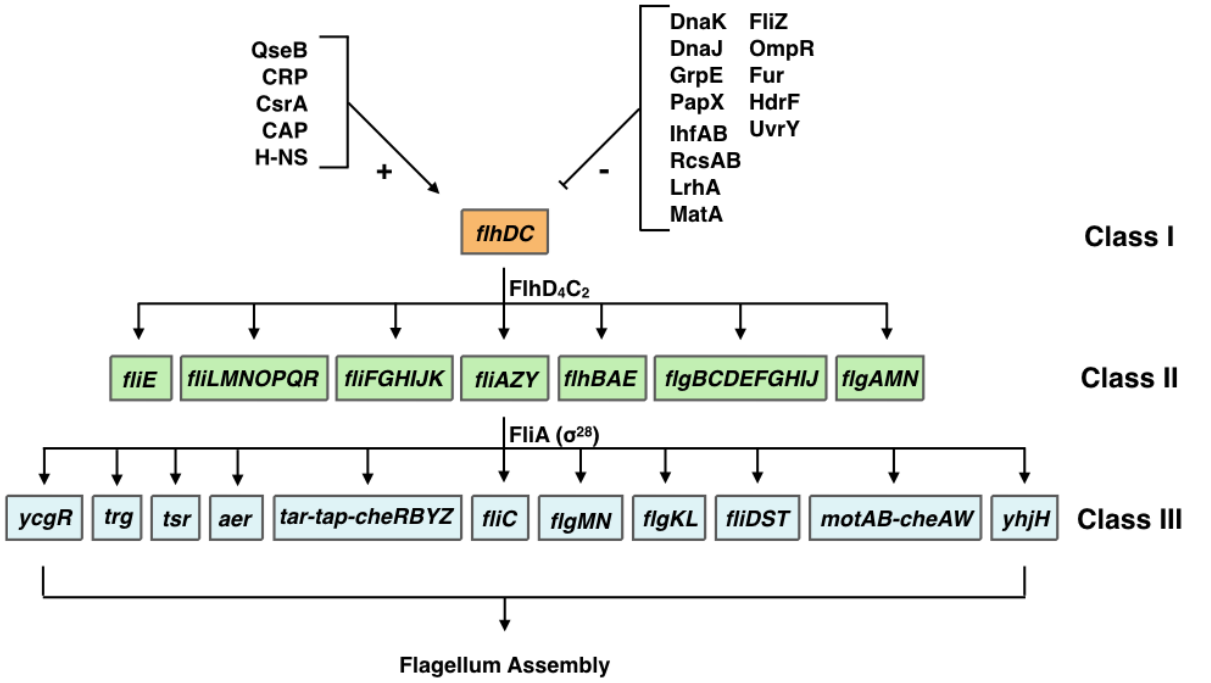

Figure 1.3 Genes encoding structural and regulators of flagellum production are expressed in a transcriptional hierarchy
flhDC encodes the heteromeric $FlhD_4C_2$ transcription factor that promotes the expression of class II genes found within multiple operons (represented by green boxes). FliA is an alternative sigma factor that is required for the expression of multiple Class III genes (represented by blue boxes). *flhDC* expression can be positively (+) or negatively (-) regulated by a variety of transcription factors that either directly bind to DNA sites within the *flhDC* promoter or indirectly affect *flhDC* expression through interactions with another transcriptional regulator.

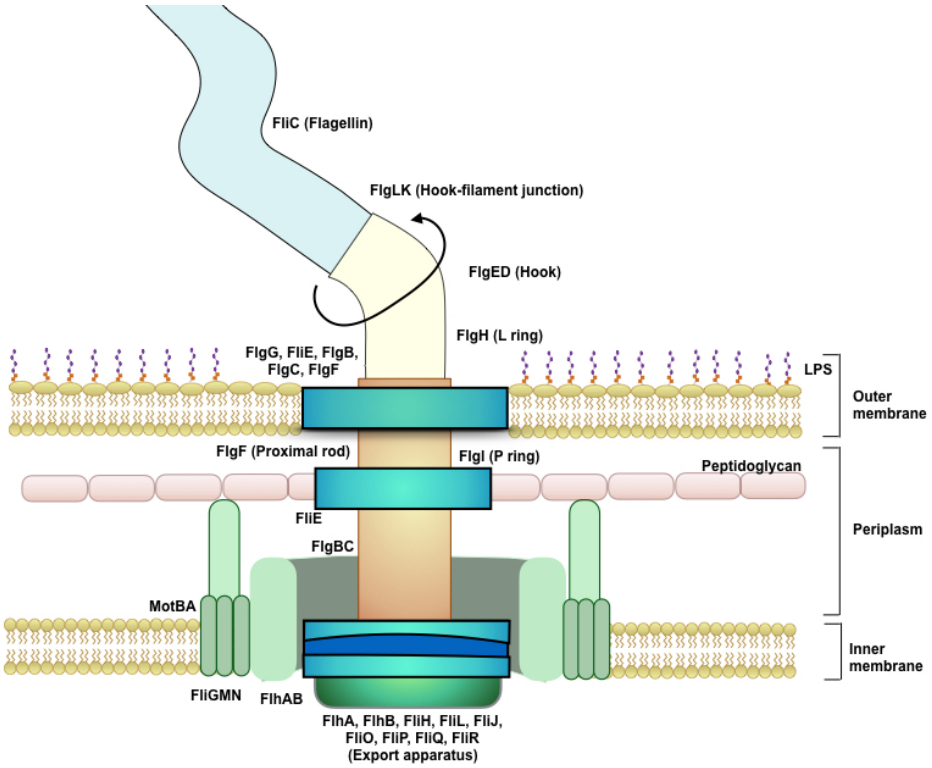

Figure 1.4 Schematic of proteins involved with the assembly of the hook, basal apparatus and flagellum in *E. coli*

Flagellum exportation occurs after the cytoplasmic export apparatus, basal body, and hook (shown in yellow) have all been assembled. The flagellum is a long (5 to 10 mm), hollow extracellular structure that is constructed of > 20,000 FliC proteins, which are secreted through export apparatus and assembled underneath a FliD cap (not shown). The motor switch complex, uses energy generated by a proton motive force across the inner membrane to rotate the flagellum

Motility is resource-intensive with each flagellum constituting approximately 1% of the total cellular proteins (85-87). Additionally, the rigid helical flagellum structure often breaks under viscous shear forces experienced during rotation (87). While flagella can be rebuilt, the released monomeric form of flagellin can be detected by the host Toll-like receptor 5 (TLR5) which can trigger a robust innate immune response targeting the invading bacteria (88). Therefore, the investment into motility comes at a cost to survival and must be managed appropriately to be advantageous for nutrient acquisition and survival. A benefit of the tiered regulatory network of flagellar genes is the ability to rapidly control flagella production through minor modifications in the expression of *flhDC*.

Expression of *flhDC* is a key regulatory point to promote or inhibit flagella biosynthesis. Therefore, as expected, regulation of *flhDC* is complex. Numerous transcription factors, post-transcription factors, and insertion elements are involved in the regulation of *flhDC* expression, including CAP, OmpR, PapX, CsgD, CpxR, and CsrA (89, 90). As a consequence of the multifaceted regulation of *flhDC*, the expression of *flhDC* can be affected by changes in osmolarity, pH, oxygen levels, carbon source, temperature, growth-phase signal, and nutritional availability (91-96).

For example, the transcription factor OmpR can regulate the expression of *flhDC* in response to the nutritional state of the cell and changes in extracellular osmolarity (97, 98). OmpR encodes a transcriptional regulator that is involved in the two-component system EnvZ/OmpR. Under conditions of high osmolarity, OmpR becomes phosphorylated and functions as a negative regulator of *flhDC* transcription (92, 98). Additionally, limited nutrient availability can elevate the intracellular acetyl phosphate levels resulting in elevated phosph-OmpR production and a subsequent decrease in motility (99). OmpR is only one of many

regulators of *flhDC*, emphasizing that the regulation of *flhDC* is an intricate network of multiple transcriptional regulators at the *flhD* promoter.

Flagella-mediated motility promotes ascension of the urinary tract

Motility is critical for UPEC ascension of the urinary tract. Flagellar genes have been identified as fitness factors for colonization of the bladder and the kidneys in the murine model of UTI (100-103). Indeed, Lane *et al.* constructed a *fliC* deletion in the UPEC strain CFT073 and determined by cochallenge infection in the murine model that the inability to produce flagella resulted in lower levels of early colonization of the bladder and faster clearance from bladder and kidneys over the course of two weeks (104). Bacterial ascension of the urinary tract happens rapidly, as UPEC can be isolated from the murine kidneys as early as 4 hours following intraurethral inoculation. However, expression of flagellar genes is transient during a UTI. Indeed, transurethral inoculation of mice with a CFT073 mutant encoding a luciferase reporter for *fliC* transcription demonstrated that flagellar gene expression was coincident with ascension of the ureters and repressed following entry into the bladder and kidneys (101). Yet, the transcriptional regulators of motility responsible for the early ascension of the urinary tract are not well characterized.

Approximately 70% of UPEC strains isolated from women experiencing cystitis displayed motility when tested under *in vitro* conditions (102). However, non-motile UPEC strains have been also isolated from the urine of women experiencing cystitis or pyelonephritis (105). Therefore, while motility provides an advantage for early colonization and persistence within the urinary tract, it is not required for the establishment of a UTI. Additionally, flagellar genes are poorly expressed during *in vitro* culture in human urine and in UPEC isolated from the

urine of women experiencing cystitis, as well as during *in vitro* culture in human urine (106). Therefore, the production of flagella is likely tightly regulated during a UTI as a strategy to avoid detection via the TLR5 of the host immune system (107, 108). Furthermore, flagellated bacteria are more likely to be targeted for phagocytosis by host immune cells and thereby eliminated during infection (109, 110). Therefore, prolonged expression of flagellar genes may trigger a more robust immune response and be detrimental to prolonged survival within the urinary tract (103). Thus, a UPEC-associated regulatory mechanism to mediate rapid transitions in flagellar gene expression would likely be advantageous during infection (101).

Involvement of adherence factors in uropathogenesis

Bacteria can attach to a variety of biotic and abiotic surfaces and often switch between motile and adherent states in response to different environmental signals (110, 111). Bacterial adherence is mediated by the production of extracellular fimbrial and nonfimbrial adhesins. A single bacterium often encodes multiple types of adhesins with different binding specificities, expanding the number of possible attachment sites (111, 112). The mechanism of bacterial attachment occurs in two phases: a brief reversible initial contact mediated by hydrodynamic and electrostatic interactions followed by an irreversible attachment to the surface via an adhesin (113).

Bacterial adherence to host cells is critical for initial colonization and persistence during a UTI. UPEC encode a variety of fimbrial adhesins (e.g. P, F1C, S, type 1, and Dr) and nonfimbrial adhesins (e.g. TosA) that bind to cells found within the urinary tract (114, 115). A major intrinsic host defense mechanism within the urinary tract is the constant flow and accumulation of urine that washes bacteria from cell surfaces and expels free-floating bacteria

from the urinary tract during voiding (116). Thus, bacterial adherence to the uroepithelium limits the effect of shear forces produced by urine flow and thereby improves colonization (117). Adherence to host cells also provides a number of additional fitness advantages, including evasion of host immune defenses and more effective delivery of bacterial toxins. Adherence can also trigger signaling pathways in both the bacterium and the host cell that may modulate gene transcription, host chemokine production, or cytoskeletal organization promoting bacterial invasion of host cells (118-128). Therefore, bacterial adhesins are critical for pathogenesis, as many of these virulence-associated pathways require close contact between bacteria and host cells. There is extensive cross-talk between multiple fimbrial types as well as flagellar genes. Thus, investigating the transcriptional regulators (i.e. TosR, PapX, and FocX) associated with adhesins is critical for understanding what environmental and host factors promote adherence and motility during infection.

TosA: a non-fimbrial adhesin

Non-fimbrial adhesins are a heterogeneous group of protein structures that are secreted through either a type 1 secretion system (T1SS), T5SS or are autotransported across the outer membrane and anchored to the extracellular surface (129). The TosA adhesin, encoded by the *tosRCBDAEF* operon, is a member of the Repeat-in-Toxin (RTX) protein family. TosA is secreted through a T1SS, comprised of TosCBD, and subsequently attached to the outer membrane (130, 131). The *tos* operon is located on the PAI-*aspV,* and UPEC strains isolated from the urine of women experiencing acute cystitis were more likely to encode the *tos* operon (25-30%) than fecal *E. coli* isolates (114). Additionally, TosA was shown to be one of the most highly produced antigens during murine UTIs, and correspondingly, *tosA* was highly expressed

in infected bladder, kidneys, spleen and livers (132). Furthermore, a *tosA* mutant in UPEC CFT073 had reduced fitness during cochallenge in the murine model of UTI and bacteremia (62, 131, 132). Intriguingly, *in vitro* induction of *tos* expression has not been observed, indicating that the regulation of the *tos* operon may depend on being within the host environment (133).

TosR is encoded by the *tos* operon and is a member of the PapB family of transcriptional regulators (134). TosR functions as a dual regulator of the *tos* operon (133, 134). Specifically, high levels of TosR correspond to decreased TosA production, while low levels of TosR correlate with increased TosA production (133). Previous work has demonstrated that TosR binds to A+T-rich DNA sequences, and a TosR binding site has been identified within the promoters of the *tos* and *pap* operon, encoding P fimbriae (133, 134). Therefore, TosR likely participates in cross-talk between adhesins. Additionally, TosR may also regulate the expression of additional adhesins as well as other virulence factors. Thus, characterization of the regulation and function of TosR will elucidate the *in vivo* signals involved in UPEC colonization and dissemination in the urinary tract.

Fimbrial adhesins: type 1, P, F1C

Chaperone-usher pili (CUP) are the most common fimbrial type encoded by *E. coli* and are morphologically characterized as being relatively thick (5-7nm diameter), rod-like fibers (112). The bulk of the pilus (or fimbria) is comprised of multiple copies (>1000) of the major fimbrial subunit and terminates with a tip adhesin and adapter complex, which often consists of multiple minor subunit proteins (135). During fimbria assembly, the major and minor subunits are shuttled to the periplasm via the general secretory pathway. Next, these subunits are linked together via a zip-in zip-out mechanism coordinated by periplasmic chaperone proteins and a

pore-forming usher protein, which acts as a scaffold for subunit assembly (129). Briefly, the N-terminal extension on an incoming pilus subunit displaces the β-strand of the chaperone protein bound to the previously-assembled subunit (135). Through this mechanism of strand exchange, pilus subunits are rapidly polymerized to form a pilus.

While there are approximately 38 different types of CUP characterized in *E. coli*, individual commensal and pathogenic *E. coli* strains encode on average 8-16 different CUP (112). However, phase variation between fimbrial types typically limits the production of fimbriae to a single type for each bacterium (136, 137). Some fimbrial types are common to both commensal and pathogenic *E. coli* strains, including Mat, Yad, Yeh and Yfc (112). However, fimbrial types that have advantageous adherence properties for colonization of a particular niche during infection are often preferentially encoded by *E. coli* pathotypes (115). For example, UPEC strains are more likely than fecal commensal *E. coli* to encode P, F1C, S, Dr, and Auf fimbriae that bind various carbohydrates located on host cells within the urinary tract (115, 138, 139). However, type 1 fimbriae, encoded by the *fim* operon, are an exception to this correlation, since the prevalence of the *fim* operon is similar across pathogenic and commensal *E. coli* isolates (>90%), yet type 1 fimbria have been confirmed as a virulence factor during murine UTI (140, 141).

The pyelonephritis isolate CFT073 encodes 12 fimbrial types, including type 1, F1C, and two copies of P fimbria (P1 and P2) (142). While fimbrial operons vary in operon organization, the majority of fimbrial operons encode at least one subunit, a chaperone protein, an usher protein. and an adhesin. However, the operons encoding P1 and F1C also contain a terminal "X" gene *papX* or *focX*, respectively, that encodes a MarR-like transcription factor that functions as a repressor of motility **(Figure 1.5)**.

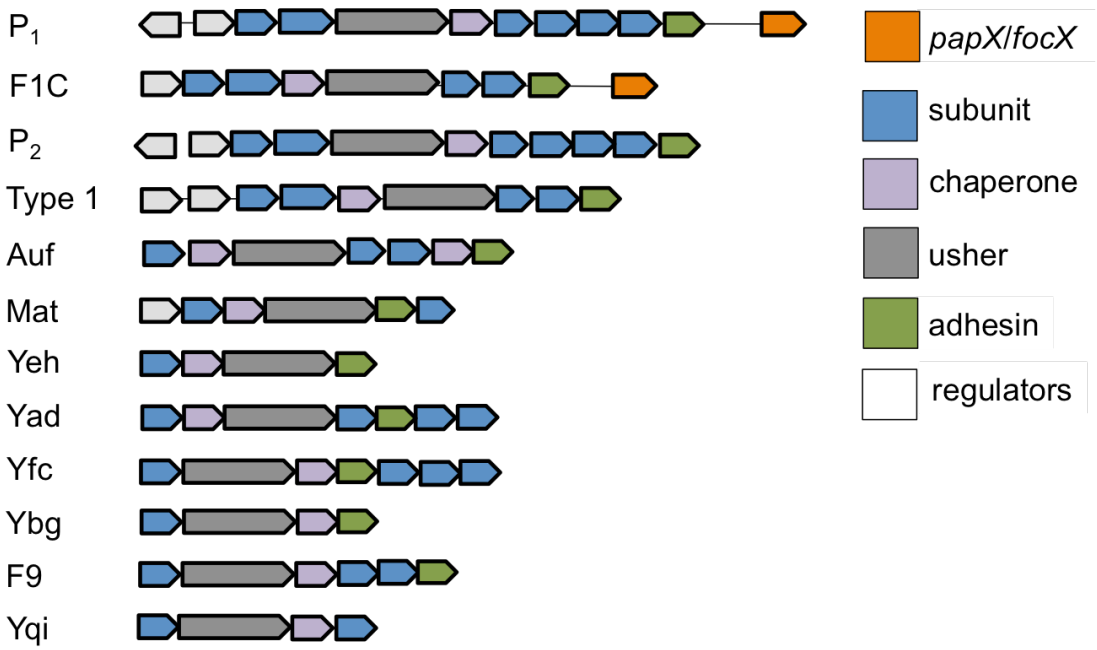

Figure 1.5 Individual *E. coli* strains encode a diversity of fimbrial types
The schematic shows that diversity of operons encoding fimbriae in the UPEC strain CFT073. While these 12 fimbrial operons differ in DNA sequence and overall gene organization, all operons contain at least one subunit, chaperone and usher protein. In CFT073, only the operons encoding P1 and F1C contain a terminal "X" gene (papX or focX, respectively) that encodes a MarR-like transcriptional regulator.

Type 1 fimbriae

Type 1 fimbriae are among the most common adhesins in *E. coli* and are encoded by the *fim* operon **(Figure 1.6)** (143). One of the earliest phenotypic characterizations of type 1 fimbriae was their ability to confer D-mannose-sensitive hemagglutination of guinea pig erythrocytes (141, 144, 145). Further characterization of the type 1 adhesin, FimH, demonstrated that type 1 fimbriae recognize mannose residues on uroplakin Ia enriched on the apical surface of urothelial cells (141, 144-146). Additionally, the receptor specificity of type 1 fimbriae correlates with virulence, as UPEC strains producing high levels of type 1 fimbriae are more robust colonizers of the murine bladder and kidneys (140)

Moreover, the production of type 1 fimbriae confers the ability to attach to the uroepithelium for nonpathogenic *E. coli* strains, as evidence by the redistribution of the asymptomatic *E. coli* strain 83972 from the murine bladder lumen to the walls following ectopic expression of the *fim* operon (147). Yet, while the *fim* genes are highly expressed in voided urine collected from the murine model of UTI, an investigation of *fimA*, encoding the major fimbrial subunit, showed that *fim* genes are overall poorly expressed in UPEC strains isolated from the urine of women experiencing acute cystitis (148-150). A host defense response to a UTI is the exfoliation of epithelial cells to remove attached bacteria (54). Therefore, voided human urine likely contains a mix of both nonadherent and adherent bacteria and may not best represent the fimbrial types needed for successful host colonization (150). Thus, the contribution of type 1 fimbriae during colonization of the bladder may not be as robust in humans compared to mice, highlighting the complexity of interacting and compensatory mechanisms of UPEC pathogenesis.

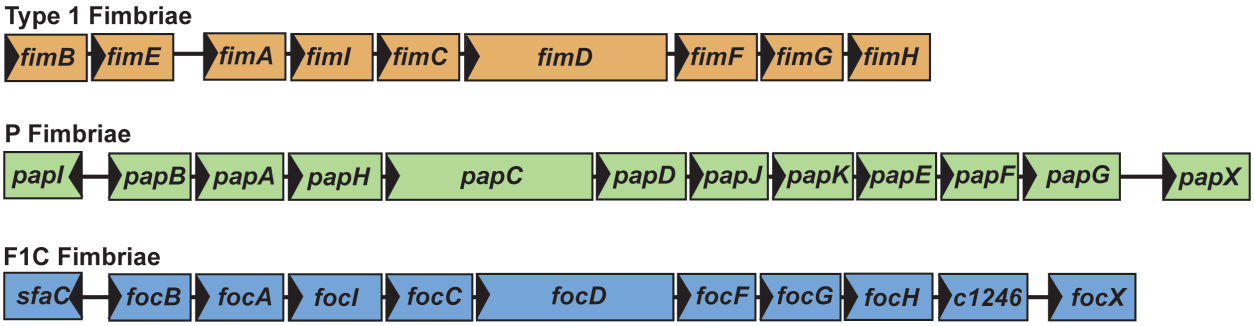

Figure 1.6 A schematic of the gene organization of the *fim*, *pap*, and *foc* gene clusters
All three fimbrial gene clusters encode the structural and regulatory genes necessary for fimbria biogenesis, including regulatory proteins (*fimB, fimE, papI, papB, sfaC, focB*), major subunits (*fimA*, *papA*, *focB*), periplasmic chaperones (*fimC*, *papD*, *focC*), ushers (*fimD*, *papC*, *focD*), and adhesins (*fimH*, *papG*, *focH*). The *foc* operon also encodes a putative phosphodiesterase (c1246), and the *pap* and *foc* operons both encode a 3' terminal MarR-like transcription factor, PapX and FocX, respectively.

P fimbriae

Pyelonephritis-associated pili (*pap*) or P fimbriae are one of the most well studied fimbrial types in *E. coli*. Multiple epidemiological studies have identified a positive correlation between UPEC genomes carrying the *pap* operon and the development of more severe clinical outcomes during UTI, notably pyelonephritis (61, 151-153). In addition, it is not uncommon for UPEC strains to carry two copies of the *pap* operon, which are found on PAI-*pheV* (*pap1*) and PAI-*pheU* (*pap2*) (64, 142, 154). In contrast to type 1 fimbriae, P fimbriae mediate mannose-resistant hemagglutination of human erythrocytes. Furthermore, biochemical analysis revealed that the P fimbrial adhesin, PapG, binds to the Gal(α1-4)Gal-containing receptor of the P blood group antigen, which is enriched on erythrocytes as well as the kidney epithelium of most humans (155, 156).

Therefore, P fimbriae binding specificity mediates binding to host cells within the kidneys. Indeed, *in vivo* competition assays in cynomolgus monkeys between the UPEC strain DS17 and a mutant unable to produce P fimbriae demonstrated that while both strains were equally adept at bladder colonization, the production of P fimbriae was critical for the establishment of pyelonephritis (157). Additionally, ectopic expression of the *pap* operon in the asymptomatic bacteriuria strain *E. coli* 83972 was sufficient to improve colonization of the human urinary tract following intravesical inoculation (158). Therefore, the production of P fimbriae promotes a more robust and rapid establishment of bacteriuria.

However, these *in vivo* infections were conducted using an avirulent bacteriuria *E. coli* strain, which is capable of persisting within the urinary tract undetected from host immune defenses and therefore likely uses a different strategy than pathogenic *E. coli* strains to remain within the urinary tract. Additionally, in the pyelonephritis UPEC isolate CFT073, which carries

both copies of the *pap* operon, independent infections in the murine model between wild type CFT073 and an isogenic mutant unable to produce P fimbriae did not result in a fitness defect (153). Therefore, the contribution of P fimbriae in the mouse to colonization requires additional investigation. In addition to promoting adherence within the upper urinary tract, attachment of P fimbriae to host cells stimulates the production of the pro-inflammatory cytokines IL-6 and IL-8, as well as the release of ceramide, an agonist for the TLR4 (159-162). Asymptomatic bacteriuria (ABU) strains do not encode P fimbriae as frequently (<20%) as pyelonephritis (90%) or cystitis (33%) isolates (163). Thus, the production of P fimbriae in ABU strains may hinder their ability to hide from the host immune responses.

The production of P fimbriae requires the *papBAHCDJKEFGX* operon, encoding the structural, transport, and regulatory machinery for fimbria assembly **(Figure 1.6)** (164). The pilus consists of the adhesin PapG, the adhesin tip complex, comprised of the minor subunits PapEFK, and >1000 copies of the major subunit PapA, making up the bulk of the structure. Individual units are shuttled by the periplasmic chaperone protein PapD to the usher PapC, which acts as a scaffold for subunit assembly on the extracellular surface of the bacterium (165). *papB* and the divergently transcribed *papI* encode transcriptional regulators that function as both positive and negative regulators of the *pap* operon. The function of *papB* and *papI* depends on the accessibility of the *pap* promoter, which is affected by Leucine-responsive protein (Lrp) and DNA adenine methylase (Dam) that bind to multiple DNA binding sites within the *pap* promoter (154, 166-168).

PapX

Located at the 3' terminal end of the majority (60%) of *pap* operons is *papX*, which encodes a 17 kDa winged helix-turn-helix (wHTH) transcription factor belonging to the Multiple antibiotic resistance (MarR)-like protein family (169, 170). The MarR-like protein family represents a large class of DNA-binding proteins (>12,000) found in both Eubacteria and Archaea. Yet, all MarR-like proteins share conserved structural homology to the canonical protein MarR, which was characterized in *E. coli* and functions as a repressor of the multiple antibiotic resistance operon *marRAB* (171-173). Members of the MarR protein family regulate a variety of bacterial processes, including toxin secretion, antibiotic resistance, metabolism, and motility (171, 174-176).

Even through *papX* is transcribed as part of the *pap* operon, PapX does not contribute to the regulation or assembly of P fimbriae (170, 176). Instead, work by Reiss *et al.,* demonstrated that PapX binds to a palindromic DNA sequence centered -410 bp upstream of the ATG start site of *flhD*, and the binding of PapX to this DNA site repressed the transcription of *flhDC* and subsequently swimming motility (169, 177). Therefore, PapX functions as a regulatory link between adherence and motility in UPEC and is therefore predicted to contribute to colonization and ascension of the urinary tract. However, it has been challenging to identify a fitness contribution of *papX* during murine UTI as a *papX* mutant in UPEC CFT073 colonized the murine bladder and kidneys to the same extent as wild type (176).

PapX is part of a class of 17 kDa fimbrial-associated transcription factors (e.g. *prsX*, *sfaX*, and *focX*) that are all located at 3' terminal end of a fimbrial operon, share a low GC content (~37-40%) and have high sequence and structural homology (169, 178). Thus, "X" genes are predicted to share a similar function as repressors of motility. Moreover, this function may

also be conserved across uropathogens, as overexpression of *papX* in *Proteus mirabilis* was able to inhibit its flagella production (170). Therefore, uropathogens may be more likely than commensal isolates to use fimbrial-associated transcription factors as a mechanism to coordinate the production of adhesins and flagella. The investigation of the similarities between "X" proteins may elucidate common mechanisms for the regulation of motility in uropathogens.

F1C fimbriae

Similar to type 1 and P fimbriae, F1C fimbriae, encoded by the *foc* operon, also mediate adherence to cells found within the urinary tract. In fact, UPEC cystitis isolates are more likely to carry the *foc* operon (14-38%) than fecal *E. coli* isolates (7%) (138, 179-181). The F1C adhesin, FocH, binds to various glycosphingolipids, including galactosylceramides that are prevalent on epithelial cells found within the kidneys, ureters and bladder, and globotriaosylceramides found on kidney cells (182, 183). Furthermore, the attachment of F1C fimbriae to human renal epithelial cells induces the secretion of the cytokine IL-8, and elevated IL-8 levels in urine is a common indication of an ongoing UTI (182). Therefore, while F1C-mediated binding promotes colonization of the human urinary tract, F1C-mediated attachment to the uroepithelium could also stimulate a mucosal immune response targeting bacteria for clearance. Furthermore, *foc* genes are poorly expressed in bacteria collected from the urine of women experiencing acute cystitis. Thus additional *in vivo* studies are necessary to confirm the role of F1C as a virulence factor during human UTI (106, 184).

The *foc* operon shares high sequence identity and gene organization with the *sfa* operon, encoding S fimbriae (138, 185). Specifically, the F1C main pilus is composed of >1000 copies of FocA and terminates in an adhesin complex comprised of the minor subunits FocFG and the

adhesin FocH **(Figure 1.6)** (183). The export and assembly of F1C subunits mimics the mechanism responsible for P fimbriae biogenesis with individual F1C fimbrial subunits being secreted through the general secretory pathway and shuttled via the chaperone protein FocC to the outer membrane usher FocD for pilus assembly (185). The *foc* operon also encodes the transcription factors SfaC and FocB that share structural homology with PapI and PapB encoded by the *pap* operon and have been shown to regulate the expression of both the *foc* and *pap* operons (186).

In contrast to the *pap* operon, the *foc* operon carries c1246 (also termed *focY* or *pdeY*) encoding a putative phosphodiesterase, which contains an EAL domain and is predicted to bind c-di-GMP (187). In some bacteria, an increase in c-di-GMP levels can promote biofilm formation and the deletion of c1246 in CFT073 enhanced biofilm formation when cultured in salt-free LB (187). Additionally, F1C fimbriae are required for biofilm formation on abiotic surface in the commensal *E. coli* strain Nissle 1917, and the production of F1C fimbriae improved persistence within the intestine of infant mice (188). Therefore, in addition to mediating adherence to the urinary tract, production of F1C fimbriae may also contribute to biofilm formation in a context-dependent manner.

FocX

Similar to the *pap* operon, the *foc* operon includes a 3' terminal gene, *focX,* encoding a MarR-like wHTH transcription factor that shares high amino acid sequence identity (96.7%) with PapX (169). While only 60% of *pap* operons include *papX*, the majority (>90%) of *foc* operons carry *focX* (169). FocX is predicted to share the same function as PapX. However, the

contribution of FocX to motility and pathogenesis has not established and remains a gap in our understanding of how "X" genes regulate motility in UPEC.

Coordinated regulation of adherence and motility

It is counterproductive for a single bacterium to produce both adhesins and flagella at the same time. Bacteria swimming at a high velocity are unable to remain stationary long enough to attach to a surface, and conversely, an adherent bacterium wastes energy by simultaneously being motile. Thus, it is important to understand the coordinated regulation between adherent and motile states in UPEC since transitioning between these states is presumably advantageous for pathogens within a dynamic and resource-restrictive environment, such as the urinary tract. Both the *pap* and *foc* operons encode PapX and FocX, respectively, which likely mediate the switch between adherence and motility. However, it is not known if FocX shares the same function as PapX as a repressor of motility. In this work, I first assess the role of P fimbriae as a virulence factor in the murine model of UTI and then characterize the involvement of the fimbrial transcription factors PapX and FocX and the non-fimbrial transcription factor TosR in mediating cross-talk between adherence and motility.

Chapter Outline

Chapter II: Signature-tagged mutagenesis and co-infection studies demonstrate the importance of P fimbriae in a murine model of urinary tract infection

Chapter III: Cross-talk between MarR-like transcription factors coordinates the regulation of motility in uropathogenic *Escherichia coli*

Chapter IV: TosR-mediated regulation of adhesins and biofilm formation in uropathogenic *Escherichia coli*

Chapter II: Signature-tagged mutagenesis and co-infection studies demonstrate the importance of P fimbriae in a murine model of urinary tract infection

Notes

This chapter was reprinted and modified with permission from the authors Luterbach, C.L., Buckles, E.L., Wang, X., Lockatell, C.V., Johnson, D.E., Mobley, H.L.T., and Donnenberg, M.S. Signature-tagged mutagenesis and co-infection studies demonstrate the importance of P fimbriae in a murine model of urinary tract infection. *FEMS Pathogens and Disease*, 73, 2015

Abstract

Escherichia coli is the leading cause of urinary tract infections (UTIs), one of the most common infections in humans. P fimbria was arguably the first proposed virulence factor for uropathogenic *E. coli*, based on the capacity of *E. coli* isolated from UTIs to adhere to exfoliated epithelial cells in higher numbers than fecal strains of *E. coli*. Overwhelming epidemiologic evidence has been presented for involvement of P fimbriae in colonization. It has been difficult, however, to demonstrate this requirement for uropathogenic strains in animal models of infections or in humans. In this study, a signature-tagged mutagenesis screen identified a P-fimbrial gene (*papC*) and 18 other genes as being among those required for full fitness of cystitis isolate *E. coli* F11. A P-fimbrial mutant was outcompeted by the wild-type strain in cochallenge

in the murine model of ascending UTI, and this colonization defect could be complemented with the cloned *pap* operon. To our knowledge, this study is the first to fulfill molecular Koch's postulates in which a pathogenic strain was attenuated by mutation of *pap* genes and then complemented to restore fitness, confirming P fimbria as a virulence factor in a pathogenic clinical isolate.

Introduction

Extraintestinal pathogenic *Escherichia coli* (ExPEC) strains are capable of colonizing niches distinct from the gut environment and can cause severe infections in humans, including neonatal meningitis, urinary tract infections (UTIs) and sepsis. UTIs are among the most prevalent bacterial infections in humans and in some cases can require extensive medical attention. Each year, as many as 1–2 million people suffering from UTIs visit the emergency department and almost 400 000 infections are severe enough to require hospitalization (189). Antimicrobial drug resistance among ExPEC, steadily on the rise, adds further to the difficulty of treating these infections (190, 191). Total costs to the healthcare system exceed 3 billion dollars annually, making UTIs also a substantial economic burden (189). The majority of UTIs progress stepwise from initial colonization by microorganisms of the periurethral area, followed by entrance into the urethra, and ascension into the bladder, resulting in inflammation or cystitis. More severe complications of UTIs can occur when bacteria travel through the ureters into the kidneys, producing pyelonephritis and, in some cases, later bypass the kidney parenchyma to reach the bloodstream or lymphatic sys- tem, resulting in bacteremia and potentially sepsis.

Adhesion organelles, known as fimbriae, mediate colonization by ExPEC of the urinary tract, a necessary step in the establishment of UTIs (10, 153, 192, 193). Epidemiologic studies

have shown a positive correlation between ExPEC strains and the presence of genes encoding for type 1, P, S, F1C, Dr and Auf fimbriae, as well as other non-fimbrial adhesins (115, 140, 153, 194-196). Among these fimbriae, only type 1 fimbriae, which are encoded by the *fim* operon, have been proven in animal models as a virulence factor according to the conditions of molecular Koch's postulates (140). It was demonstrated in the murine model of UTI using clinical isolates that mutations within the *fimH* adhesin gene or associated with its promoter resulted in reduced virulence. Virulence was restored following complementation with a plasmid encoding a functional *fim* operon (140).

Although P fimbria was arguably the first virulence determinant associated with ExPEC strains (197), it has been difficult to directly demonstrate a requirement for P fimbria as a colonization factor in UTI. Clinical studies have shown a positive correlation between ExPEC strains that cause pyelonephritis and the presence of the genes encoding P fimbriae (198, 199). However, in a murine model of ascending UTI, no differences could be detected in colonization or histological findings between pyelonephritis ExPEC strain CFT073 and its isogenic mutant strain deleted for genes in both copies of the *pap* operon and unable to produce fully assembled P fimbria (153). Conversely, in a primate model in which bacteria were inoculated directly into the ureter, pyelonephritis ExPEC strain DS17 persisted significantly longer in the urinary tract than its isogenic *papG* mutant, which was unable to cause acute pyelonephritis (157). However, the *papG* mutant was still capable of colonizing the bladder, resulting in cystitis, similar to what was observed with the wild-type strain. Complementation studies were not performed in either study, and therefore molecular Koch's postulates were not fulfilled (200). A volunteer study using *E. coli* 83972, which was isolated from a case of asymptomatic bacteriuria and also does not express functional P fimbriae, showed that following transformation with the *pap* operon,

bacteriuria was established faster and to a higher concentration than wild-type *E. coli* 83972 (158). However, this study was not conducted using a virulent isolate, and by using a plasmid-based operon, was not a comparison of isogenic mutants. Furthermore, the data suggest that P and type 1 fimbriae were not required for persistence of *E. coli* 83972 in the human urinary tract, since both the isogenic *papG* and *papGfimH* mutants of this avirulent strain were still able to colonize the human bladder up to 3 months following infection (147).

The lack of a defined set of virulence factors in ExPEC strains suggests that a combination of known and unidentified virulence factors may dictate fitness during infection. Signature-tagged mutagenesis (STM) is a useful and unbiased technique to identify genes involved with bacterial survival *in vivo* by screening a pool of mutants simultaneously within a limited number of animals (201). This method has been successfully used to both discover and confirm virulence and fitness genes in other pathogens (202-204). Previously, we applied STM to the pyelonephritis ExPEC strain CFT073 using a mouse model of ascending UTI to identify 19 mutants with reduced fitness from a non-saturating library of 2049 mutants (205). Of these 19 mutants, 8 had mutations in six different sites within the type 1 fimbrial locus. Several other survival-defective mutants had disruptions in genes responsible for the production of extracellular polysaccharides, metabolic pathways as well as within genes of unknown function. However, that study had a number of limitations. It was performed using a single strain of a particular serotype (O6:K2:H1), originally isolated from a case of pyelonephritis. Furthermore, in the murine model of UTI, this strain regularly colonizes the kidneys, and therefore may not be fully representative of other ExPEC.

In this study, we continue to take advantage of STM and the CBA murine model of ascending UTI to identify virulence or fitness genes in the cystitis isolate ExPEC strain F11.

Escherichia coli F11 is a member of a clonal group commonly found in human UTI that includes the prototypic serotype O6:K15:H31 isolate 536. F11 is highly pathogenic in the murine model of ascending UTI, as it is capable of colonizing the bladder to a higher concentration and more rapidly than ExPEC pyelonephritis isolate CFT073 (199). We tested the hypothesis that some virulence or fitness factors are unique to cystitis and pyelonephritis strains and can be identified using techniques such as STM. In the original STM study (205), we did not identify a P-fimbrial mutant. However, we recognized that doing so was unlikely given that there are two complete and functional *pap* operons in strain CFT073 (142, 153). Here we report that an STM screen of a cystitis strain that carries only a single *pap* operon did yield an attenuated *papC* mutant deficient in synthesis of P fimbriae. In cochallenges of the murine model, *pap*-negative mutants were outcompeted by the wild-type strain, and the loss of fitness could be complemented with the *pap* operon *in trans*. Thus, we have satisfied molecular Koch's postulates and conclude that P fimbriae contribute to the full colonization potential of ExPEC strains.

Materials and Methods

Bacterial strains, growth conditions and plasmids.

Table 2.1 lists the bacterial strains, growth conditions and the plasmids used for this study. *Escherichia coli* strain F11, originally cultured from a case of cystitis, served as the recipient strain during transposon mutagenesis (199, 206). Donor strains consisted of *E. coli* S17 λ*pir* strains trans- formed with pUT/mini-Tn5km2 (Amp^R Kan^R) plasmid carrying a unique pUT/mini-Tn5 sequence. All pUT/mini-Tn5 signature tags were tested for non-cross-reactivity (207, 208). Bacteria were cultured at 37°C in Luria-Bertani (LB) medium or on Luria agar with the addition of the appropriate antibiotics to provide selective pressure at the following

concentration: ampicillin 50 μg mL^{-1}; chloramphenicol, 50 μg mL^{-1}; nalidixic acid, 50 μg mL^{-1} ; and rifampin 50 μg mL^{-1}. Strains were stored at –70°C in a 1:1 ratio of glycerol and LB medium. For RNA preparation, *E. coli* was cultured on Luria agar for 18 h at 37° C with biological replicates being inoculated on independent plates to induce *pap* gene expression (209). Bacteria were resuspended in phosphate-buffered saline (PBS) to a final OD_{600} of 1.0. Bacteria were treated with a stop solution (5% phenol, 95% EtOH), harvested by centrifugation (13,000 rpm, 10 min, 4° C), and the pellet was stored at –20° C prior to RNA extraction.

Table 2.1. Bacterial strains and plasmids used in this study

Strains	Description	References
E. coli		
F11	UPEC strain (cystitis isolate, O6:K2:H31); Nal^R	(206)
F11 L-ON	F11 with *fim* invertible element phase locked on	(210)
F11 L-OFF	F11 with *fim* invertible element phse locked off	(210)
S17 λ*pir*	Conjugative donor strain	(211)
CFT073	UPEC strain (pyelonephritis isolate, O6:K2:H1)	(142)
UPEC76	Deletion derivative of *E. coli* CFT073 with both copies of P fimbrial operon disrupted	(153)
DH5α	Donor strain for cloning	(212)
Plasmids		
pUT/mini-Tn5km2	Suicide vector for transposon delivery ($Amp^R Kan^R$)	(207)
Cosmid 1-B10	Encodes for CFT073 genes *papIAHCDJKEFG_2*	(153)
Cosmid 1-E8	Encodes for CFT073 genes *papIAHCJKEFG_2*	(153)
pWSK29	Empty cloning vector	(213)
pXLW34	pWSK29 containing *papIAHCJKEFG_2* between the BamHI and SalI sites	This study

Construction of *E. coli* F11 signature-tagged mutant library

For conjugation, overnight cultures of S17 λ*pir* donor strains, each being transformed with a unique signature tag carried on the pUT/mini-Tn5km2 ($Amp^R Kan^R$) plasmid (201), and *E. coli* F11 (Nal^R) were mixed 1:1 in the wells of a 96-well microtiter plate. Aliquots of each mixture were plated on LB agar (201, 202). To confirm transposon insertion, isolated colonies were cultured overnight at 37°C on LB supplemented with nalidixic acid and kanamycin. Additional screening for ampicillin sensitivity confirmed the loss of the pUT plasmid among the transconjugants. This process was repeated to generate 1334 transposon mutants each carrying 1 of the 46 unique sequence tags. Transposon mutants were grouped and placed into individual wells of a 96-well microtiter plate, resulting in 29 pools with each pool having one representative of each of the uniquely tagged sequences. Each pool also contained two controls for identification of cross-reactivity with the blotting membrane. Mutants were stored in LB containing 20% glycerol at –70°C.

Mouse model of ascending UTIs

Infections were carried out in a previously described CBA mouse model of ascending UTI (214, 215). For the mutant screen, 6 to 8-week-old female mice (Harlan Sprague-Dawley) were anesthetized with pentobarbital and 50 μL suspensions of overnight bacterial cultures containing 10^8 CFU of a pool of 48 uniquely tagged mutants were inoculated transurethrally. The input pool was standardized by calculating the optical density at 600 nm of a 1 mL sample of the initial inoculum and stored as a centrifuged pellet at –20°C. Mice were sacrificed at 48 h by the administration of an overdose of isoflurane. The bladder and kidneys were collected aseptically and homogenized in 1 mL aliquots of PBS. Homogenizations were plated on LB agar containing

kanamycin and nalidixic acid. Following incubation, bacteria, now representing the output pools, were collected by washes with PBS (pH 7.2). The samples were standardized at an optical density of 600 nm, centrifuged and stored at –20° C.

Cochallenge infections were used to confirm attenuation of STM mutants. A total of 10^8 CFU per inoculum comprised of a 1:1 mixture of independent overnight cultures of wild-type *E. coli* F11 (5×10^7 CFU) and a single STM mutant (5×10^7 CFU) was inoculated into five mice. The inoculum was quantified by plating dilutions onto LB agar containing the appropriate antibiotics to provide selective pressure. For studies of P fimbriae in UTI, CFT073 containing the plasmid pWSK29, representing the control empty vector, was tested and compared to double *pap* mutant UPEC76 (153) transformed with either the complementing pXLW34 carrying *papIAHCDJKEFG* under control of their native promoter or the control empty vector. At 48 h, urine samples were collected and the bladder and kidneys were isolated, weighed and homogenized. A spiral plater was used to plate dilutions of the collected samples onto selective medium containing the appropriate antibiotics. Following overnight incubation, viable counts were represented as CFU mL^{-1} urine or CFU g^{-1} tissue with 10^2 CFU mL^{-1} urine or CFU g^{-1} tissue acting as the lower limit of detection for samples lacking colonies. A competitive index (CI) for each mutant from each sample site was calculated by dividing the ratio of mutant to wild-type strains in the output pool by the input pool, or inoculum, values of the same ratio.

Statistical analysis

For the independent infections, comparisons of the CFU mL^{-1} or CFU g^{-1} distributions were analyzed using the Mann–Whitney test. In contrast, the cochallenge data were analyzed using a repeated measure of analysis of variance with rank order data (STATA software) (205). P

values less than 0.05 were considered significant. For quantitative real-time PCR (qPCR) experiments, an unpaired Student's *t*-test was used to analyze differences in gene expression between F11 and F11 L-ON (Prism; GraphPad Software).

Screening of STM mutants

To obtain DNA template for sequencing, more than 5000 CFUs were scraped from the plated output samples of the collected bladder or kidneys and resuspended in PBS. Samples were normalized to the same OD_{600} (201). Proteinase K was used to lyse a fraction of each sample. Chromosomal DNA was used to generate labeled PCR products of the input and output pools using primers targeting the transposon insertion site **(Table B.1)**. The PCR products were labeled with digoxigenin-dUTP (Roche) before hybridization to a prepared DNA dot-blot membrane carrying the original uniquely tagged plasmids. Two controls to evaluate cross-hybridization were included with one tag being absent on the blot but common to the probes, while the other tag was only present in the blot. For the primary screen, mutants were considered to be attenuated in vivo and were further pursued if the output hybridization signal was weaker than the input hybridization signal in all three blots derived from the same organ or in at least four of the possible six blots. Confirmation of weak hybridization signals were conducted by testing the potentially attenuated mutants in single competition assays with wild-type strain F11. If found to be attenuated, DNA adjacent to the transposon junctions was amplified and sequenced. After several attenuated mutants with insertions in known fitness factors were identified in this manner, specifically colanic acid biosynthesis genes and the *fim* operon, the order of the screen was changed to sequence all mutants with confirmed weak hybridization signals, reserving confirmatory co-infection studies for mutants with insertions in previously unconfirmed genes.

Identification of *pap* cosmid clones and subcloning of the *pap* operon

PCR primers, Donne646 and Donne792, specific to sequences located 7 bp upstream of the *papA2* start codon and 42 bp downstream of the *papG2*, were used to locate the *pap* operon from a previously generated chromosomal DNA library of CFT073 (153). The CFT073 library is arranged across 19 microtiter plates and is comprised of approximately 1834 clones. Initial PCR, using the eLongase enzyme system, involved isolating the plasmid DNA from clones pooled from each microtiter plate. A total of 14 of the 19 pooled samples contained the *pap* cosmid clones. From a selected positive plate, pooled plasmid DNA from each row and column was PCR amplified leading to the identification of two cosmid clones, 1-B10 and 1-E8, carrying the *pap* genes. *Escherichia coli* DH5α was transformed with cosmid 1-B10 or cosmid 1-E8 and passaged on LB agar plates with antibiotic selection. The presence of functional P fimbriae was confirmed using a previously described hemagglutination assay using human and sheep erythrocytes in the presence or absence of 50 mM α-methyl D-mannoside (205). The cosmid 1-E8 was selected for subcloning of the *pap* operon after confirming the presence of P fimbriae by positive agglutination.

Cosmid clone 1-E8 was digested using the restriction enzymes BamHI and SalI to yield a fragment approximately 10.7 kb containing the *papIAHCDJKEFG*2 genes (the second of two *pap* operons in strain CFT073). The 10.7 kb BamHI/SalI fragment was isolated from an agarose gel and ligated into BamHI and SalI digested pWSK29 (213). The modified plasmid was transformed into *E. coli* DH5α to generate the recombinant clone, pXLW34, containing the *papIAHCDJKEFG*2 genes.

RNA extraction and cDNA synthesis

Total RNA was isolated using the RNeasy Kit (Qiagen) according to the manufacturer's protocol. To remove contaminating DNA, RNA samples were treated with DNase (Ambion). The absence of chromosomal DNA was confirmed by PCR using Taq DNA polymerase. For cDNA synthesis, the RNA samples were reverse transcribed using the SuperScript II system for first-strand cDNA synthesis (Invitrogen). Briefly, a total of 1.5 μg of RNA was mixed with 50 ng random hexamers and 10 mM dNTPs based on the manufacturer's protocol. cDNA was purified using a PCR Purification Kit (Qiagen) and stored at –20°C.

Quantitative real-time PCR

RNA was harvested from *E. coli* F11 strains that were cultured for 18h at 37°C on LB agar plates. Isogenic mutants of F11 were constructed by disrupting the invertible element that regulates *fim* expression so that expression of *fim* genes is no longer phase variable but is either locked on (L-ON) or locked off (L-OFF)(210). Primers were generated for F11 *fimA* (forward—5'TGCACAAACAACCCTGAATAAC3' and reverse 5'AAGGTCGCATCCGCATTAG3') and for F11 *papA* (forward 5'GGGACGCTAATCTCCTGAAAG3' and reverse 5'AGGTTGCGACTGCAGAAA3'). Expression of *gapA* was used for normalization and was measured using previously published primers (104). To measure gene expression, 30 ng of cDNA was combined with Brilliant III Ultra Fast SYBR green QPCR mix (Agilent), 300 nM of forward and reverse primers, and Rox, which acted as a reference dye. Comparative quantitation was performed by the 2 ΔΔCt method (Livak and Schmittgen 2001) with F11 L-OFF serving as the calibrator for F11 and F11 L-ON. Experiments were performed using three biological replicates.

Results

Screening of *E. coli* F11 signature-tagged mutants in a CBA mouse model of ascending UTI.

A library of 1334 signature-tagged mutants of *E. coli* F11 was constructed, and a total of 48 uniquely tagged transposon mutants, including two controls for cross-hybridization, were assembled into 29 screening pools. All mutants were kanamycin-resistant and ampicillin-sensitive, indicating a legitimate transposition event.

For screening in the CBA mouse model of UTI, an input pool (10^8 CFU) of 48 mutants (~2×10^6 CFU of each mutant) was transurethrally inoculated into the bladders of three female CBA mice. Two days post-inoculation, bacteria were cultured from urine, bladder and kidneys, and represent the output pools. Mutants were identified by PCR amplification of the unique sequence tags from both the input and output pools and hybridization of these identifiers with dot blots containing plasmids carrying the original sequence tags. Mutants from the initial screens with reduced hybridization signals in the output pools were regrouped and assayed by a secondary screen of single competition assays in five mice. The secondary screening yielded a total of 23 (1.7% of the total bank) putatively attenuated mutants **(Table 2.2)**.

Table 2.2. Confirmed attenuated STM mutants

Mutant	Gene/homolog	Accession no.	Function	K-12[b]	CFT073[c]
5-A3	*fimA*	EDV68690	type 1 fimbrial subunit	+	+
20-A4	*fimD*	EDV68628	type 1 fimbrial usher	+	+
29-G4	*fimD*	EDV68628	type 1 fimbrial usher	+	+
3-H2	EcF11_0984	EDV69299	Colanic acid biosynthesis	-	+
21-E6	*galE*	EDV69028	Colanic acid biosynthesis	-	+
22-B3	EcF11_0986	EDV69113	Colanic acid biosynthesis	-	+
25-B3	*cpsB*/EcF11_0983[d]	EDV69166/EDV69210	Colanic acid biosynthesis	+/-	+/+
5-C3	*papC*	EDV68631	P fimbrial usher	-	+
2-H1	*kdpA*	EDV65279	Potassium transport	+	+
5-E3	*nark*	EDV68420	Nitrate/nitrite transport	+	+
12-B3	*ycjV*	AAN80256	Putative ABC transporter ATP-binding protein	+	+
5-C5	*uidR*	EDV65917	Repressor of β-glucuronidase (*uid*)	+	+
11-E6	*yeeP*	EDV67436	Putative GTPase	+	+
6-B3	*evgA*	EDV65560	Positive transcriptional regulator of EvgSA two-component system	+	+
24-E2	*cpxA*	EDV66646	Sensor histidine kinase	+	+
18-C3	*nadB*	EDV65323	L-aspartate oxidase	+	+
25-E2	*Wzy*	EDV69037	Enterobacterial common antigen biosynthesis	-	+
29-A4	None	AAN80576	Hypothetical protein	+	+
2-F1	EcF11_3365	EDV65997	Hypothetical protein	-	+
19-E5	*yegP*	EDV69027	Hypothetical protein	+	+
28-G6	None[e]				
7-E3	None[e]				
28-H2	None[e]				

[a]Genetic locus with the closest match to the sequence interrupted by the transposon in each mutant

[b]+, present in the genome of *E. coli* K-12 strain MG1655; -, absent from the MG1655 genome

[c]+, present in the genome of *E. coli* strain CFT073; -, absent from the CFT073 genome

[d]Sequence data unable to differentiate between homologous genes

[e]Genetic locus was not sequenced

Confirmation of attenuation in *E. coli* F11 by competitive cochallenge assays

Following identification by repeat screening of mutants putatively attenuated for colonization of the murine urinary tract, we performed competition colonization experiments by coinoculating the wild-type strain F11 and each mutant in a 1:1 ratio. After 48 h, the urine, bladder and kidneys were collected, homogenized and CFU were calculated by plating onto selective medium. A CI was calculated for each mutant, and statistical analysis was performed to quantify the differences between the recovered ratios of mutant to wild type. A total of 23 mutants (1.7% of the pool) were confirmed that exhibited statistically significant attenuation in cochallenge or had transposon insertions in genes that had already been identified as virulence factors **(Table 2.2)**. In some cases, we observed multiple independent transposon events affecting the same gene, resulting in a final tally of 19 candidate genes. These genes can be described initially as 'fitness factors' until mutants are assessed in independent challenge and subjected to complementation.

Among these mutants, three carried insertions disrupting *fim* operon genes encoding type 1 fimbriae, four mutants had insertions in colanic acid biosynthesis genes and one had an insertion in *wzy* encoding enterobacterial common antigen. All of these loci had previously been identified in an STM screen using pyelonephritis isolate CFT073 (205).

Additionally, a number of genes involved in transport across membranes were also identified including *kdpA*, an ATP-dependent P-Type ATPase potassium transporter, *narK*, a nitrate/nitrite antiporter and *ycjV*, a putative ABC transporter. Mutants carrying insertions in genes encoding transcriptional regulators *uidR* and *evgA* were also attenuated. As well, *yeeP*, a predicted GTP-binding protein, and *nadB*, an L-aspartate oxidase involved in nicotinamide adenine dinucleotide (NAD) biosynthesis, were identified as fitness genes from our screen.

Finally, we observed that insertion in *papC*, encoding the usher for P-fimbria biogenesis, resulted in attenuation during colonization of the murine model.

Measurement of cross-talk between *fim* and *pap* gene expression in *E. coli* F11

In CFT073, the production of type 1 and P fimbriae are coordinated such that the expression of *fim* genes results in a decrease in the expression of both *pap* operons (216). qPCR was used to measure cross regulation of type 1 and P- fimbrial genes in *E. coli* F11. Expression of *fimA* and *papA* was quantified in F11 and in two isogenic strains that have been mutated such that the invertible element that controls *fim* gene expression is phase locked to either constitutively express *fimA* (F11 L-ON) or to repress expression of *fimA* (F11 L-OFF) (210). All strains were cultured independently on LB agar for 18 h at 37°C to favor production of P fimbriae (209). F11 L-OFF was set as the baseline 'calibrator', and expression of *gapA* acted as the normalizing internal control. As expected, qPCR demonstrated that *fimA* expression was 22.7-fold higher in F11 and 344-fold higher in F11 L-ON compared to F11 L-OFF **(Figure 2.1)**. Expression of *fimA* was significantly higher in F11 L-ON compared to F11 ($P < 0.01$). However, *papA* expression was only 7.77- fold higher and 3.93-fold higher in F11 L-ON compared to F11 L-OFF, and the expression of *papA* in F11 and F11 L-ON was not statistically different ($P = 0.403$). Thus, expression of type 1 fimbriae does not influence expression of P fimbriae in F11.

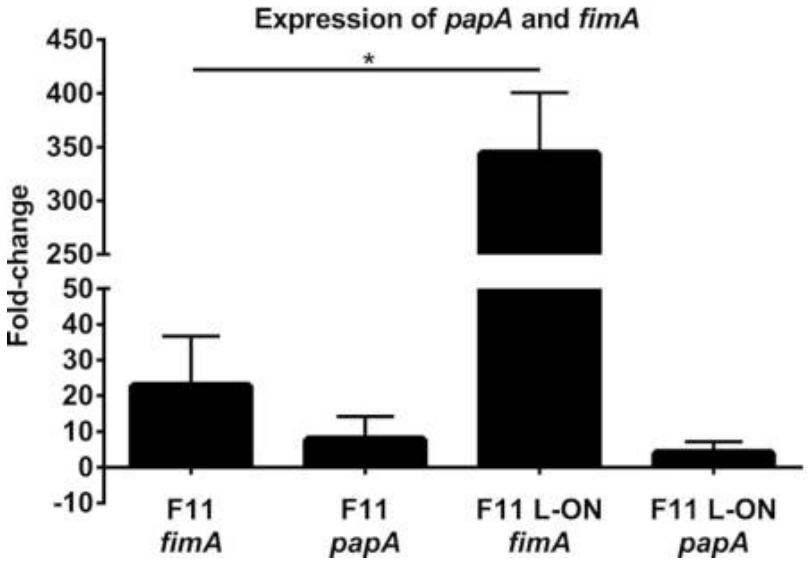

Figure 2.1 *fim* expression does not affect *pap* expression
qPCR analysis of *fimA* and *papA* expression in *E. coli* F11 and type 1 fimbrial phase-locked mutants. The black bars represent the change in gene expression (*n*-fold) of *fimA* and *papA* between wild type F11 and F11 L-ON. F11 L-OFF was used as the calibrator for calculating the fold-change in expression of *fimA* and *papA*. Results represent three independent experiments, and the error bars show standard deviation. Significant differences in gene expression were determined using an unpaired Student's *t*-test. *, $P < 0.01$.

P fimbriae enhance urinary tract colonization by CFT073

In prior studies, no difference in urinary tract colonization was detected in independent challenges using a wide range of inoculum doses (10^5–10^9 CFU) between strain CFT073 and mutant construct UPEC76, which had deletions in both of its *pap* operons (153). However, the identification and confirmed attenuation of an *E. coli* F11 *papC* mutant in the current screen prompted us to re-examine the contribution of P fimbriae in the murine model of UTI by a more sensitive co-infection method. Accordingly, we cloned one of the *pap* operons from strain CFT073 into a low-copy-number plasmid and transformed the plasmid, designated pXLW34, into UPEC76 (the double *pap* mutant).

Consistent with expression of functional P fimbriae, clones were capable of mannose-resistant hemagglutination of human and sheep erythrocytes (data not shown). Therefore, plasmid pXLW34 restored the ability of UPEC76 to produce functional P fimbriae. To control for the effect of the plasmid, we transformed the empty vector into both CFT073 and UPEC76. Then, we compared CFT073 containing the vector to either UPEC76 with the vector or UPEC76 with the cloned pap operon in co-infection studies.

In 20 mice, CFT073 significantly outcompeted UPEC76 in cultures from urine (median 2.4×10^4 versus 1.4×10^3 CFU mL^{-1}, respectively, $P = 0.003$), bladder (median 2.6×10^5 versus 7.8×10^4 CFU g^{-1}, respectively, $P < 0.001$) and kidneys (median 1.9×10^5 versus 6.7×10^4 CFU g^{-1}, respectively, $P < 0.001$), when both strains had the control vector plasmid **(Figure 2.2A)**. These results suggest that P fimbriae are important during colonization throughout the urinary tract.

To exclude the possibility that the difference in colonization between CFT073 and UPEC76 was due to an inadvertent mutation other than the deliberate deletion of both copies of

the *papG* adhesin genes, we compared CFT073 containing the control plasmid vector to UPEC76 containing the pap operon plasmid in co-infection of 20 mice **(Figure 2.2B).** In contrast to the results in the absence of complementation, we found no significant difference between CFT073 containing the control plasmid and UPEC76 containing the complementing plasmid in ability to colonize the urine (median 1.2×10^5 versus 4.3×10^4 CFU mL^{-1}, respectively, P = 0.325) or bladder (median 5.7×10^5 versus 6.4×10^5 CFU g^{-1}, respectively, P = 0.118). However in the kidneys, the wild-type strain outcompeted the complemented mutant (median 9.6×10^4 versus 5.9×10^4 CFU g^{-1}, respectively, P = 0.035).

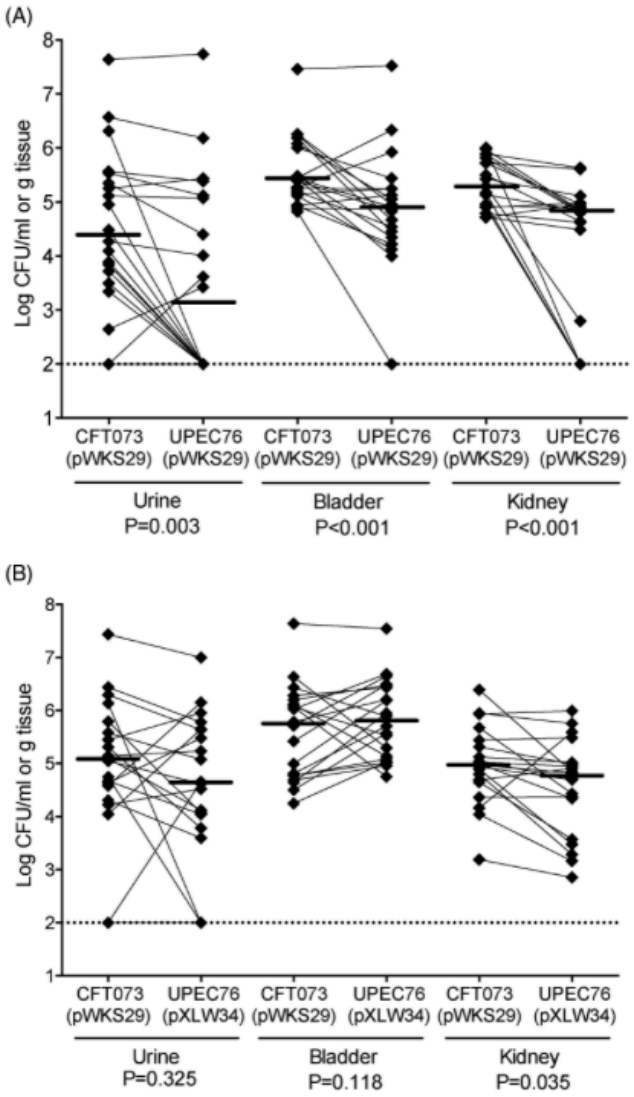

Figure 2.2 P fimbriae contribute to bladder and kidney colonization
(A) Cochallenges of mice with *E. coli* CFT073 and *pap* operon mutant UPEC76. A total of 20 mice were transurethrally inoculated with a 1:1 mixture of the wild-type and mutant strains. After 48 h, the mice were sacrificed and urine, bladder and kidneys were collected. Each data point represents the CFU per milliliter of urine or per gram of tissue collected, and a solid line indicates the median. Paired results from individual mice are connected. pWSK29 acts as the empty vector. **(B)** Cochallenges of mice with *E. coli* CFT073 and *pap* operon mutant UPEC76 transformed with pXLW34 encoding for *papIAHCDJKEFG2*. A total of 20 mice were transurethrally inoculated with a 1:1 mixture of the wild-type and mutant strains. The mice were sacrificed after 48 h, and urine, bladder and kidneys were collected. Each data point represents the CFU per milliliter of urine or per gram of tissue collected, and a solid line indicates the median. Paired results from individual mice are connected.

Discussion

Compared to commensal *E. coli*, ExPEC strains are more likely to carry additional virulence or fitness factors that enable more effective colonization and extended persistence within the urinary tract (115, 153, 217) (14, 194, 199). However, efforts to identify a defined set of requisite virulence and fitness factors remain incomplete. The aim of our study was to identify novel genes in ExPEC that are required for fitness during infection. In this study, we describe screening of signature- tagged mutants of *E. coli* F11, a cystitis strain originally isolated from a human case of uncomplicated UTI, in the murine model of UTI and the identification of 19 candidate fitness genes. STM is an effective technique to screen an array of transposon mutants in parallel in an animal model of infection. Indeed, STM has been used previously on ExPEC pyelonephritis strain CFT073 and *Proteus mirabilis* in the murine model of UTI (205, 218-220). This work identified novel fitness factors in cystitis isolate *E. coli* F11 and provides support for previously identified virulence or fitness factors, including *fimD*, *wzy* and colanic acid biosynthesis genes (205). In addition, our study has for the first time successfully fulfilled molecular Koch's postulates for P fimbriae (*papC*) as a virulence factor.

To conduct this trial, mutants in *E. coli* F11 were generated by transposon mutagenesis using unique sequence tags that allowed for detection of individual mutants following passage in the CBA murine model of UTI (201). The final library consisted of 1334 transposon mutants. Pools of 48 mutants were transurethrally inoculated into 6 to 8-week-old CBA mice. Urine, bladder and kidneys were collected at 48 h and suspensions were analyzed by dot-blot hybridization to identify absent or attenuated mutants. We initially identified 27 candidate fitness genes necessary for bladder or kidney colonization (2% of the bank). A subset of 19 fitness

genes were confirmed by co-infection of each mutant with wild-type strain F11 in the CBA murine model.

Importantly, one gene identified was *papC*, which encodes the chaperone required for P-fimbriae biogenesis. Additionally, *papC* , like the rest of the *pap* operon, is found more frequently among UPEC strains than in fecal *E. coli* strains (152, 153, 194). P fimbriae are extracellular adhesion organelles that bind to the P blood group antigen found on erythrocytes as well as to the Galα(1-4)βGal moieties of glycosphingolipids found on renal epithelial cells (221). While overwhelming epidemiologic evidence supports a role for P fimbriae during the development of UTI, heretofore, no specific studies have satisfied molecular Koch's postulates, demonstrating P fimbria as a complementable virulence determinant.

P fimbriae have been shown to participate in coordinate regulation with type 1 fimbriae in an inverse manner, and deletion of Pap-related fimbrial clusters in the pyelonephritis strain *E. coli* 536 resulted in increased fim expression (163, 216). Transcription of the *fim* operon is dependent on the orientation of a σ^{70} consensus promoter located on an invertible element (222). PapB has been shown to block expression of *fim* by inhibiting the site-specific recombinase FimB, which mediates switching of the invertible element to either on or off orientation, while concurrently promoting expression of FimE, which can only mediate switching from on to off (163, 223, 224). Conversely, microarray analysis in CFT073 demonstrated that when *fim* expression was phase L-ON, and thereby constitutively expressed, there was a subsequent decrease in expression of both *pap* gene clusters with the *pheU*-associated *pap*2 being more strongly repressed than the *pheV*-associated *pap*1 (216). Additionally, inhibition of *fim* expression in the L-OFF phase resulted in an increase in the expression of both pap operons, further supporting the presence of cross-talk. This coordinated regulation has also been verified

by qRT-PCR in CFT073 where expression in the wild type and L-ON backgrounds led to repression of papA2 expression compared to L-OFF (216).

Unlike CFT073, cross-talk between type 1 and P fimbriae has not been as well characterized in the F11 strain (216). To characterize coordinated regulation between type 1 and P fimbriae in F11, we cultured wild-type, L-ON and L-OFF strains on LB agar for 18 h at 37°C, which are conditions that have been shown to favor *pap* expression (209). We performed qPCR to quantify fold-change gene expression in *fimA* and *papA* using F11 L- OFF as the relative measure for comparison. As we expected, *fimA* expression was elevated in wild type compared to L-OFF and dramatically increased in L-ON. Despite this elevated *fimA* expression, there was only a subtle decrease in *papA* gene expression in the L-ON background compared to wild type, which was not statistically significant. Our results demonstrated that *fimA* expression did not impact *pap* expression when cultured under these conditions. F11 carries a different subset of fimbrial types including only one copy of *pap*, compared to the two copies found in CFT073, which may influence the degree of cross-talk between type 1 and P fimbriae. Additionally, F11 has been shown to have a higher percentage of phase-on *fim* switches than CFT073 at 24 h in the CBA murine model of UTI demonstrating that fimbrial expression can vary between UPEC strains (149).

The *E. coli* F11 genome has only one *pap* operon, which may explain why our current study was able to identify *papC* as a candidate fitness gene in contrast to previous work with pyelonephritis isolate CFT073, carrying two copies of the *pap* operon (153). Since our competition data already gave us a strong indication that *papC* is important for *in vivo* fitness of cystitis strain F11, we chose to further validate our screen and extend our study to multiple strains by pursuing molecular Koch's postulates in the pyelonephritis strain, CFT073.

Previous studies revealed no differences in colonization during murine UTI between wild-type CFT073 and an isogenic mutant UPEC76, lacking both *pap* operons. However, this initial work compared colonization by independent infections. It is now understood that cochallenge experiments are more sensitive for detecting attenuation during infection (225). To this end, we were able to observe attenuation of UPEC76 when cochallenged with CFT073. We were also able to complement expression of the *pap* operon in UPEC76 (double pap mutant), which restored its ability to colonize the urinary tract. This is the first time that a gene within the *pap* operon (*papC* in this case) has been identified using STM.

In addition to *papC*, we identified three mutants harboring a transpson within the *fim* operon, which encode for type 1 fimbriae. Type 1 fimbria is one of the most common fimbrial types carried by *E. coli* strains, found in nearly all strains and multiple studies have shown that type 1 fimbriae are critical for colonization of mice by both cystitis and pyelonephritis strains (136, 140, 226, 227). Therefore, we did not pursue cochallenge experiments with these mutants. We applied the same reasoning to genes involved with the biosynthesis of colanic acid, a group I capsule-associated extracellular polysaccharide. Colanic acid has been previously identified virulence factor of ExPEC (205). Nevertheless, the current study adds weight to the conclusion that surface polysaccharides and type 1 fimbriae are preeminent urovirulence factors.

Bacteria must overcome a unique combination of environmental stresses for successful colonization of the urinary tract, including high osmolarity, high urea concentration, variable pH and limited nutrient availability (106, 228). Previous data suggest that ExPEC strains are able to take advantage of the carbon and nitrogen sources within the urinary tract more effectively than commensal E. coli strains (229-231). Our screen identified a number genes in *E. coli* F11 associated with metabolism that when disrupted resulted in a reduction of *in vivo* fitness during

UTI. One mutant was identified in *uidR*, which is a negative regulator of the *uidAB* operon. UidAB is involved with the transport and hydrolysis of glucuronides (232). Imported glucuronides are catabolized into 2-keto-3-deoxy-6-phosphogluconate (KDPG) for utilization in the Entner–Doudoroff (ED) pathway, an alternative pathway to classic glycolysis (233). KDPG can also be generated by the phosphogluconate dehydratase Edd using gluconate as the input carbon source, and disruption of *edd* in commensal *E. coli* reduces gut colonization (234). However, despite genes involved with the ED pathway being upregulated (2–5-fold) in strain CFT073 during ascending UTI, an *edd* mutant does not show a loss of fitness during UTI infection (106, 231). Further complementation and knockout studies are needed to ascertain if disruption of *uidR* in our study results in a polar mutation that affects regulation of the *uidAB* operon. However, our data suggest that upon entering the urinary tract, maintaining regulation of glucuronide import into the ED pathway is important for fitness.

Another fitness factor identified was *nadB*, encoding for a flavoenzyme involved with *de novo* biosynthesis of NAD. NAD plays a central role in metabolism (235), yet the role of NAD during ascending murine UTI model is unclear. Nicotinamide auxotrophy did not show an influence on bladder colonization by strains CFT073 or UTI89 during UTI (236). Our identification of *nadB* in strain F11 suggests that NAD metabolism contributes to survival within the urinary tract. Another mutant identified was in *narK*, which is one of two nitrate transport genes in *E. coli* and is contributes to anaerobic nitrate respiration (237). *narK* encodes for a nitrate/nitrite antiporter that couples nitrate uptake to nitrite excretion (238). *narK* is upregulated in CFT073 during in vitro growth in human urine in comparison to growth in LB broth (106). Our data supports a role for *narK* as a fitness factor during UTI and suggests an advantageous contribution of increased anaerobic respiration within the urinary tract.

Our screen also identified *ycjV*, an uncharacterized member of the ATP-binding cassette (ABC) superfamily of transporters and may be involved in sugar transport. It was shown to be upregulated in an antibiotic-resistant strain of *Klebsiella pneumoniae* compared to a susceptible isolate, suggesting that it could act as a novel active efflux mechanism (239). However, its role during UTI in *E. coli* has not been fully investigated.

ExPEC strains have adapted various strategies to maintain cellular homeostasis despite variable osmolality and elevated urea levels within the urinary tract (240, 241). Our screen identified two genes that were critical during ascending infection of the urinary tract and are also involved with limiting the effects of osmotic stress. One mutant that we identified was *kdpA*, which is part of the *kdpFABC* operon. The *kdpFABC* operon encodes a high-affinity ATP-driven potassium transporter (242). KdpA is the K^+-translocating subunit and is essential for Kdp-ATPase function (243). In prokaryotes, potassium is vital in regulating intracellular pH levels and maintaining turgor pressure in response to stress-inducing environments (244). In response to low external K^+ levels or osmotic upshock, expression of the *kdpFABC* operon is upregulated, which differs from the only other K^+ transporters in *E. coli*, Trk and Kup, that are constitutively expressed (245). Recent RNA-seq experiments done by the Mobley lab using clinical samples showed that *kdpA* was selectively expressed during UTI (246) (Subashchandrabose et al. 2014). Our work supports the supposition that the Kdp system is critical during infection of the urinary tract. Our screen also identified *evgA*, which encodes one subunit of a two-component signal transduction system EvgAS (247) (Utsumi et al. 1992). EvgA regulates the expression of multiple genes including those related to osmotic stress, acid resistance and antibiotic resistance (248-251). Further studies are needed to investigate the exact role of EvgA in the context of a UTI. However, we hypothesize that given the high osmolality of the urinary tract, EvgA is

critical for regulating expression of additional genes needed to maintain osmotic homeostasis during UTI. We also identified the mutant *cpxA*, which is the sensor kinase of the CpxRA two-component signal transduction system. CpxRA is triggered by changes in pH, envelope stress, interaction with hydrophobic surfaces or high osmolarity (252-255). In response to these triggers, CpxA–CpxR modulates porin expression as well as activates proteases and folding proteins (256, 257). Deletion of *cpxRA* operon reduced fitness and virulence in both UTI89 during colonization of the murine bladder and in CFT073 during localized and systemic infections in zebrafish embryos (258). Our results support these findings and advocate that CpxA is also important in F11 during colonization of the murine urinary tract.

In contrast to P fimbriae, which we show here to be required for full urovirulence, additional complementation studies should be conducted with the identified transposon mutants to confirm their importance during UTI. Another limitation of this current study is the limited number of mutants screened. Thus, additional genes required for UTI likely remain to be identified.

This study demonstrates the advantages of cochallenge experiments and the use of transposon mutagenesis to identify novel fitness factors. We were able to confirm, after decades of study, that P fimbriae are important during UTI as well as support previously identified virulence factors. At this time, there has been no identification of a defined group of virulence and fitness factors in ExPEC suggesting that ExPEC strains may express combinations of virulence and fitness genes resulting in different strategies for survival within the urinary tract.

Chapter III: Cross-talk between MarR-like transcription factors coordinate the regulation of motility in UPEC

Courtney L. Luterbach and Harry L.T. Mobley

Infection and Immunity (In Review)

Abstract

The MarR-like protein PapX represses transcription of the flagellar master regulator *flhDC* in uropathogenic *Escherichia coli* (UPEC), the primary cause of uncomplicated urinary tract infections (UTIs). PapX is encoded by the *pap* operon, which also encodes the adherence factor P fimbriae. Both adherence and motility are critical for productive colonization of the urinary tract. However, the mechanisms involved in coordinating the transition between adherence and motility are not well characterized. The UPEC strain CFT073 carries both *papX* and a homolog *focX*, located in the *foc* operon encoding F1C fimbriae. In this study, we characterized the dose-effects of "X" genes on flagellar gene expression and cross-talk between *focX* and *papX*. We found that FocX and PapX both repress *flhD* transcription. However, we determined that the Δ*papX* mutant was hypermotile, while the loss of *focX* did not affect motility. We further investigated this phenotype and found that FocX represses *papX* transcription. Additionally, we identified a proximal imapromoter upstream of both *focX* and *papX* and assessed the expression of *focX* and *papX* during culture in human urine and on LB

agar plates compared to LB medium. Finally, we characterized the contribution of PapX and FocX to fitness in the ascending murine model of UTI, and observed a subtle, but not statistically significant, fitness defect in colonization of the kidneys. Altogether, these results expand our understanding of the impact of encoding multiple "X" genes on coordinated regulation of motility and adherence in UPEC.

Introduction

Escherichia coli is a common, and typically commensal, bacterial species that regularly colonizes the human gastrointestinal tract (259, 260). Some strains of *E. coli*, broadly referred to as extraintestinal pathogenic *E. coli* (ExPEC), are equipped with virulence and accessory genes that are lacking from their commensal counterparts and promote infections outside of the intestine, including urinary tract infections (UTIs) (11). Uropathogenic *E. coli* (UPEC) are the primary cause of approximately 80% of all community-acquired UTIs, which are a pervasive and costly public health burden afflicting approximately half of all women and one-fifth of men at least once in their lifetime (261, 262). Most UTIs are established when bacteria contaminate the periurethral area and migrate to the bladder via the urethra. While many UTIs are self-limiting and resolve within a few days, in some cases UPEC may further ascend via the ureters and cause a more severe secondary infection in the kidneys called pyelonephritis, increasing the risk of renal scarring, sepsis, and death (33).

Extracellular polymeric filaments called flagella promote swimming motility in bacteria and facilitate UPEC ascension of the urethra and ureters during UTI (103, 263). While the ability to produce flagella is not required for colonization of the urinary tract, strains capable of flagella-mediated motility persist longer within the bladder and kidneys and colonize to higher levels

(100, 102). Moreover, expression of *fliC*, the subunit that polymerizes to form the flagellum, coincides with ascension of the urinary tract and colonization of the kidneys in the murine model of UTI (101). However, *fliC* is poorly expressed in UPEC strains isolated from the urine of women experiencing acute cystitis, as well as, during *in vitro* culture in human urine (150, 246). Additionally, flagella are energetically costly to produce and monomeric FliC can be detected by the Toll-like receptor 5 (TLR5) found on the uroepithelium (107, 108). Thus, expression of flagella during UTI may be detrimental for UPEC survival and contribute to the transient expression of flagellar genes observed during infection (101, 106).

During a UTI, bacteria transition between motile and adherent states through coordinated cross-talk between genes encoding flagella and adherence factors, termed fimbriae (101, 104, 170). Adherence of bacteria to host cells is critical for colonization of the urinary tract, and UPEC isolates are more likely to encode fimbriae that bind to cells found within the urinary tract (61, 140, 264). The UPEC strain CFT073 genome carries 12 fimbriae, including F1C and two separate P fimbriae (142). F1C fimbriae, encoded by the *foc* operon, bind glycolipids found on the kidney epithelium and endothelium, and cystitis UPEC isolates were more likely than fecal *E. coli* isolates to encode F1C fimbriae (138, 182, 183). Similarly, pyelonephritis-associated pili (Pap), or P-fimbriae, bind the P-blood group antigen enriched on human kidney epithelial cells and erythrocytes, and UPEC strains harboring the *pap* operon are more likely to cause pyelonephritis (153, 265).

Differing from most fimbrial operons, one of the two *pap* operons and the single *foc* operon carry a 3' terminal gene encoding a MarR-like transcription factor PapX and FocX, respectively. MarR-like proteins share a winged helix-turn-helix structure (wHTH), bind as dimers to palindromic DNA sequences, and have been shown to mediate the regulation of

numerous genes, including those involved with resistance to antibiotics, oxidative stress and low pH, as well as motility (175, 266-268). We have previously shown that PapX binds to a 29 bp palindromic DNA sequence located 410 bp upstream of the *flhDC* translational start site, encoding the master transcriptional regulator $FlhD_4C_2$ of flagellar gene expression. Overproduction of PapX represses the transcription of *flhD* and subsequently reduces swimming motility (169, 170, 176). PapX was also identified in a TraDIS screen for genes affecting motility in a different UPEC strain EC958 (269). Thus, PapX is involved in regulatory cross-talk between genes associated with adherence and motility.

FocX shares 96.7% amino acid sequence identity with PapX and therefore is predicted to also function as a repressor of motility. However, the function of FocX in UPEC has not been well characterized, and the impact of encoding multiple homologous "X" proteins on motility in UPEC is poorly understood. In this study, we found that PapX and FocX both repress *flhD* expression as well as swimming motility when ectopically expressed. However, we have discovered that FocX can also repress the expression of *papX,* and that cross-talk between "X" genes affect motility. Additionally, we characterized an independent proximal promoter for *focX* and *papX*, suggesting that *focX* and *papX* can be expressed independently from their respective fimbrial operons. However, we found that the expression of *papX* positively correlates with *pap* expression during *in vitro* culture on LB agar plates. Furthermore, we assessed the relative fitness of either the single Δ*papX* or double Δ*focX*Δ*papX* mutants compared to wild type by *in vivo* competitive cochallenge in CBA/J mice, and observed a slight, but not statistically significant, decrease in kidney colonization. Since UPEC isolates are more likely than commensal strains to encode at least two "X" genes, investigating the interactions between PapX

and FocX is imperative to understand how UPEC regulates motility and responds to environmental signals within the urinary tract.

Results

PapX and FocX share high sequence and structural similarities.

The *E. coli* CFT073 genome harbors both the *pap* and *foc* operons, which encode the homologous MarR-like proteins PapX and FocX, respectively **(Figure 3.1A)** (142). The predicted structures of PapX and FocX were created using I-TASSER and were modeled as dimers based on the solved dimer structure of the MarR-like protein, HucR (270). While MarR-like proteins contain a conserved winged helix-turn-helix DNA-binding motif, the majority of these proteins share limited amino acid sequence identity (~25-35%)(271). Despite being encoded by different fimbrial operons, PapX and FocX share high amino acid sequence identity (96.7%) **(Figure 3.1B)** and predicted structural homology **(Figure 3.1C)** (169). In MarR-like proteins, key structural motifs include the dimerization domain between subunits, the DNA recognition helices that bind palindromic DNA sequences within the major groove, and the wing domain that interacts with residues within the minor groove (172, 272). Therefore, amino acid changes within these structural domains are more likely to alter DNA binding site recognition and protein function. There are three amino acid differences within key structural areas between PapX and FocX, respectively: T35A within the dimerization domain, A97T within the DNA binding helix, and M103T within the wing domain. Therefore, while we predict that PapX and FocX share the same function based on their high structural and amino acid sequence similarities, it is not known if these substitutions affect protein function.

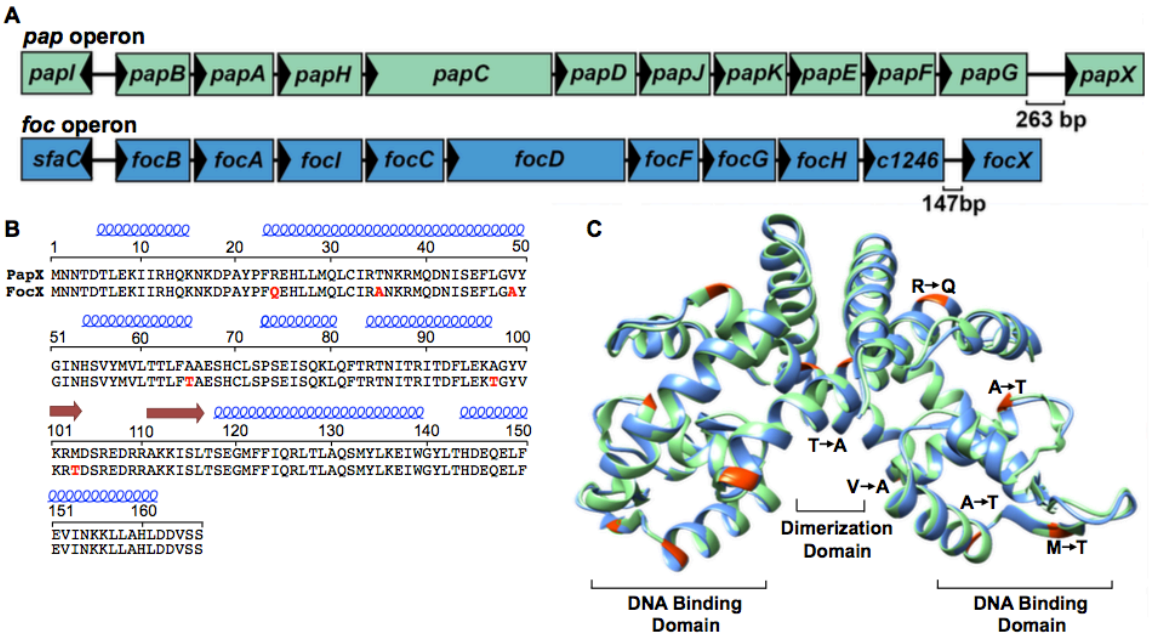

Figure 3.1 PapX and FocX share high sequence and structural homology.
(A) A schematic of the *pap1* and *foc* operons in CFT073. **(B)** The amino acid sequences of PapX and FocX were manually aligned and residues in red signify differences between FocX and PapX. The predicted location of α-helices (blue) and β-sheets (red arrows) are shown above the amino acid sequence. **(C)** The predicted dimer structures of PapX (green) and FocX (blue) were created using I-TASSER and aligned using Chimera to the known structure of the dimer HucR (not shown). Amino acid differences between FocX and PapX are highlighted in red and labeled on one monomer.

The loss of *papX,* but not *focX,* increases swimming motility.

To determine the effect of PapX and FocX on motility, we measured the motility of CFT073 wild type, Δ*focX*, Δ*papX*, and the double mutant Δ*focX*Δ*papX* strains using a swimming motility assay. We observed that the loss of *focX* did not increase swimming motility **(Figure 3.2A)**. In contrast, the loss of *papX* resulted in a hypermotile phenotype, and this result was consistent with previous studies showing PapX represses motility (169, 170, 176, 273). Interestingly, the loss of both *focX* and *papX* resulted in an increased level of swimming that was significantly greater than wild type, but not as robust as the Δ*papX* mutant, suggesting that there may be cross-talk between *focX* and *papX*.

E. coli strains differ in their capacity for motility in part due to heterogeneity in the presence of insertion sequence elements upstream of *flhDC* as well as variability in the encoded transcriptional regulators of flagellar genes (89, 274, 275). Therefore, to compare the function of PapX in additional UPEC strains, we compared the motility between wild type and a Δ*papX* mutant in the UPEC cystitis isolates F11 and HM69 **(Figure 3.3)**. Both strains F11 and HM69 carry the *pap* operon, including *papX*, but not the *foc* operon. We observed that the deletion of *papX* resulted in a significant increase in motility compared to wild type in F11 (121%) and HM69 (117%); however, the hypermotile phenotypes were not as robust as what was observed in CFT073 (161%) **(Figure 3.2A)**. Therefore, these data support that PapX functions through a conserved mechanism in UPEC, but that the impact of PapX on motility is dependent on the strain background.

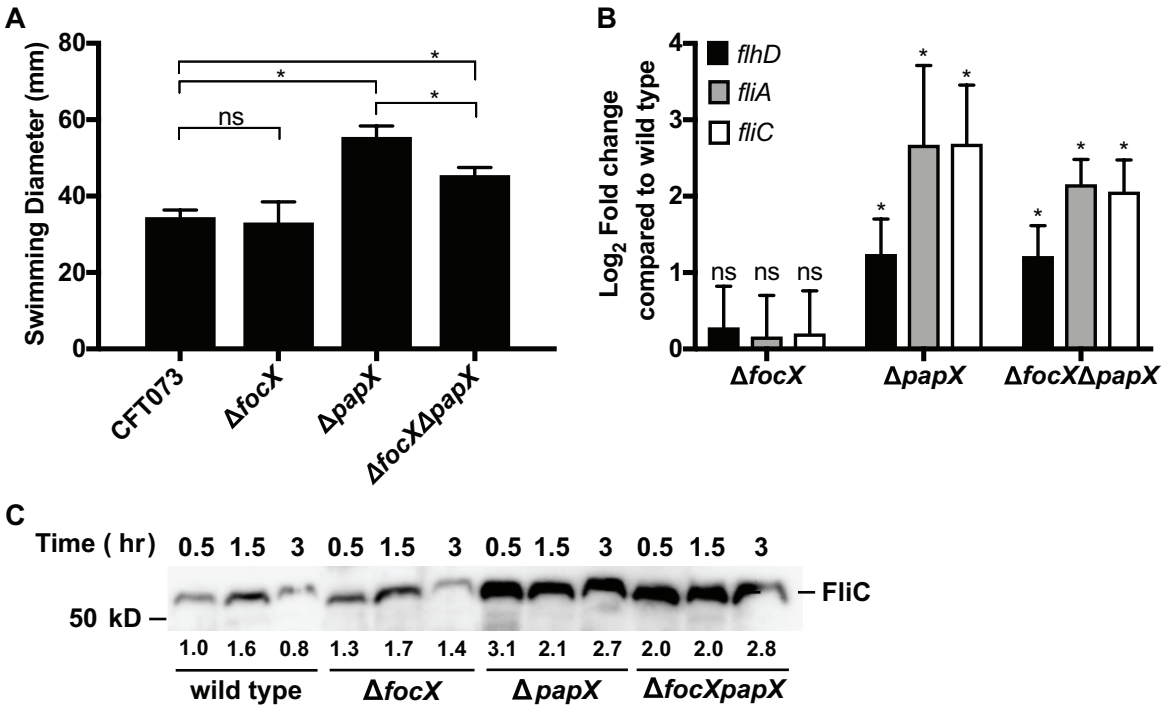

Figure 3.2 Effect of *focX* and *papX* expression on swimming motility
(A) Swimming diameter (mm) was measured for CFT073 and isogenic mutants after 16-18 hr incubation at 30°C. Data represent five biological replicates with the error bars showing the standard deviation. Tukey's multiple-comparisons test following ANOVA was used for statistical analysis. *, $P < 0.05$; ns (not significant) **(B)** qPCR of flagellar genes *flhD*, *fliA*, and *fliC* using cDNA collected from *E. coli* CFT073 wild type and Δ*focX*, Δ*papX*, and Δ*focX*Δ*papX* constructs cultured in tryptone media until OD_{600} of 0.3 (~1.5 hr). Data represent the average of three experiments. Standard deviation is shown and a Student's *t*-test was used for statistical analysis. *, $P < 0.05$. No statistical difference was found between Δ*papX* and Δ*papX*Δ*focX* using a Mann-Whitney test. **(C)** Immunoblot detecting FliC levels from whole cell lysates in CFT073 wild type and the Δ*focX*, Δ*papX*, and Δ*papX*Δ*focX* constructs cultured in tryptone broth. Relative quantification of FliC (shown underneath the protein band) was obtained using Image Lab 5.2.1 and represents the average fold change of two independent experiments compared to FliC levels of wild type at 0.5 hr and normalized to a conserved nonspecific band.

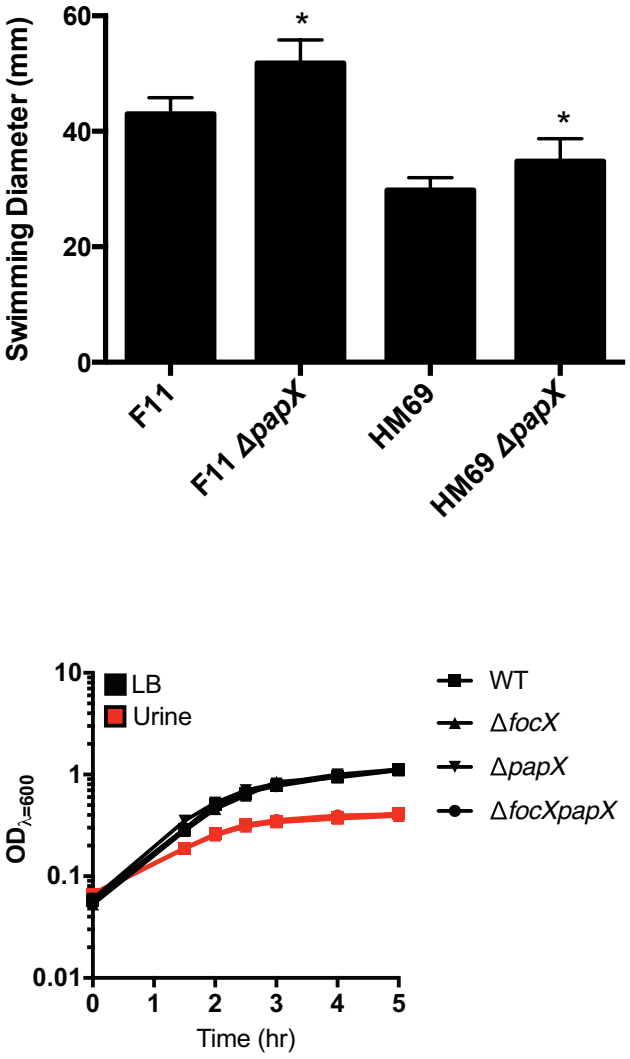

Figure 3.3 The loss of *papX* in the cystitis UPEC isolates F11 and HM69 increases motility **(A)** The bars represent the average diameter (mm) of swimming motility of bacteria following 16-18 hr incubation at 30°C (N=6). The error bars represent the standard deviation, and a Student's *t* test was used for statistical analysis. *, $P < 0.05$. **(B)** Growth curves showing similar levels of bacterial growth between CFT073 wild type and the Δ*focX,* Δ*papX,* Δ*focXpapX* constructs. Bacteria were diluted 1:100 from overnight cultures into either fresh pooled, sterilized human urine (red) or LB media (black) and cultured with aeration at 37°C for 5 hrs. OD_{600} measurements were taken over time and plotted on the $\log_{10}$ scale.

We have previously shown that PapX inhibits swimming motility by repressing the expression of *flhDC*, resulting in the downregulation of additional flagellar genes (169, 176, 273). To verify that the observed motility phenotypes correspond to changes in the expression of flagellar genes, we performed qPCR to quantify the changes in mRNA abundance of *flhD*, *fliA*, and *fliC* between CFT073 and the Δ*focX*, Δ*papX*, and Δ*focX*Δ*papX* constructs. RNA was collected from bacteria cultured in tryptone medium to an OD_{600} of 0.3. Growth conditions were chosen based on previous work demonstrating that the production of flagella in CFT073 is elevated during early logarithmic growth in tryptone medium (104). Consistent with our swimming results, the loss of *focX* did not alter the expression of *flhD*, *fliA*, or *fliC* **(Figure 3.2B)**. However, we did observe a significant increase in the expression of *flhD*, *fliA*, and *fliC* in both the Δ*papX* (Log_2 Fold Change (FC): 1.2-2.7) and the double Δ*focX*Δ*papX* (Log_2 FC: 1.2-2.1) mutants compared to wild type.

To determine if the qPCR results correlated to an increase in flagellum production, we performed an immunoblot comparing FliC levels between CFT073 wild type and the Δ*focX*, Δ*papX*, and Δ*focX*Δ*papX* constructs. Bacteria were cultured in tryptone medium and the levels of FliC were assessed from normalized whole cell lysates collected at 0.5, 1.5, and 3 hours, representing early, mid and late logarithmic growth **(Figure 3.3B)**. In wild type CFT073, we observed a peak in FliC production at 1.5 hours, and this result was consistent with previous studies characterizing the temporal production of FliC **(Figures 3.2C)** (104). Additionally, we observed an increase in FliC production in the Δ*papX* and Δ*focX*Δ*papX* constructs at all collected time points, which were quantified by densitometry based on the average of two replicates. While we detected an increase in FliC production in the Δ*focX* construct compared to wild type at 0.5 hrs, we did not observe a difference in FliC production at later time points.

Therefore, these results show that the deletion of *papX*, compared to *focX*, has a greater impact on swimming motility, flagellar gene expression and FliC production in CFT073.

PapX and FocX both function as repressors of motility.

Based on the amino acid sequence and structural similarities between PapX and FocX, we predicted them to share the same function as transcriptional repressors of motility. Yet compared to wild type, the deletion of *focX* did not significantly increase swimming motility. Therefore, to assess PapX and FocX function independent of their native expression, we expressed *papX* (pLX-*papX*) or *focX* (pLX-*focX*) *in trans* in CFT073 and performed a swimming motility assay **(Figure 3.4A)**. Previous work demonstrated that, in the absence of IPTG, *papX* expression was increased 11-fold in CFT073 carrying pLX-*papX* compared to the empty vector (176). Compared to CFT073 carrying the empty vector pLX3607, expression of either *papX* (pLX-*papX*) or *focX* (pLX-*focX*) resulted in approximately a 50% reduction in swimming motility. To assess whether this phenotype was specific to CFT073, we repeated this assay in the cystitis isolate F11 and observed a comparable decrease in motility following overproduction of either FocX or PapX. We have previously shown that the commensal *E. coli* K-12 MG1655 strain lacks the PapX binding site upstream of *flhDC*, and therefore the overproduction of PapX does not reduce motility (169). To determine if the function of FocX also depends on the presence of the PapX binding site upstream of *flhDC*, we assessed the swimming motility of K-12 MG1655 carrying pLX3607, pLX-*papX*, or plx-*focX*. We observed that the expression of either *papX* or *focX* did not decrease motility compared to the empty vector. Therefore, these data support that PapX and FocX function as repressors of motility, and that this mechanism is dependent on the presence of the PapX binding site upstream of *flhDC*.

To determine if the reduction in motility following overexpression of *focX* or *papX* was a result of decreased expression of flagellar genes, we used qPCR to assess the gene expression of *flhD*, *fliA*, and *fliC* in the double Δ*focX*Δ*papX* mutant carrying pLX3607, pLX-*papX*, or pLX-*focX*. We assessed flagellar gene expression in the double mutant background, versus wild type, to eliminate any interference due to native levels of PapX and FocX. RNA was collected from bacteria cultured to an OD_{600} of 0.3 in tryptone medium. We found that expression of either *papX* or *focX*, compared to the empty vector, resulted in a comparable decrease in the transcription of *flhD*, *fliA*, and *fliC* **(Figure 3.4B)**. To verify that our qPCR data correlated with a decrease in flagellum production, we performed an immunoblot for FliC using Δ*focX*Δ*papX* carrying pLX3607, pLX-*focX*, or pLX-*papX*. Bacteria were cultured in tryptone medium, and whole cell lysates were collected at 0.5, 1.5, 3, and 6 hours and normalized by OD_{600}. We observed that overexpression of either *focX* or *papX* resulted in a decrease in FliC production at all collected time points compared to the empty vector **(Figure 3.4C)**. These data support that both FocX and PapX when ectopically expressed can repress *flhD*, resulting in decreased flagellar production and motility.

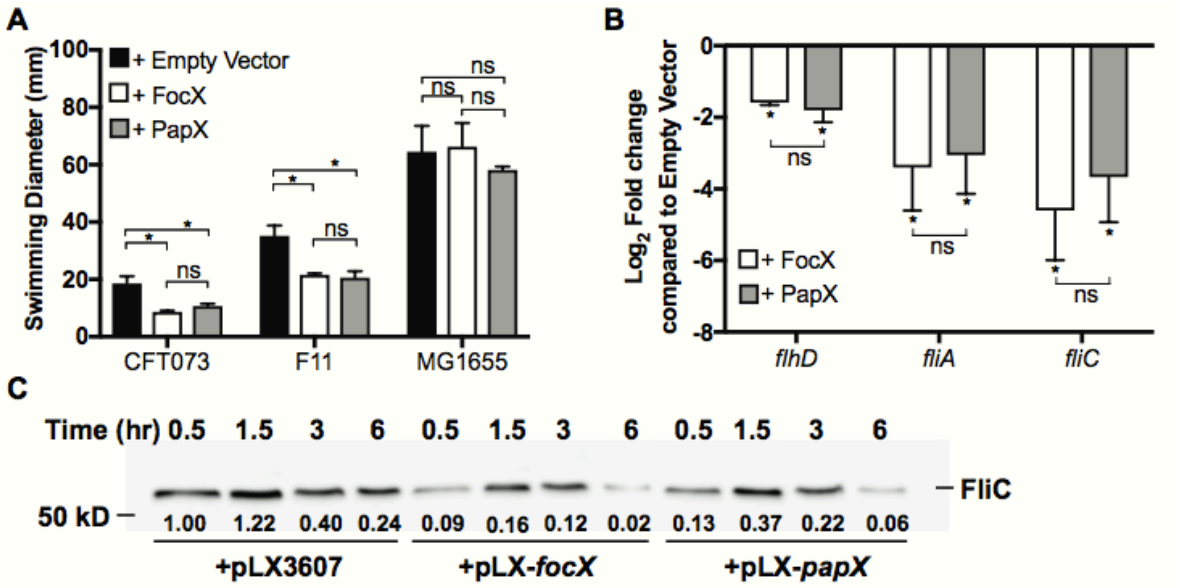

Figure 3.4 Expression of either *focX* or *papX* represses flagellar gene expression and motility

(A) Bars represent the average diameter (mm) of swimming motility of bacteria following 16-18 hr incubation at 30°C. Data represent five biological replicates with the error bars showing the standard deviation. Tukey's multiple comparisons test following ANOVA was used for statistical analysis. *, $P < 0.05$; ns (not significant) **(B)** qPCR of flagellar genes *flhD*, *fliA*, and *fliC* using cDNA synthesized from mRNA collected from *E. coli* CFT073 Δ*papX*Δ*focX* carrying pLX3607, pLX-*focX*, or pLX-*papX* cultured in tryptone media until OD_{600} of 0.3. Data represent the average of three experiments with standard deviation. A Student's *t*-test was used for statistical analysis **(C)** Immunoblot detecting FliC levels from whole cell lysates in CFT073 wild type carrying pLX3607, pLX-*focX*, or pLX-*papX*. Relative quantification of FliC was obtained using Image Lab 5.2.1 and represents the average fold-change of two independent experiments compared to FliC levels of Δ*papX*Δ*focX* +pLX3607 at 0.5 and normalized to a conserved non-specific band.

***focX* and *papX* are transcribed from a proximal promoter.**

We have previously shown that *papX* is transcribed as part of the *pap* operon and have confirmed that *focX* is also transcribed as part of the *foc* operon **(Figure 3.5)** (176). However, the *papX* homolog, *sfaX*, is transcribed as part of the *sfa* operon as well as from an independent proximal promoter (276). Since the upstream DNA sequences of *papX*, *focX*, and *sfaX* share high sequence identity, *papX* and *focX* likely share a similar proximal promoter. We used 5' Rapid Amplification of cDNA Ends (RACE) to map the transcriptional start sites of both *papX* and *focX* to an adenosine residue located 144 bp upstream of their predicted ATG start codon **(Figure 3.6)**. We manually identified a putative -10 and -35 region separated by a 19 bp spacer that resembles the consensus sequence of a bacterial σ^{70} promoter. This site was shared between *papX* and *focX* but was located 44 bp upstream of the transcriptional start site identified for *sfaX* (276). The presence of an additional proximal promoter upstream of *focX* and *papX* suggests that these genes can both be transcribed independently and from their associated fimbrial operons.

Expression of *papX* or *focX* trends with the expression of the preceding fimbrial operon.

Since *focX* and *papX* may be also transcribed from an independent proximal promoter, we investigated the expression of *focX* and *papX* compared to the *foc* and *pap* operons, respectively, under different environmental conditions. Previous work by Hancock *et al*. determined that the *pap* and *foc* genes are upregulated in CFT073 during planktonic growth in human urine compared to MOPS, but the expression of *focX* or *papX* was not investigated (277). Therefore, we used qPCR to quantify the expression of *papA*, *papX*, *focA*, *focX,* and *fliC* in CFT073 wild type during culture to mid-logarithmic growth in pooled human urine compared to LB medium. We included *fliC* to assess correlations between *focX* and *papX* with motility under these growth conditions. We found that culture in human urine compared to LB medium led to a

significant increase in the transcription of *focA* (Log_2 FC: 2.8) and *papX* (Log_2 FC: 1.3), but we did not detect a statistically significant change in *focX* or *papA* **(Figure 3.7A)**. Additionally, we observed a decrease in *fliC* expression (Log_2 FC: -5.48), and this finding was consistent with previous work showing decreased motility in UPEC strains when cultured in human urine (150)

Additionally, previous studies have shown that the production of P fimbriae is elevated in the *E. coli* CFT073 strain when cultured on LB agar plates compared to planktonic growth (209). Therefore, we assessed the expression of *papA*, *papX*, *focA*, *focX,* and *fliC* by qPCR following 24 hr incubation on LB agar plates at 37°C compared to culture in LB medium to mid-logarithmic growth. Consistent with previous findings, we observed that expression of *papA* (Log_2 FC: 2.7) and *papX* (Log_2 FC: 1.5) was significantly increased but did not observe a change in the expression of *focA* and *focX* **(Figure 3.7B)**. Additionally, *fliC* expression was decreased (Log_2 FC: 2.8) following incubation on LB agar plates.

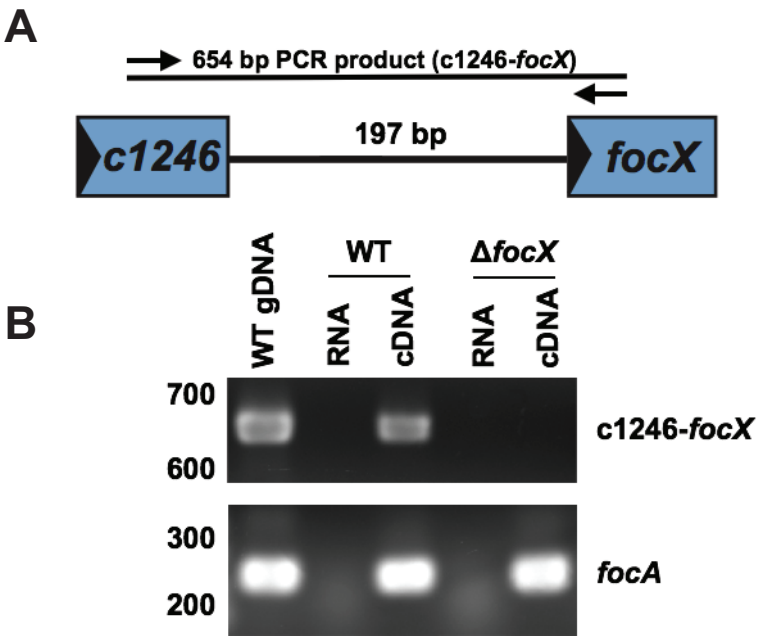

Figure 3.5 *focX* is transcribed as part of the *foc* operon
(A) Schematic of the c1246 and *focX* genes in the *foc* operon of CFT073. *focX* is 196 bp downstream of the c1246 allele. **(B)** PCR using Taq polymerase was performed to determine whether *focX* is transcribed with c1246. Arrows indicate the location of the primers (c1246-Fpcr/focX-Rpcr) used to PCR amplify a 654 bp product (c1246-*focX*). Additional primers (papA-Fpcr/papA-Rpcr) were included that amplified a 240 bp product from *focA*, which is included as a positive control confirming cDNA synthesis. CFT073 gDNA acts a positive control, and extracted RNA samples from CFT073 wild type and Δ*focX* were DNase treated and serve as a negative control for contaminating gDNA.

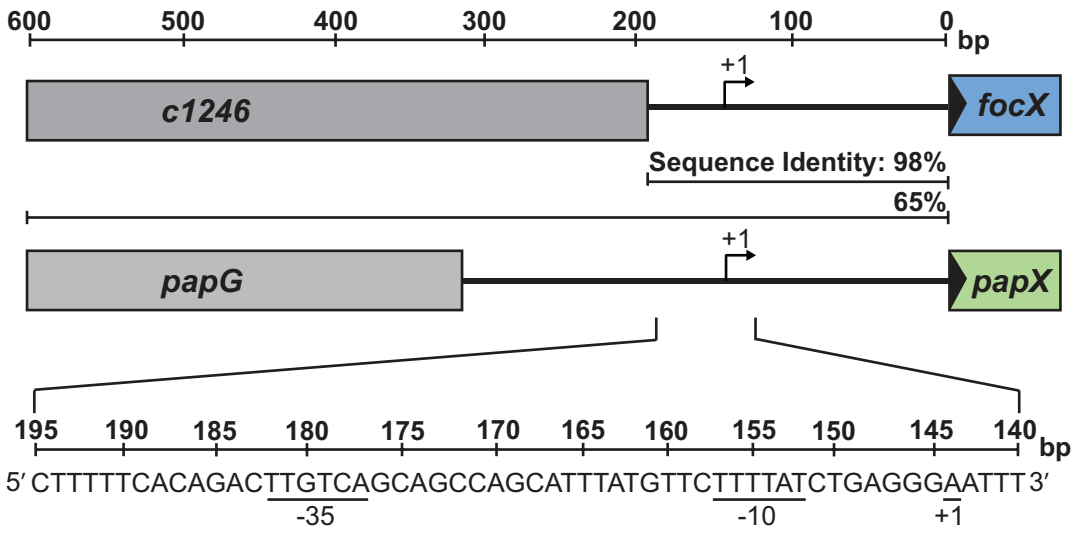

Figure 3.6 *focX* and *papX* are transcribed from a proximal promoter
Schematic of the transcriptional start sites of focX and papX identified using 5'RACE on cDNA synthesized from mRNA collected from either Δ*papX* or ΔfocX, followed by DNA sequencing. Putative -10 and -35 sites with similarity to the bacterial σ70 promoter are underlined. A 144-bp distance between the ATG translational start site of *focX* or *papX* and the transcription start site (+1) is indicated above the figure.

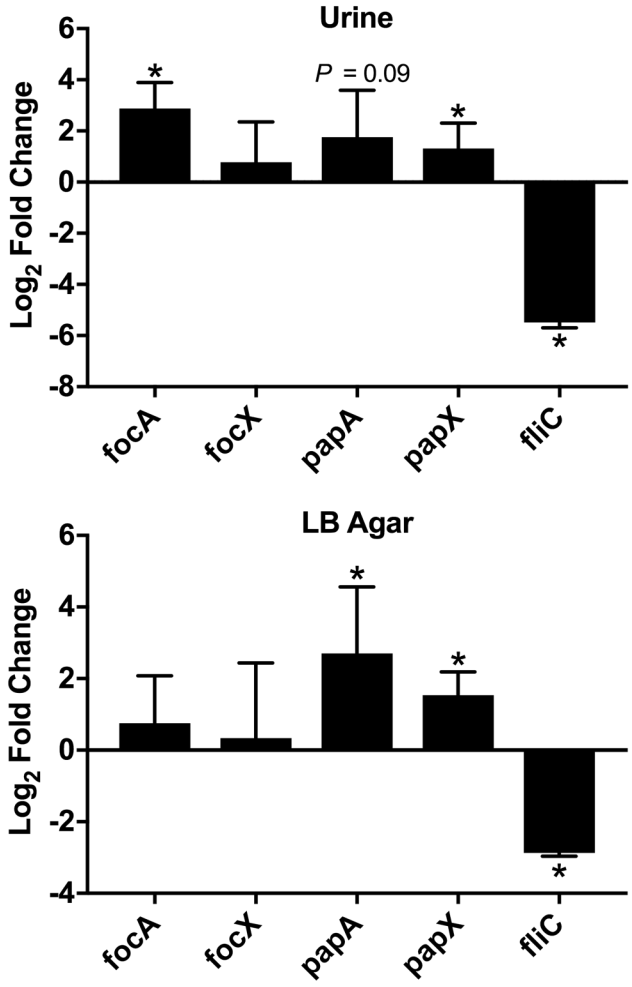

Figure 3.7 Expression of *foc*, *pap*, and *fliC* when cultured in human urine or on LB agar qPCR of *focA*, *focX*, *papA*, *papX*, and *fliC* using cDNA collected from *E. coli* CFT073 wild type cultured in human urine **(Top)** until OD_{600} of 0.3 or on LB agar **(Bottom)** for 24 hr compared to cDNA collected from bacteria cultured to mid-logarithmic growth in LB medium. Data represent the average of three experiments with error bars showing standard deviation. A Student's *t*-test was used to calculate statistical significance. *, $p < 0.05$

FocX functions as a repressor of *papX*.

We have previously shown in CFT073 that the deletion of *papX* does not affect the production of P fimbriae; however, the effect of FocX on the expression of genes within the *foc* operon has not been characterized (176). Therefore, we performed qPCR to assess the changes in gene expression of *focA, focX, papA* and *papX* following the deletion of either *focX* or *papX*. cDNA was synthesized from mRNA collected from CFT073 wild type and the Δ*focX* and Δ*papX* constructs cultured to mid-logarithmic growth in tryptone medium. We found that the deletion of *focX* did not affect *focA* or *papA* expression, but did result in higher expression of *papX* (Log_2 FC: 2.06) **(Figure 3.8A)**. In contrast, deletion of *papX* did not result in any significant changes in the gene expression of *focA*, *focX*, or *papA*. These data suggest that FocX functions as a repressor of *papX* and that the regulatory mechanism is not a result of decreased expression of the *pap* operon. Therefore, FocX may bind to a DNA site upstream of *papX* and affect transcription of the proximal *papX* promoter. However, we did not identify a DNA sequence upstream of either *focX* or *papX* that matched with the PapX binding site characterized upstream of *flhDC*, suggesting that regulation of *papX* by FocX may be indirect or occurs through a degenerate DNA binding site (169).

We also assessed the changes in the gene expression of *focA, focX, papA*, and *papX* in CFT073 when either *focX* or *papX* was ectopically expressed. cDNA was synthesized from mRNA collected from CFT073 harboring pLX3607, pLX-*focX*, or pLX-*papX* cultured to mid-logarithmic growth in tryptone medium. We found that the production of FocX did not affect the expression of *focA, papA,* or *papX* **(Figure 3.8B)**. Similarly, production of PapX did not impact the expression of *focA, focX*, or *papA*. Therefore, the function of FocX as a repressor of *papX*

may be dependent on protein concentration, as we did not observe a decrease in *papX* expression in response to increased *focX* transcription.

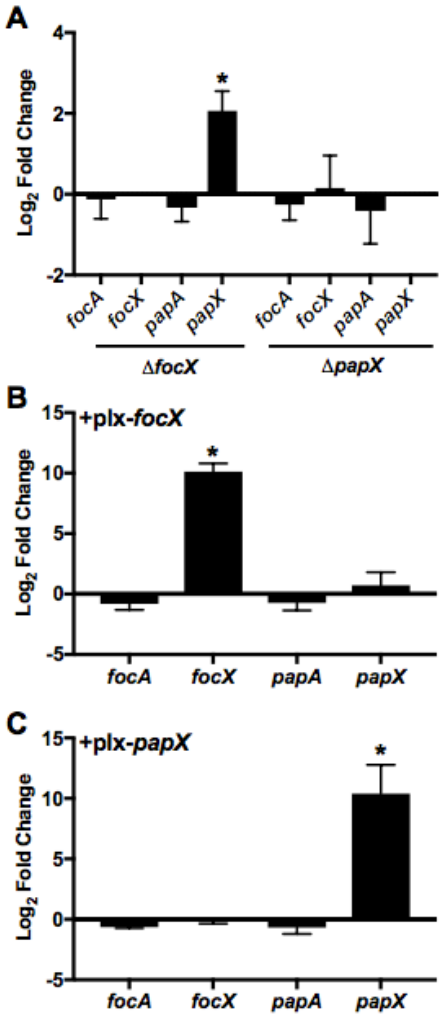

Figure 3.8 Loss of *focX* results in elevated *papX* expression
qPCR was performed to calculate the average (N=3) Log_2 fold change of mRNA abundance of *focA*, *focX*, *papA* and *papX* using cDNA collected from *E. coli* **(A)** CFT073 wild type, Δ*focX*, or Δ*papX* or wild type carrying pLX3607, **(B)** pLX-*focX*, or **(C)** pLX-*papX* cultured in tryptone media until an OD_{600} of 0.3. Error is shown as standard deviation, and statistical significance was calculated using Student's *t*-test, *, $p < 0.05$.

***papX* provides a subtle fitness advantage in colonization of the kidneys during murine UTI**

While P fimbriae have been shown to promote colonization of the kidneys during murine UTI, *papX* has not been confirmed as a fitness factor during *in vivo* infection (278, 279). Instead, PapX has been hypothesized to negatively impact colonization during UTI as a Δ*papX* mutant showed a slight increase in kidney colonization compared to wild type CFT073 during an experimental cochallenge in transurethrally-inoculated CBA/J mice (176). However, the contribution of PapX during an ascending UTI may be more observable following intraurethral inoculation, since transurethral inoculation places a high number of bacteria directly into the bladder and increases the occurrence of vesicoureteral reflux into the kidneys in the murine model (280). Indeed, previous work by Lane *et al.* demonstrated flagella as a fitness factor for colonization of the bladder and kidneys through independent infections in CBA/J mice between wild type CFT073 and a Δ*fliC* mutant following intraurethral inoculation (100, 101). Therefore to assess the contribution of *papX* to *in vivo* colonization, we performed an independent infection of CBA/J mice intraurethrally-inoculated with either CFT073 wild type or the Δ*papX* mutant. Mice were sacrificed at 24 and 48 hrs and the bladder, kidneys and spleen were homogenized and plated to enumerate bacterial load. We did not observe any significant differences between wild type and the Δ*papX* mutant in colonization of the bladder, kidneys, or spleen after either 24 or 48 hrs **(Figure 3.9A and Figure 3.9B)**. While we did observe high levels of colonization of three spleens infected with the Δ*papX* mutant, due to limited replicates we did not have sufficient statistical power to make any conclusions about the role of *papX* in dissemination.

In some cases, a co-challenge model has been shown to be more sensitive than independent challenge for the detection of subtle fitness defects during UTI (225). Thus to measure relative fitness, CBA/J mice were intraurethrally-inoculated with a 1:1 ratio of CFT073

wild type and the Δ*papX* mutant. We did not observe any statistically significant differences between wild type and Δ*papX* in colonization of the bladder, kidneys, or spleen after either 24 or 48 hrs **(Figure 3.9C)**. However, the Δ*papX* mutant had a slight decrease in colonization of the kidneys after 24 hrs (P = .063).

It is possible that FocX can compensate for PapX during UTI and thereby mask fitness defects of the Δ*papX* mutant during infection. Therefore, we performed a cochallenge infection in CBA/J mice transurethrally-inoculated with a 1:1 ratio of CFT073 wild type and the double Δ*focX*Δ*papX* mutant. Mice were sacrificed at 48 hrs and the bladder, kidneys and spleen were homogenized and plated to enumerate bacterial load. We did not observe any fitness defect in colonization of the bladder or spleen, but did observe a subtle, but not statistically significant, decrease in colonization of the kidneys (P = .061) **(Figure 3.9D)**.

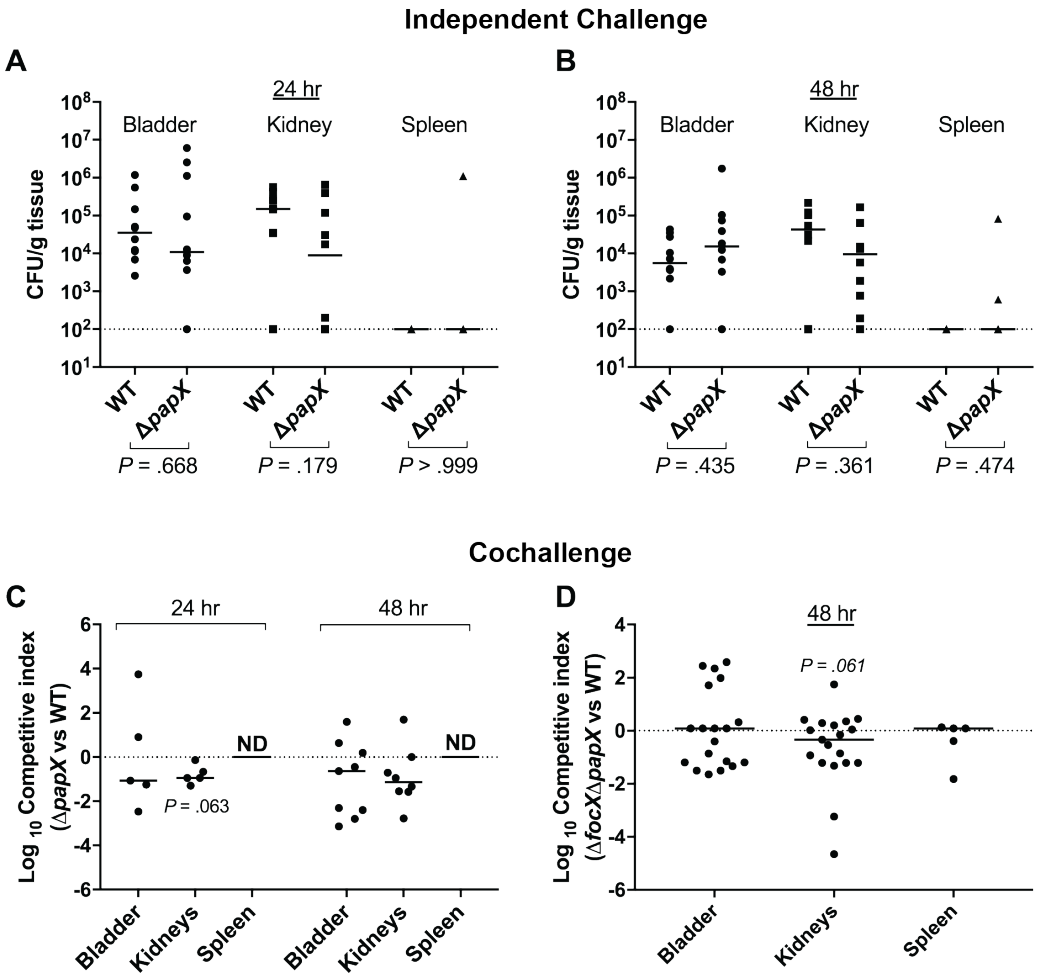

Figure 3.9 The contribution of PapX to *in vivo* colonization is subtle and only observable following intraurethral inoculation

Independent challenges of CBA/J mice (N=10) inoculated with a 10-µl suspension of 10^7 cfu/ml of either wild type CFT073 or Δ*papX* directly into the urethra. Mice were sacrificed at either 24 **(A)** or 48 **(B)** hrs post inoculation (hpi), and the bladders, kidneys, and spleens were homogenized and plated to enumerate bacterial load and presented as cfu/g of tissue. **(C)** Cochallenge infection of mice (N=10) using a 1:1 mixture of wild type and Δ*papX* mutant. CBA/J mice were intraurethrally inoculated with a 10-µl suspension of a total 10^7 cfu/ml. Mice were sacrificed at either 24 (N=5) or 48 (N=10) hpi, and the bladders, kidneys, and spleens were homogenized and plated to enumerate bacterial load. Relative fitness is presented as a competitive index. **(D)** Cochallenge infection of mice (N=20) using a 1:1 mixture of wild type and *ΔfocXΔpapX*. Mice were transurethrally inoculated with a 50-µL suspension of total 10^8 cfu/mL. Relative fitness after 48hpi is presented as a competitive index. Horizontal bars represent the median values of the populations, and the dotted line represents the limit of detection (2 x 10^2 cfu/g). Statistical differences in colonization were determined using a Wilcoxon signed-rank test. *, $P < 0.05$

Discussion

UPEC rely on flagella and fimbriae to successfully ascend and colonize the diverse niches within the urinary tract (102, 103). Yet, it is not practical for a bacterium to be both motile and adherent simultaneously. Thus, UPEC isolates likely possess mechanisms that mediate a rapid transition between adherent and motile states in response to environmental signals during UTI. One such mechanism is through the MarR-like protein, PapX, which is encoded as part of the *pap* operon and functions as a transcriptional repressor of the flagellar master regulator *flhDC* (169, 170, 176). PapX is a representative member for various 17-kDa MarR-like proteins encoded within fimbrial operons that have been identified in *E. coli*, and raises the notion that harboring multiple MarR-like "X" proteins may result in cooperative regulation of motility(169). Hence, the study of PapX and its homologs is central to our understanding of UPEC ascension and colonization of the urinary tract.

In this study, we investigated the regulation of *focX* and *papX* gene expression and characterized the effect of encoding multiple PapX homologs on motility. We found that ectopic expression of *focX* or *papX* resulted in comparable inhibition of motility that corresponded with decreased *flhD, fliA* and *fliC* gene expression and reduced FliC production. Therefore, FocX and PapX share the same function as repressors of motility. However, we found that in general expression of *focX* and *papX* mimicked the expression of their preceding fimbrial operons during *in vitro* culture on LB agar plates as elevated expression of *papA* was paralleled by an increase in *papX* expression.

In *E. coli*, a single bacterium typically expresses one dominant fimbrial type, and since *focX* and *papX* are encoded within different fimbrial operons, they are likely expressed at different times (178, 216). Therefore, strains encoding multiple "X" proteins may be better suited

to rapidly repress motility in response to a range of niche-specific cues. Since both P and F1C fimbriae mediate adherence to renal cells, the function of PapX may be particularly important during kidney colonization (182, 265). We predicted that the production of PapX improves the success of *in vivo* attachment of bacteria to the renal epithelium by decreasing interference from swimming motility. Also, reducing flagella production likely allows bacteria to better evade host defenses, as the monomeric flagellum subunit, FliC, is recognized by TLR5 found on host epithelial cells, leading to the rapid recruitment of neutrophils, inflammation, and bacterial clearance (88, 107) However, we observed during co-challenge in the murine model of ascending UTI that an isogenic Δ*papX* mutant had only a slight decrease in colonization of kidneys ($P < 0.06$). Additionally, while we predict that FocX shares the same function as PapX, deletion of both "X" genes did not substantially affect kidney colonization ($P < 0.06$) and evaluation of the relative fitness of the double Δ*focX*Δ*papX* mutant instead by intraurethral inoculation may demonstrate a greater effect on colonization. Since there are few studies in the literature exploring the effects of hypermotility on kidney colonization during UTI, further investigation of the function of "X" genes during infection would broaden our understanding of the role of motility in the development of pyelonephritis. Indeed, another "X" genes, *vatX*, has also been identified in strain CFT073 (281). While VatX share 44% amino acid identity with PapX, neither mutation nor overexpression of *vatX* impacted motility of CFT073 (282).

In this study we also identified a conserved transcriptional start site located 144-bp upstream of the ATG start codon of both *focX* and *papX*, suggesting that *focX* and *papX* can also be regulated independently of their fimbrial operon. A similar transcriptional schema has also been observed for the *papX* homolog, *sfaX*, which is transcribed from an independent promoter in addition to being expressed by the *sfa* operon, encoding S fimbriae (276). Thus, dual

transcription from two promoters appears to be a conserved regulatory feature of MarR-like proteins encoded within fimbrial operons. Interestingly, the transcriptional start site of *sfaX* was located 44 bp downstream from the start site identified for *focX* and *papX.* In the case of *papX* and *focX*, regulation from an independent promoter may allow for control over flagellar gene expression while independently preserving appropriate regulation of fimbriae production, allowing for fine-tuned transitions in the regulation of adherence and motility factors during ascension from the bladder to the kidneys.

Additionally, an independent proximal promoter may also serve as a site for cross-talk between "X" genes or other transcription factors. Genes encoding MarR-like proteins are commonly autoregulated, where increased protein production creates a negative feedback loop that inhibits transcription (171, 283). We observed that FocX functions as a repressor of *papX*, and this regulation likely occurs at the proximal independent promoter of *papX* as we did not observe any changes in the expression of the rest of the *pap* operon. Since FocX and PapX share the same function, we predict that PapX is capable of autoregulation, however future studies are needed to confirm this regulatory mechanism. We did not observe that PapX repressed expression of *focX*, and it is not clear if a required regulatory element is absent from the *focX* promoter or if expression is better observed under a different condition. Thus, cross-talk between *focX* and *papX* may serve as a mechanism to limit negative consequences of extended repression of motility due to excessive "X" protein production.

Regardless, maintenance of "X" protein levels appears to be critical for the mechanism behind repression of motility by PapX and FocX, as we observed in our swimming motility assays that the deletion of *focX* had no effect on motility, while the double Δ*focXpapX* mutant had an intermediate motility phenotype compared to the hypermotile Δ*papX* mutant. We propose

that increased levels of PapX in the *focX* mutant may compensate for the loss of *focX* and thus result in a similar degree of motility compared to wild type. However, in the double mutant it may be that the loss of both *focX* and *papX* affects the recruitment of a transcriptional activator of *flhD* or allows another regulator of *flhDC* expression to partially compensate for the absence of "X" proteins, resulting in an intermediate motility phenotype. The mechanism of PapX and FocX regulation of *flhDC* is not clearly defined. The PapX binding site upstream of *flhDC* does not overlap with binding sites of other characterized transcription factors and the impact of PapX binding within the *flhDC* promoter on DNA bending and promoter access for other regulators of *flhDC* is not well characterized (76, 169, 284). Thus, it may be that the binding of FocX or PapX interferes with DNA access within the *flhDC* promoter for other regulatory elements, including other transcription factors and DNA insertion elements. The complex interplay of regulators of *flhDC* expression emphasizes the lengths that bacteria employ to control motility, and in the context of UTIs, MarR-like "X" proteins may provide a mechanism to mediate fine-tune coordinated transitions between motility and adherence allowing for better evasion of the host immune systems and improved colonization of the upper urinary tract.

Materials and Methods

Bacterial strains and culture conditions.

Strains used in this study are listed in **Table 3.1**. Unless otherwise noted, bacteria were cultured in LB medium (10 g Tryptone, 5 g Yeast extract, 0.5 g NaCl / 1 L) at 37°C with aeration. UPEC strain CFT073 was isolated from the blood and urine of a patient hospitalized with acute pyelonephritis, and strains F11 and HM27 were isolated from the urine of women experiencing cystitis (206, 246, 285). Human urine was collected from at least three women,

pooled, filter-sterilized and stored at -20°C in accordance with the University of Michigan Institutional Review Board (HUM00004949). When necessary, antibiotics were added at the following concentrations: ampicillin (100 μg/mL), kanamycin (25 μg/mL), and chloramphenicol (20 μg/mL).

Table 3.1. Bacterial strains and plasmids used in this study

Strain	**Genotype/Resistance/Use**[a]	**Source**
CFT073	Pyelonephritis isolate (O6:K2:H1)	[Mobley, 1990]
ΔfocX	CFT073 *ΔfocX::cat* (Cam^R)	This Study
ΔpapX	CFT073 *ΔpapX::kan* (Kan^R)	(176)
ΔfocXΔpapX	CFT073 *ΔfocX::cat ΔpapX::kan* (Cam^R, Kan^R)	This Study
E. coli F11	Cystitis isolate (O6:K2:H31)	(206)
E. coli F11 *ΔpapX*	F11 *ΔpapX::kan* (Kan^R)	This Study
E. coli HM69	Cystitis isolate	(65)
E. coli HM69 *ΔpapX*	HM69 *ΔpapX::kan* (Kan^R)	This Study
Top10 *E. coli*	Used for cloning	ThermoFisher Scientific
Plasmid	**Relevant Characteristics**	**References**
pLX3607	IPTG-inducible vector (Amp^R)	(170)
pLX-*focX*	pLX3607+*focX* (Amp^R)	This Study
pLX-*papX*	pLX3607+*papX,* also known as pDRM001 (Amp^R)	(170)
pKD4	Vector carrying a FRT-flanked *kan* gene (Amp^R, Kan^R)	(286)
pKD3	Vector carrying a FRT-flanked *cat* gene (Amp^R, Cam^R)	(286)
pKD46	Vector carrying phage λ Red recombinase (Amp^R)	(286)

a: cam-chloramphenicol, kan-kanamycin, amp-ampicillin, R-resistant

Mutant and plasmid construction

The primers used in our study are listed in **Table D.2**. The Δ*papX* mutant was constructed previously (273). Lambda Red-mediated recombineering was used to construct the Δ*focX* and Δ*focXpapX* mutants. In brief, the chloramphenicol resistance gene (*cat*) was amplified from pKD4 by PCR using EasyA polymerase (Agilent) and the primers focXKO-F/focXKO-R and then transformed into competent CFT073 carrying pKD46 harboring the Lambda *red* operon. Transformed bacteria were cultured at 30°C for 2.5 hrs, plated on LB agar containing chloramphenicol, and cultured overnight at 37°C. The resulting colonies were screened by PCR using Taq polymerase (New England BioLabs) and the primers scrnF/scrnR for deletion of *focX*. The same strategy was used to construct the Δ*papX* mutants in *E. coli* F11 and HM69 but the kanamycin resistance gene (*kan*) was instead amplified from pKD3 for transformation.

To construct the double Δ*focXpapX* mutant, the primers KO-F/KO-R, which have homology to both *papX* and *focX*, were used with EasyA polymerase to PCR amplify the *cat* gene from pKD3. The resulting PCR product was transformed into competent CFT073 carrying pKD46. Colonies were screened by PCR using Taq polymerase and the primers scrnF/scrnR to verify deletion of either *focX* or *papX.* To remove the second "X" gene, the kanamycin resistance gene was PCR amplified from pKD4 using the primers KO-F2/KO-R2, which flank the first set of primers, and transformed into the competent single mutant strain carrying pKD46. The primers scrnF2/scrnR2 were used with Taq polymerase to screen for deletion of the second "X" gene, and the deletion of both *focX* and *papX* was verified by DNA sequencing.

To induce expression of *papX*, we previously cloned *papX* into the vector pLX3607 under the control of an IPTG-inducible promoter, referred to as pLX-*papX* (170). A similar strategy was used to control the expression of *focX*. In brief, *focX* was amplified by PCR using

EasyA polymerase and the primers focplx-F/focplx-R from CFT073 Δ*papX*. The resulting PCR product and pLX3607 were both digested by NcoI and HindIII, ligated together using T4 DNA Ligase (New England BioLabs) to generate pLX-*focX*, and transformed into competent Top10 *E. coli*. Transformants were plated on LB with ampicillin and the resulting colonies were screened by PCR to verify plasmid construction. pLX-*focX* was obtained using a miniprep kit (Qiagen) from overnight cultures of Top10 *E. coli* and transformed into CFT073. We relied on leaky expression for induction of *papX* and *focX* from pLX-*papX* and pLX-*focX*, respectively.

Swimming Motility Assay

Overnight stationary cultures were diluted to an OD_{600} of 1.0 and stab-inoculated into 0.025% agar motility plates (10 g Tryptone, 5 g NaCl, 1.25 g Agar / L). Plates were incubated for 16-18 hrs at 30°C, and the diameter of bacterial spread was averaged as a quantification of swimming motility. Tukey's multiple comparisons test following ANOVA was used for statistical analysis with the error bars representing the standard deviation.

qPCR

Stationary cultures were diluted 1:100 into 25 mL of either LB medium, tryptone medium (10g Tryptone, 5g NaCl / L), or sterilized pooled human urine with ampicillin when needed for plasmid maintenance. Strains were cultured at 37°C with aeration until mid-logarithmic growth was reached, and then an aliquot was collected for RNA extraction and treated with a stop solution (95% EtOH, 5% phenol) to preserve RNA stability. RNA was also collected from bacteria that were plated on LB agar and incubated at 37°C for 24hr. Plated bacteria were resuspended in 1x PBS (137 mM NaCL, 2.7 mM KCl, 4.3 mM Na_2HPO_4, 1.47 mM KH_2PO_4 /

1L, pH 7.4) and treated with the stop solution. For RNA extraction, bacterial cells were lysed using 1 mg/mL of lysozyme, and RNA was purified using the RNeasy kit (Qiagen) following the manufacturer's guidelines. RNA samples were treated with DNaseI (Ambion), and the removal of genomic DNA was confirmed by PCR using Taq polymerase and the primers gapA-F/gapA-R. RNA was converted to cDNA using SuperscriptIII (Invitrogen) and purified using the PCR cleanup kit (Epoch Life Science). qPCR was conducted using PowerUP SYBR Green (Invitrogen), 4ng of total cDNA as template, and the primers listed in Table S2. CT values were normalized to *gapA*, a housekeeping gene, and analyzed using the ΔΔCT method (287). Data are shown as the $\log_2$ fold change (FC) of three biological replicates. A Student's *t*-test was used for statistical analysis.

Immunoblot for FliC detection

Production of FliC was determined by immunoblot using standardized whole cell lysates using a previously described method (273). Stationary bacterial cultures were diluted 1:100 in 20 mL of Tryptone medium and cultured at 37°C with aeration. Samples were taken at 0.5, 1.5, 3 and 6 hrs, centrifuged at 1500 rpm for 10 min to limit the shearing of flagellum, suspended in 2x SDS loading buffer (100 mM Tris-CL (pH 6.8), 4% SDS, 0.2% bromophenol blue, 20% glycerol, 200 mM DTT) and boiled for 10 min at 95°C. Whole cell lysates were normalized by OD_{600} and electrophoresed on a 10% SDS-polyacrylamide gel followed by transfer to a polyvinylidene difluoride membrane (Immobilon-P; Millipore Corp.). The blot was incubated with 1:10,000 dilution of rabbit polyclonal antiserum to H1 flagella (Statens Serum Institute, Copenhagen, Denmark) followed by secondary incubation with 1:20,000 dilution of peroxidase-conjugated goat anti-rabbit immunoglobulin G (Sigma). The Clarity Western ECL Substrate kit

(BioRad) was used to develop the blot.

5' Rapid Amplification of cDNA Ends (RACE)

Overnight cultures of Δ*papX* and Δ*focX* strains were diluted 1:100 in LB medium and cultured at 37°C to mid-logarithmic growth. An aliquot was collected for RNA extraction and treated with a stop solution (95% EtOH, 5% phenol) to preserve RNA stability. To determine the transcription start site of *papX* and *focX*, we used the 5' Rapid Amplification of cDNA Ends (RACE) kit (Invitrogen) following the Manufacturer's guidelines and the primers are listed in Table S2. cDNA was inserted in pCR2.1-TOPO via the TOPO TA cloning kit (Invitrogen) and transformed into competent Top10 *E. coli*. Transformants were plated on LB with ampicillin and plasmids were isolated by miniprep and sequenced to determine the *papX* and *focX* transcription initiation sites.

Co-challenge and independent infections in the murine model of UTI

Six-to eight-week-old female CBA/J mice (Jackson Laboratories) were infected as previously described (101, 199, 214). Briefly, bacteria were grown to stationary phase in LB medium, and then to induce motility, were diluted 1:50 in fresh LB medium and cultured with aeration at 37°C until an OD_{600} of ~0.3 was reached. Bacteria were harvested by centrifugation (1500 RPM), resuspended in sterile PBS, and adjusted by OD to a final total concentration of 10^7 CFU/mL. For independent intraurethral infections between *E. coli* CFT073 and Δ*papX*, mice were inoculated over a 6 second period with a low-dose inoculum (10 µl of 10^7 CFU/mL) of each strain into the proximal end of the urethra. For cochallenge infections, mice were inoculated

intraurethrally (10 μL of 10^7 CFU/mL) with a 1:1 mixture of wild type and Δ*papX* for cochallenge infection.

A transurethral infection model was used for cochallenge infections between *E. coli* CFT073 and the Δ*focX*Δ*papX* construct. Bacteria were grown to stationary phase in LB medium, and then harvested by centrifugation (4000 RPM), resuspended in sterile PBS, and adjusted by OD to a final total concentration of 10^8 CFU/mL. Mice were transurethrally inoculated (50 μl of 10^8 CFU/mL) with a 1:1 mixture of wild type and the Δ*focX*Δ*papX* mutant. Dilutions of the initial inoculums were plated to verify input CFU/mL.

For all infections, after either 24 and/or 48 hrs post inoculation, mice were sacrificed and the bladder, kidneys and spleen were removed, homogenized in PBS (GLH homogenizer, OMNI International), and plated onto LB agar using an Autoplate 400 spiral plater (Spiral Biotech). Bacterial counts were enumerated using a QCount automated plate counter (Spiral Biotech) to determine the output CFU/g of tissue. Competitive indices (CI) were calculated as the ratio of mutant to wild type in the output over the ratio of mutant to wild type in the input inoculum. Statistically significant differences were determined using a Wilcoxon signed-rank test. All animal protocols were approved by the Institutional Animal Care and Use Committee (IACUC) at the University of Michigan (PRO00007111).

Chapter IV - TosR-mediated regulation of adhesins and biofilm formation in uropathogenic *Escherichia coli*

Notes

This chapter was reprinted and modified with permission from the authors Luterbach, C.L., Forsyth, V.S., Engstrom, M.D., and Mobley, H.L.T. TosR-mediated regulation of adhesins and biofilm formation in uropathogenic *Escherichia coli. mSphere,* 2018.

Abstract

Uropathogenic *Escherichia coli* utilize a variety of adherence factors that assist in colonization of the host urinary tract. TosA (type one secretion) is a non-fimbrial adhesin that is predominately expressed during murine urinary tract infection (UTI), binds to kidney epithelial cells, and promotes survival during invasive infections. The *tosRCBDAEF* operon encodes the secretory machinery necessary for TosA localization to the *E. coli* cell surface, as well as the transcriptional regulator TosR. TosR binds upstream of the *tos* operon and, in a concentration dependent manner, either induces or represses *tosA* expression. TosR is a member of the PapB family of fimbrial regulators that can participate in cross-talk between fimbrial operons. TosR also binds upstream of the pap operon and suppresses PapA production. However, the scope of TosR-mediated cross-talk is understudied and may be underestimated. To quantify the global effects of TosR-mediated regulation on the *E. coli* CFT073 genome, we induced expression of *tosR*, collected mRNA, and performed RNA-Seq. These findings show that production of TosR

affected the expression of genes involved with adhesins including P, F1C, and Auf, nitrate/nitrite transport, microcin secretion, and biofilm formation.

Importance

Uropathogenic *E. coli* cause the majority of UTIs, which are the second most common bacterial infection in humans. During a UTI, bacteria adhere to cells within the urinary tract using a number of different fimbrial and non-fimbrial adhesins. Biofilms can also develop on the surfaces of catheters, resulting in complications such as blockage. In this work, we further characterized the regulator TosR, which links both adhesin production and biofilm formation and likely plays a crucial function during UTI and disseminated infection.

Introduction

Uropathogenic *Escherichia coli* (UPEC) are the primary cause of uncomplicated urinary tract infections (UTIs), a widespread public health issue with approximately half of all women and one-fifth of men experiencing at least one UTI in their lifetime (261, 288). Most uncomplicated UTIs arise when bacteria from the intestine contaminate the periurethral area, traverse the urethra and colonize the bladder, resulting in cystitis (43). In some cases, bacteria ascend the ureters and infect the kidneys, resulting in pyelonephritis. From the kidney, bacteria are capable of crossing the epithelial and endothelial barriers to spread via the bloodstream, which in severe cases can lead to urosepsis and death (289).

Compared to commensal *E. coli*, UPEC genomes encode numerous accessory genes, including adhesins, toxins, and siderophores, which provide a fitness advantage during colonization of the host urinary tract system (290-292). Many of these virulence genes reside on

large regions of horizontally acquired DNA, termed pathogenicity-associated islands (PAIs) (293, 294). Indeed, the pyelonephritis isolate CFT073 encodes 13 genomic islands (GIs) that account for nearly one-fifth of the genome (64, 285, 295). Of these GIs, seven have been confirmed as PAIs (62, 64, 294, 296). We have previously shown that PAI-*aspV* harbors the *tosRCBDAEF* operon, which encodes the repeat-in-toxin (RTX) family member TosA (62, 132). RTX protein family members are frequently encoded on large open reading frames and can perform a range of functions, including pore-forming, biofilm formation, and adherence to host cells (130, 297, 298).

TosA functions as an RTX non-fimbrial adhesin and can adhere to human kidney epithelial cells (132). Additionally, production of TosA occurs during both murine and human UTI, and a mutant lacking *tosA* was attenuated for colonization of the bladder and kidneys in the murine model of UTI (62, 131). TosCBD mediate production and export of TosA, while TosE and TosF have an unknown regulatory function associated with suppression of motility (132, 134). The *tos* operon is regulated by TosR and the global regulatory proteins H-NS and Lrp (133). Our laboratory has previously shown that TosR functions as both an activator and repressor of the *tos* operon (133, 134). We found that low levels of TosR correlate with increased TosA production, while high levels of TosR inhibit TosA production (133).

TosR is a member of the PapB family of transcriptional regulators, which includes the fimbrial-associated regulators PapB and FocB (134, 186, 209, 299, 300). PapB and FocB bind as oligomers to AT-rich DNA motifs to mediate positive and negative regulation of the *pap* and *foc* operons, which encode the UPEC-associated P and F1C fimbriae respectively (186, 299, 301). Pyelonephritis-associated pili, or Pap, bind Gal(α1-4)Gal moieties of the P-blood group-antigen located on kidney cells and erythrocytes (153, 302, 303). F1C fimbriae bind glycosphingolipids

found on kidney cells and also promote biofilm formation in the commensal *E. coli* isolate Nissle 1917 (182, 188, 304). Cross-regulation between fimbrial operons has been extensively studied. For example, PapB and FocB mediate the cross-talk between the *pap*, *foc*, and *fim* operons, the latter encoding type 1 fimbriae (137, 154, 163, 224, 299, 305). While PapB and FocB share over 80% amino acid sequence identity, they differ in their function as regulators of fimbrial operons. In particular, FocB is a positive regulator of the *pap* operon and a dual regulator of the *foc* operon; PapB is a dual regulator of the *pap* operon and a repressor of the *foc* operon; and both FocB and PapB are negative regulators of the *fim* operon (216, 224, 300, 301, 306).

TosR shares only 27.7% amino acid sequence identity with PapB, but may share a similar function in regulating fimbrial expression based on predicted structural homology (134). Indeed, we have previously shown that TosR binds upstream of the *pap* operon and suppresses PapA production, the major structural subunit of P fimbria (133). However, it is unclear if TosR regulates additional fimbrial genes, as observed with PapB and FocB, or additional non-fimbrial genes. Thus, the focus of this study was to further define TosR-mediated effects on gene expression, in particular on other adhesin genes, we ectopically expressed *tosR*, collected mRNA, and performed RNA sequencing (RNA-Seq). We discovered that TosR significantly affects gene expression of multiple functional gene categories including adhesins, biofilm formation, microcins, and nitrite/nitrate transport. Specifically, when *tosR* was overexpressed, we observed dramatic upregulation of the *auf* operon, encoding Auf fimbriae, and downregulation of the *pap* and *foc* operons. UPEC isolates are more likely to encode Auf fimbriae, and production of Auf fimbriae occurs *in vivo* during murine UTI (115, 139). We also observed that *tosR* overexpression led to increased Congo red and Calcofluor white binding and this phenotype was more robust in a mutant deficient in expression of the *auf* operon.

Additionally, we observed that induction of *tosR* increased biofilm formation in lysogeny broth (LB) and human urine. Thus, our study shows the depth of TosR-associated regulation in a global network connecting genes encoding adhesins and other biofilm promoting factors important in persistence and fitness during UTI (292, 307).

Results

Induction of *tosR* results in differential expression of both fimbrial and nonfimbrial genes

To identify genes affected by TosR, we performed RNA-Seq on mRNAs derived from *E. coli* CFT073 harboring either pBAD-*tosR*-His_6 or pBAD empty vector, because *tosR* is poorly expressed *in vitro* (132). Bacteria were cultured at 37°C in LB with aeration to mid-logarithmic growth, mRNAs were extracted and RNA-Seq was performed. RNA sequence reads ranged from 10-15 million per sample with 98.8-99.5% of these reads mapping to sequences in the reference *E. coli* CFT073 genome. Additionally, we excluded genes with variable or low expression by applying a cutoff requiring at least 3 of our counts per million (CPM) mapped reads for a given gene to be greater than 2. In total, overexpression of *tosR* resulted in the differential expression of 200 genes (123 upregulated and 77 downregulated) with a $\log_2$ fold change (FC) greater than or equal to ± 1.5. The top 25 genes upregulated and downregulated ($\log_2$ FC 10.1 to -6.2) in response to *tosR* overexpression are noted in **Table 4.1** and **Table 4.2**, respectively.

E. coli genetic diversity is often mediated by horizontal gene transfer of large GIs, which frequently carry genes with accessory functions that are advantageous for host colonization, pathogenesis or immune evasion (63, 64, 295, 308). The UPEC isolate CFT073 encodes 13 GIs with 7 being confirmed as PAIs (62, 64). We mapped the genomic location of genes differentially expressed following overproduction of TosR to determine whether these genes are

preferentially localized to GIs **(Figure 4.1)**. We found that a larger percentage of these genes, 68 out of 945 (7.2%), are located on GIs compared to the rest of the genome, 132 out of 4476 (2.9%) ($p<0.0001$; two-tailed Fisher's exact test). In CFT073, the majority of GIs differ in G+C content compared to the rest of the genome (50.5%)(64). Since TosR is predicted to bind AT-rich sequences, we determined the association between the number of genes differentially regulated following induction of *tosR* and the total G+C content of the GI **(Table 4.3)**(64, 133). We found that GIs with higher A+T content were more likely (8.3-20.4% vs 0-4.5% genes/kB) to harbor genes differentially expressed following TosR overproduction with the exception of GI-*selC* that did not have any genes affected by TosR-mediated regulation. Additionally through *in silico* analysis, we identified an AT-rich motif enriched in the upstream regions of differentially expressed genes (44.9%, N=129) compared to non-differentially expressed genes (11.5%, N=52) **(Figure 4.2, Table 4.4)**. Of the top 50 differentially expressed genes, the TosR binding motif was located more frequently greater than 100 bp upstream of the ATG start site of positively expressed genes (75%) compared to negatively expressed (14%) **(Figure 4.3)**. Therefore, the location of the TosR binding motif may influence whether TosR functions as a positive or negative regulator.

Table 4.1. Top 25 genes upregulated in response to *tosR* overexpression[a]

Gene Name	Gene Locus[b]	Protein Function	log_2FC	P value	FDR
tosR	C_RS26215, c0359	PapB family transcription factor	10.1	8.3E-50	2.7E-46
c4594	C_RS21660, c4594	Uncharacterized protein	7.0	5.4E-47	8.6E-44
c0092	NA, c0092	Uncharacterized protein	6.6	2.3E-19	5.6E-17
aufF	C_RS19920, c4208	Auf fimbrial chaperone	6.6	8.6E-15	1.2E-12
c4924	C_RS23275, c4924	Putative hippuricase	6.6	2.1E-21	6.1E-19
aufC	C_RS19935, c4212	Auf fimbrial usher	5.6	1.5E-21	4.7E-19
aufD	C_RS19930, c4210	Auf minor fimbrial subunit	5.5	5.8E-16	1.1E-13
aufB	C_RS19940, c4213	Auf fimbrial chaperone	5.4	7.8E-22	2.8E-19
aufA	C_RS19945, c4214	Auf fimbrial major subunit	5.3	4.5E-32	3.6E-29
yqiL	C_RS18015, c3791	Yqi fimbrial subunit	5.3	8.3E-23	3.8E-20
yfcV	C_RS13680, c2884	Yfc fimbrial adhesin	5.2	4.4E-23	2.3E-20
c4423	C_RS20890, c4423	Uncharacterized protein	5.1	6.3E-15	9.2E-13
pitB	C_RS17665, c3724	Phosphate transporter	4.9	1.0E-18	2.2E-16
aufE	C_RS19925, c4209	Auf fimbrial minor subunit	4.4	3.2E-14	4.1E-12
yicP	C_RS21630, c4589	Adenine deaminase	4.4	4.6E-20	1.2E-17
c0325	C_RS01495, c0325	Uncharacterized protein	4.4	1.0E-14	1.4E-12
tosC	C_RS01650, c0360	TolC homolog	4.3	6.0E-19	1.4E-16
efuD	C_RS01485, c0322	Oligogalacturonide transporter	4.2	1.7E-23	1.1E-20
yjjQ	C_RS25720, c5444	Putative transcriptional regulator	3.7	2.9E-11	2.7E-09
efuE	C_RS01490, c0323	Exopolygalacturonate lyase	3.6	4.0E-22	1.6E-19
c2408	C_RS11410, c2408	Uncharacterized protein	3.5	7.3E-14	8.3E-12
c3178	NA, c3178	Uncharacterized protein	3.4	5.5E-15	8.3E-13
c1936	C_RS09090, c1936	F9 fimbrial major subunit	3.3	2.5E-12	2.8E-10
c0435	C_RS02025, c0435	Uncharacterized protein	3.3	7.1E-11	6.0E-09
tsx	C_RS23130, c4894	Nucleoside-specific channel	3.3	1.0E-10	8.1E-09

a: NA-Not Available, FC-Fold Change, FDR-False Discovery Rate

b: Gene locus tags contain the current NCBI annotation and the discontinued NCBI annotation, repectively

Table 4.2. Top 25 Genes downregulated in response to *tosR* overexpression[a]

Gene Name	Gene Locus[b]	Protein Function	log_2FC	P value	FDR
narK	C_RS07865, c1684	Nitrite extrusion protein 1	-6.2	5.2E-38	5.5E-35
sdiA	C_RS11040, c2330	Transcription Factor	-3.6	2.8E-18	5.6E-16
c3655	C_RS17360, c3655	Antigen 43	-3.2	2.3E-05	7.7E-04
narX	C_RS07855, c1682	Histidine kinase	-2.7	3.6E-14	4.4E-12
papH2	C_RS24515, c5187	P fimbrial minor subunit	-2.7	1.6E-11	1.5E-09
yhcS	C_RS18950, c3998	Transcription Factor	-2.5	5.5E-09	3.6E-07
focC	C_RS05825, c1241	F1C fimbrial chaperone	-2.4	4.9E-10	3.5E-08
yffB	C_RS14240, c2998	ArsC protein family reductase	-2.4	7.0E-09	4.4E-07
sfaD	C_RS05820, c1240	F1C fimbrial minor subunit	-2.4	4.9E-10	3.5E-08
papB	C_RS17045, NA	P fimbriae regulatory protein	-2.3	9.7E-11	8.0E-09
papB2	C_RS24525, NA	P fimbriae regulatory protein	-2.2	1.4E-09	9.4E-08
yeiC	C_RS12810, c2701	Pseudouridine kinase	-2.2	2.5E-03	4.2E-02
papF2	C_RS24485, c5180	P fimbrial minor subunit	-2.2	2.0E-08	1.2E-06
papA2	C_RS24520, c5188	P fimbrial major subunit	-2.2	9.4E-08	4.8E-06
hybA	C_RS17710, c3733	Hydrogenase-2 subunit	-2.1	8.9E-05	2.5E-03
papH	C_RS17035, c3591	P fimbrial minor subunit	-2.1	1.2E-06	4.9E-05
focG	C_RS05840, c1244	F1C fimbrial minor subunit	-2.0	3.5E-07	1.6E-05
pmbA	C_RS25180, c5333	Microcin B17 peptidase	-2.0	7.0E-09	4.4E-07
focH	C_RS05845, c1245	F1C fimbriae adhesin	-2.0	2.7E-07	1.3E-05
c1246	C_RS05850, c1246	F1C-associated phosphodiesterase	-2.0	2.0E-07	9.8E-06
ynjE	C_RS10200, c2158	Sulfurtransferase	-1.9	1.2E-05	4.3E-04
focF	C_RS05835, c1243	F1C fimbrial minor subunit	-1.9	4.8E-06	1.8E-04
narL	C_RS07850, c1681	Nitrate/nitrite response regulator	-1.9	2.7E-05	8.7E-04
papF	C_RS17005, c3584	P fimbrial minor subunit	-1.9	5.7E-07	2.6E-05
focA	C_RS05815, c1239	F1C fimbrial major subunit	-1.9	9.4E-07	4.0E-05

a: NA-Not Available, FC-Fold Change, FDR-False Discovery Rate

b: Gene locus tags contain the current NCBI annotation and the discontinued NCBI annotation, repectively

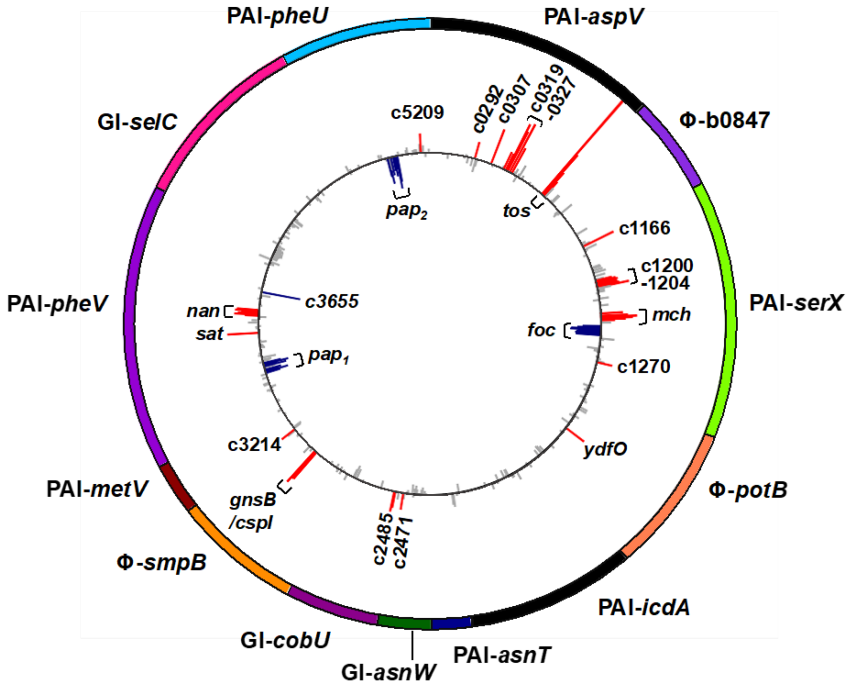

Figure 4.1 Overexpression of *tosR* affects expression of genes located on genomic islands. Schematic of genomic islands (GIs) and pathogenicity islands (PAIs) present in the CFT073 genome (outer circle). Colored segments indicate the length of each labeled DNA region. Each bar (inner circle) represents the $\log_2$ fold change for each gene present within the island with red bars indicating a $\log_2$ fold change ≥ 1.5, blue bars indicating a $\log_2$ fold change ≤ -1.5, and gray bars representing genes that were not differentially regulated. Clusters of red (upregulated) and blue (downregulated) bars are indicative of differential expression of whole operons in response to *tosR* overexpression.

Table 4.3. Characteristics of CFT073 genomic islands harboring differentially regulated genes identified by RNA-Seq

Genomic Island[a]	%G+C	Size (kb) of genomic island	# of genes[b]
PAI-*asnT*	57	32	0
PAI-*metV*	53	32	0
GI-*asnW*	53	54	1
φ-*potB*	51	44	1
PAI-*icdA*	50	54	0
GI-*cobU*	50	44	2
φ-b0847	50	33	0
PAI-*serX*	49	113	23
φ-*smpB*	49	48	4
PAI-*pheU*	48	52	9
PAI-*aspV*	47	100	12
PAI-*pheV*	47	123	16
GI-*selC*	47	68	0

a: PAI: Pathogenicity island - contains known virulence genes; GI: Genomic Island - contains genes with unconfirmed or no roles in virulence; φ**:** contains phage-rich DNA sequences
b: genes identified by RNA-Seq to be differentially regulated following induction of *tosR*

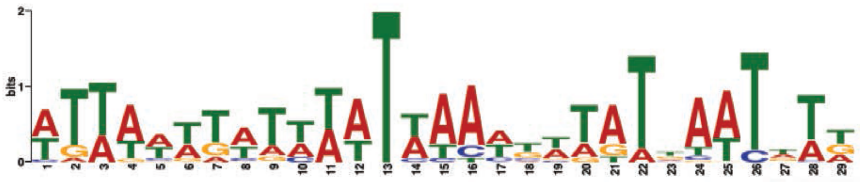

Consensus Sequence:
WTWWWWTWTWWWTWAAWKWTATKAWTDTD

Figure 4.2 Putative TosR binding consensus sequence
Multiple Em for Motif Elicitation software (MEME version 4.12.0, http://meme-suite.org) was used to identify a 29 bp consensus sequence enriched in the upstream regions of differentially regulated genes (44.9%, N=129) relative to non-differentially regulated genes (11.5%, N=52). The 36 bp TosR binding site (5'ATAACAATAATATCTATAATATAGATATTATCTGCA) was used as a template for discriminative motif discovery within 450 bp DNA sequences located upstream of the translational start ATG of differentially regulated genes.

Table 4.4. Presence of a putative TosR binding consensus sequence located upstream of differentially expressed genes

Top 25 Genes Upregulated in Response to *tosR O*verexpression				
Gene Locus	**Gene Name**	**Putative DNA binding sequence (5' è 3')**	**Start[a]**	**P value[b]**
c0359	*tosR*	AACAATAATATCTATAATATAGATATTAT	254	1.32E-07
c4594	c4594	ATATATTTTATATTTATAGTTTGATTGTT	181	2.40E-06
c0092	c0092	ATTATTGATCAATTAATGTTAAGAATTAA	117	1.42E-08
c4208	*aufF*	TTAATATATACCATTAATATATATTAAAT	3985	2.43E-07
c4924	c4924	CTTATAAAACAAATATATAAATATTTTAT	78	1.23E-06
c4212	*aufC*	TTAATATATACCATTAATATATATTAAAT	1954	2.43E-07
c4210	*aufD*	TTAATATATACCATTAATATATATTAAAT	4659	2.43E-07
c4213	*aufB*	TTAATATATACCATTAATATATATTAAAT	1138	2.43E-07
c4214	*aufA*	TTAATATATACCATTAATATATATTAAAT	360	2.43E-07
c3791	*yqiL*	ATTACTAATTAATAATATAAATTAATAAG	342	4.81E-07
c2884	*yfcV*	TATATTTATTGATTTAATTAATATTAAAT	365	3.46E-08
c4423	c4423	ATAATTAATTATTTAAATTTTTCAATCAG	299	7.40E-07
c3724	*pitB*	-[c]	-	-
c4209	*aufE*	TTAATATATACCATTAATATATATTAAAT	5077	2.43E-07
c4589	*yicP*	-	-	-
c0325	c0325	TTTTTTTCTTAATATCATTAATAAATTTA	2632	4.31E-07
c0360	*tosC*	AACAATAATATCTATAATATAGATATTAT	254	1.32E-07
c0322	*efuD*	CATATTGATATAGTTAACTAATTATCTAT	288	3.14E-06
c5444	*yjjQ*	ATTATTTAATTATAAATTAAATGAATGAG	258	1.52E-09
c0323	*efuE*	CATATTGATATAGTTAACTAATTATCTAT	1732	3.14E-06
c2408	c2408	TGTTAGTTATTTTAAAAAATATAAACTTT	71	6.17E-06
c3178	c3178	CAGAATGACACGTTTTATTAATAAATAAA	42	1.17E-07
c1936	c1936	-	-	-
c0435	c0435	-	-	-
c4894	*tsx*	-	-	-

a: # of bp upstream of ATG of the listed gene, NA-Not Annotated

b: Site P value as determined by Multiple Em for Motif Elicitation (MEME)

c: No consensus sequence identified

Top 25 Genes Downregulated in Response to *tosR* Overexpression				
Gene Locus	**Gene Name**	**Putative DNA binding sequence (5' è 3')**	**Start[a]**	**P value[b]**
c1684	*narK*	TTAAATGAGCAATAACCTTAATGAATGTG	282	2.16E-07
c2330	*sdiA*	ATAAATTATATATAAATCTTATTTATGTG	56	2.21E-09
c3655	c3655	-[c]	-	-
c1682	*narX*	CACATTCATTAAGGTTATTGCTCATTTAA	21	2.16E-07
c5187	*papH2*	-	-	-
c3998	*yhcS*	TGTAGATTGATATTTAATATATTAACGTA	58	4.44E-06
c1241	*focC*	CATGTTTACAACATAAAAAACTAAATATA	1971	4.07E-06
c2998	*yffB*	TTTAATGTTATTTAATAGTTGTTAATTTG	100	3.00E-08
c1240	*sfaD*	CATGTTTACAACATAAAAAACTAAATATA	1406	4.07E-06
NA[c]	*papB*	AATATTTACAACATAAAAAACTAAATTTA	67	1.81E-06
NA	*papB2*	-	-	-
c2701	*yeiC*	-	-	-
c5180	*papF2*	-	-	-
c5188	*papA2*	-	-	-
c3733	*hybA*	-	-	-
c3591	*papH*	AATATTTACAACATAAAAAACTAAATTTA	1224	1.81E-06
c1244	*focG*	CATGTTTACAACATAAAAAACTAAATATA	5928	4.07E-06
c5333	*pmbA*	-	-	-
c1245	*focH*	CATGTTTACAACATAAAAAACTAAATATA	6382	4.07E-06
c1246	c1246	CATGTTTACAACATAAAAAACTAAATATA	7696	4.07E-06
c2158	*ynjE*	-	-	-
c1243	*focF*	CATGTTTACAACATAAAAAACTAAATATA	5379	4.07E-06
c1681	*narL*	CACATTCATTAAGGTTATTGCTCATTTAA	1744	2.16E-07
c3584	*papF*	AATATTTACAACATAAAAAACTAAATTTA	6942	1.81E-06
c1239	*focA*	CATGTTTACAACATAAAAAACTAAATATA	778	4.07E-06

a: # of bp upstream of ATG of the listed gene, NA-Not Annotated

b: Site P value as determined by Multiple Em for Motif Elicitation (MEME)

c: No consensus sequence identified

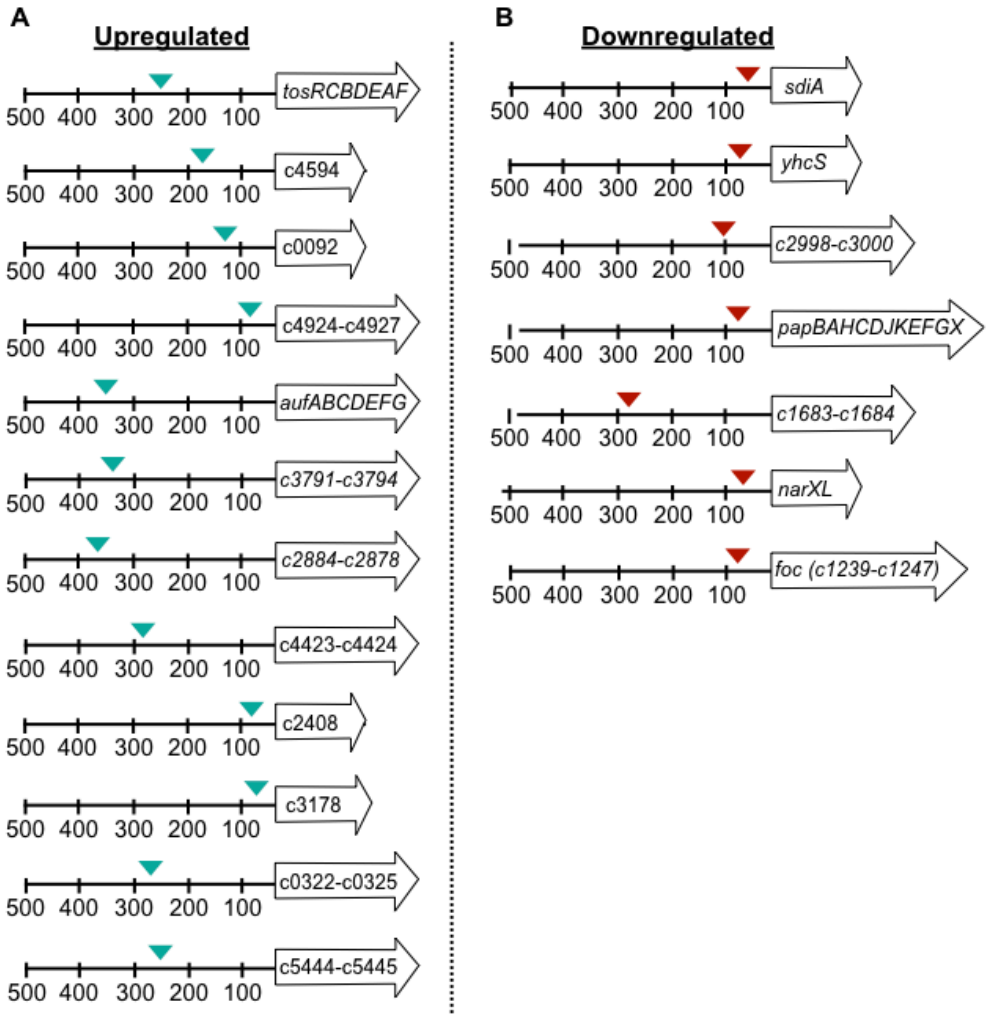

Figure 4.3 The location of the TosR binding motif upstream of differentially expressed genes

Schematic of the location of the putative TosR binding motif (shown as a triangle) upstream of the top 25 genes **(A)** upregulated (blue triangle) and **(B)** downregulated (red triangle) folllowing production of TosR. Genes lacking an upstream TosR binding motif are not shown.

TosR induces expression of multiple genes within the *tos* operon

While TosR is both a positive and negative regulator of *tos* expression, we have previously shown by immunoblot that the level of *tosR* induction used in the cells to derive mRNA for our RNA-Seq study results in an increase in TosA production (133, 134). Therefore, we predicted that overproduction of TosR would induce expression of the *tos* operon. As we expected, expression of the *tos* operon as determined by RNA-Seq revealed upregulation of *tosCBD* (log_2 FC: 1.5 to 4.3). However, we did not observe a statistically significant change in *tosA* expression (log_2 FC: 0.99), and insufficient reads for *tosE* and *tosF* precluded detection of differential gene expression **(Figure 4.4)**.

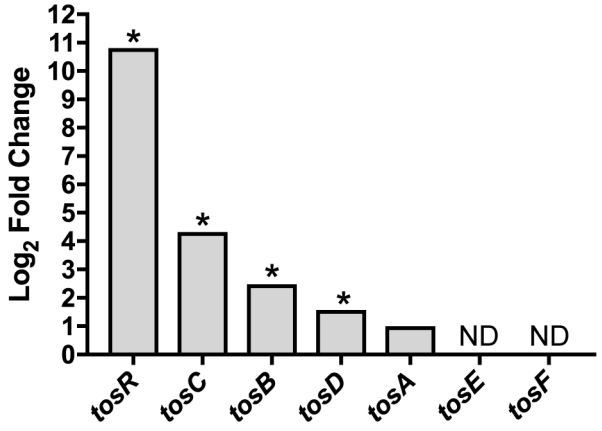

Figure 4.4 TosR-mediated induction of the *tos* operon
RNA-Seq demonstrates that overproduction of TosR promotes expression *tos* genes. Each bar represents the log_2 fold change in mRNA transcript levels of gene expression of CFT073 carrying pBAD-*tosR*-His_6 compared to CFT073 carrying pBAD as an empty vector control. ND, no data (i.e. genes that did not return a sufficient number of sequencing reads for analysis). *, log_2 FC ≥ |± 1.5| and a false discovery rate (FDR) < 0.05.

TosR mediates differential expression of nonfimbrial genes

Induction of *tosR* resulted in the differential expression of multiple nonfimbrial genes encoding proteins that participate in nitrate/nitrite transport, microcin production, quorum sensing, fucose metabolism, the transport of metabolites and nucleosides, as well as many with uncharacterized functions. *narK* was the most downregulated gene (log_2 FC: -6.22) identified using RNA-Seq in response to overexpression of *tosR* **(Table 4.2)**. *narK* is transcribed with the *narKGHJI* operon and encodes a nitrate/nitrite transporter involved with the uptake of nitrate and excretion of nitrite (309-311). *narGHJI* genes encode subunits of a nitrogen reductase, which reduces nitrate to nitrite (311). The expression of *narGHJI* genes trended towards downregulation but was not statistically significant. Nitrate serves as an electron acceptor during anaerobic respiration, and *narK* has been previously identified as a fitness factor in UPEC F11 during murine UTI (279). Additionally, *narX* (log_2 FC -2.7) and *narL* (log_2 FC -1.9), part of the *narXLQ* operon, were also within the top 25 downregulated genes identified by RNA-Seq **(Table 4.2)**. NarL and NarQ function as a two-component regulator that senses nitrate availability and subsequently induces expression of *narK* (312-314). However, direct binding of TosR to a DNA site within the promoters of the *narKGHJI* or *narXLQ* operons has not been investigated. Additionally, our RNA-Seq study assayed TosR-mediated regulation under *in vitro* conditions; therefore, the impact of TosR-mediated regulation of *nar* genes during UTI requires further investigation.

RNA-Seq also identified upregulation of all five genes of the *mchBCDEF* operon (log_2 FC: 1.8-3.0), encoding microcin H47, located within the PAI-*serX* pathogenicity island (64). Microcins are small, antibacterial peptides produced by bacteria that target the same or related species (315, 316). Microcin H47 is a known UPEC virulence factor, binds catechol receptors,

and targets the ATP synthase for bactericidal activity (317-319). The ability to eliminate susceptible bacteria may provide an advantage to pathogenic strains during colonization (320). Upregulation of *mchBCDEF* has been observed during human UTI, murine UTI and during growth in human urine, which further underscores the importance of *tosR*-mediated gene regulation during UTI (64, 106).

Overproduction of TosR affects expression of the *pap*, *foc*, and *auf* fimbrial operons

The CFT073 genome encodes 12 distinct fimbriae, including 10 of the chaperone-usher family and 2 putative Type IV pili (142). TosR shares predicted structural homology with PapB and FocB, both of which participate in fimbrial cross-talk, and is therefore predicted to also regulate other fimbriae (134). Consistent with this prediction, RNA-Seq indicated that TosR regulates multiple operons encoding fimbriae. We observed significant upregulation of the *auf* operon (*aufABCDEFG*) ($\log_2$ FC 2.6 to 6.6), which encodes Auf fimbriae **(Figure 4.5A)**. In contrast, we observed downregulation of the *pap1* ($\log_2$ FC: -2.3 to 0.38), *pap2* ($\log_2$ FC: -2.7 to -1.1), and *foc* operons ($\log_2$ FC: -2.4 to 0.15) **(Figure 4.5B-D)**. The CFT073 genome harbors two copies of the *pap* operon, designated *pap1* and *pap2*, both of which encode P fimbriae (142).

While we did identify additional differentially regulated fimbria-encoding genes within the *fim*, *yqi*, *F9*, *yad*, *yeh*, *yfc*, and *mat* operons, the majority of the genes associated with these operons were either not differentially regulated or excluded due to mapped reads below the CPM cutoff value **(Figure 4.5)**. type 1 fimbriae, encoded by the *fim* operon, bind to mannose-containing glycoproteins located on epithelial cells within the lower urinary tract and are a virulence factor for *E. coli* during colonization of the urinary tract (136, 321). We observed a decrease in *fimA* ($\log_2$ FC: -1.8), encoding the fimbrial subunit, and a modest but statistically

significant decrease in *fimB* ($\log_2$ FC: -1.2), encoding a recombinase that catalyzes the inversion of the *fim* regulatory switch (223). We did not identify significant differences in the gene expression of additional *fim* genes, which is not surprising since *fim* genes are poorly expressed during culture in aerated conditions (322, 323).

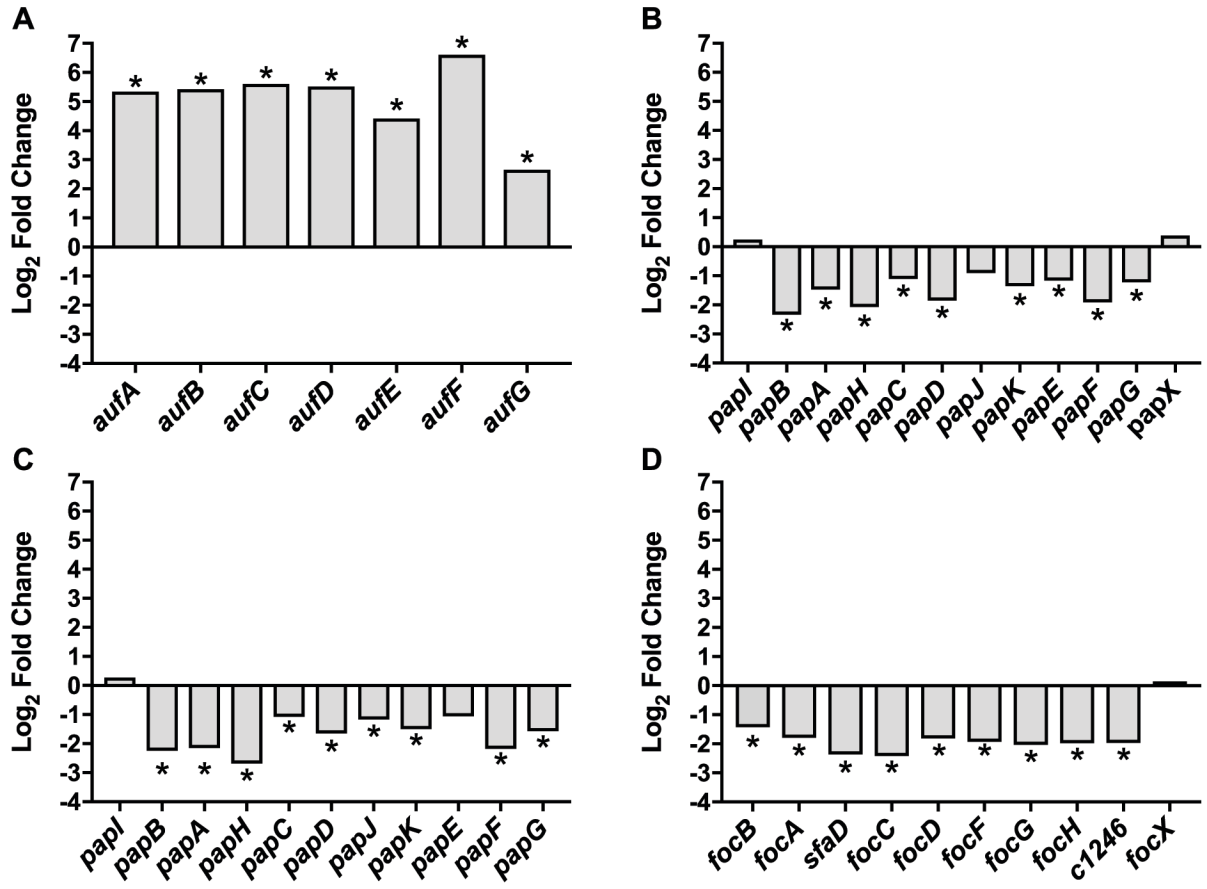

Figure 4.5 *tosR* overexpression leads to differential expression of fimbrial operons. **(A to D)** Data from RNA-Seq showing the $\log_2$ fold change in abundance of mRNA transcript levels compared between CFT073 carrying either pBAD or pBAD-*tosR*-His_6 for each gene within the *auf* **(A)**, *pap1* **(B)**, *pap2* **(C)**, and *foc* **(D)** fimbrial operons. NS, differences in gene expression are not significant; ND, no data (i.e. genes did not return a sufficient number of sequencing reads for analysis). *, $\log_2$ FC $\geq |\pm 1.5|$ and a false discovery rate (FDR) < 0.05.

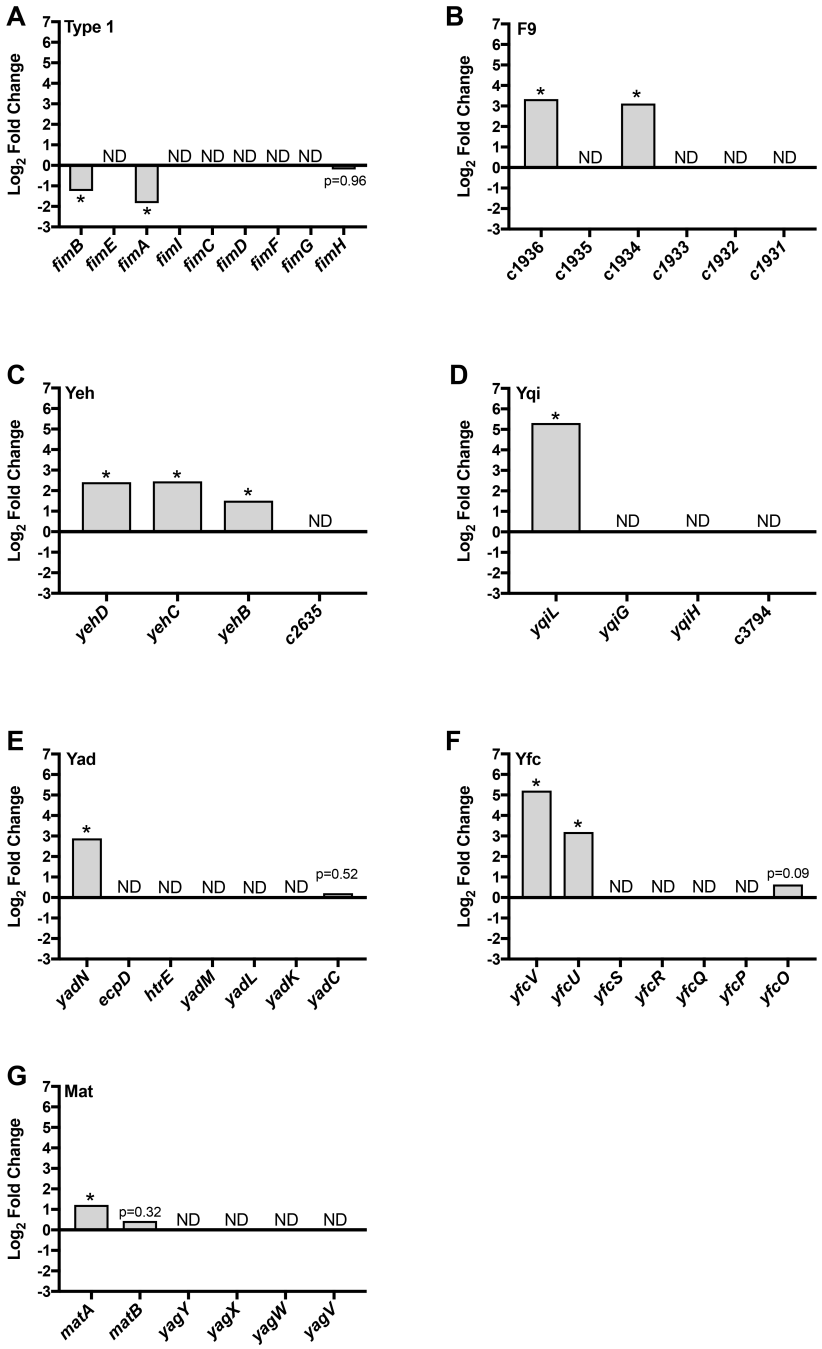

Figure 4.6 Overexpression of *tosR* affects the expression of multiple fimbrial genes
(A-D) RNA-Seq data representing the $\log_2$ fold change in mRNA between CFT073 carrying either pBAD or pBAD-*tosR*-His_6 for genes encoding **(A)** type 1, **(B)** F9, **(C)** Yeh, **(D)** Yqi, **(E)** Yad, **(F)** Yfc, and **(G)** Mat fimbriae. No data (ND) represents genes that did not return sufficient number of sequencing reads for analysis; *, $\log_2$ FC $\geq |\pm 1.5|$ and a false discovery rate (FDR) < 0.05.

Validation of differentially expressed fimbrial genes

To validate our RNA-Seq results, we performed qPCR using primers specific to the fimbrial genes *papA1, papA2,* and *aufA* to compare $\log_2$ fold change in gene expression between CFT073 carrying pBAD-*tosR*-His_6 or pBAD. Strains were cultured in a manner that replicated our RNA-Seq experiment. We observed identical trends in gene expression as compared to our RNA-Seq results. Specifically, we observed upregulation of *aufA* ($\log_2$FC: 5.2) and downregulation of *papA1* and *papA2* ($\log_2$FC: -2.3; $\log_2$FC: -2.7) **(Figure 4.7).**

We did not observe any changes in the gene expression of *papA1, papA2,* or *aufA* when comparing wild type with Δ*tosR* using qPCR, and this may be due to poor *in vitro* expression of *tosR* **(Figure 4.8)**. However, we found that overexpression of *tosR* decreased attachment to T24 human bladder epithelial cells, and this phenotype was abrogated in a mutant deficient in *auf* expression **(Figure 4.9)**.

TosR induces curli-associated genes

Curli, amyloid-like fibers, assist in UPEC adherence to human uroepithelial cells and participate in the structural development of biofilms (324-326). Curli regulatory and structural genes are encoded by the divergently expressed *csgBAC* and *csgDEFG* operons (327, 328). In response to *tosR* overexpression, we identified upregulation of two *csg* genes: *csgD* ($\log_2$ FC: 2.2) and *csgC* ($\log_2$ FC: 1.6) **(Figure 4.10)**. *csgD* encodes a transcriptional regulator that induces the expression of *csgAB* encoding CsgA, the main curli fiber subunit, and CsgB, which mediates nucleation of CsgA (327, 329, 330). CsgC inhibits toxic intracellular amyloid formation by interfering with CsgA oligomerization (331, 332). We were unable to determine if *csgA, csgB,*

csgE, and *csgF* were differentially expressed as they were excluded from the final RNA-Seq analysis due to low CPM values.

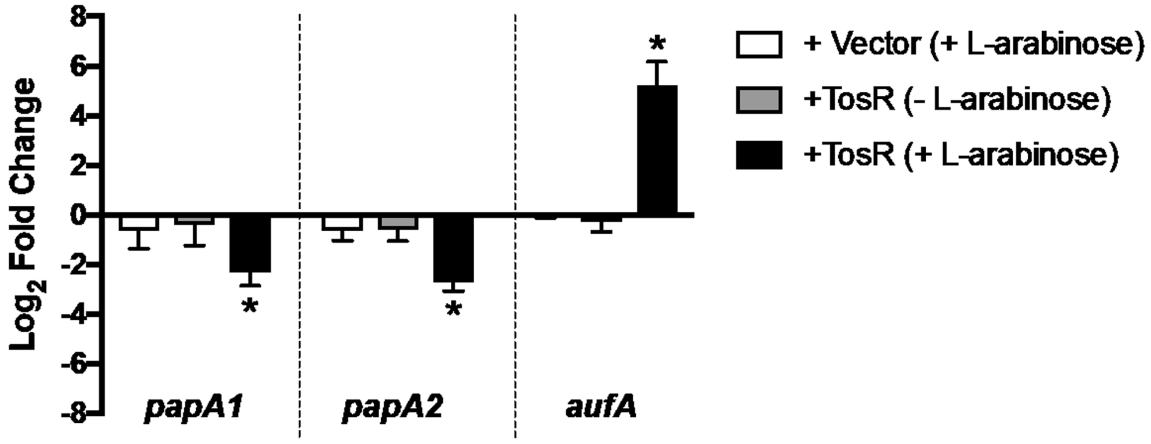

Figure 4.7 Overexpression of *tosR* represses *papA* expression and induces *aufA* expression. qPCR was performed, and bars represent the average (n = 3) $\log_2$ fold change in mRNA levels between CFT073 expressing pBAD-*tosR*-His_6 (+TosR) and CFT073 expressing pBAD (+Vector) compared to an uninduced empty vector control. Data are normalized to the housekeeping gene *gapA*. Error bars represent standard deviation, and statistical significance was determined using Student's *t* test. *, $P < 0.05$

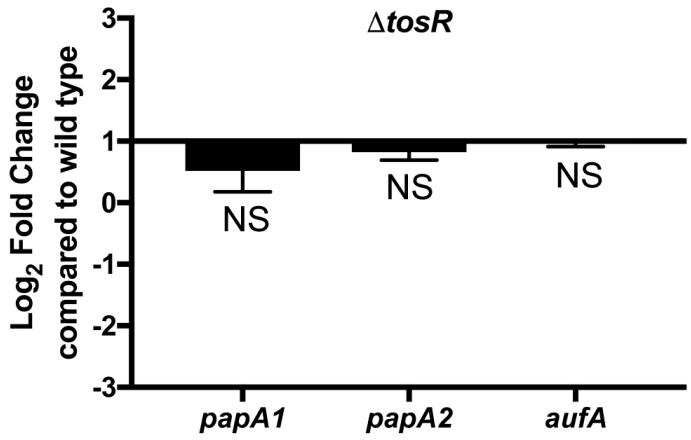

Figure 4.8 Loss of *tosR* does not affect the expression of *papA1*, *papA2*, or *aufA*
qPCR was performed and bars represent the average (N=2) fold change in mRNA levels compared between CFT073 and Δ*tosR*. Data is normalized to the housekeeping gene *gapA*. Error bars represent standard deviation, and statistical significance was determined using the Student's *t*-test; *: $P < 0.05$

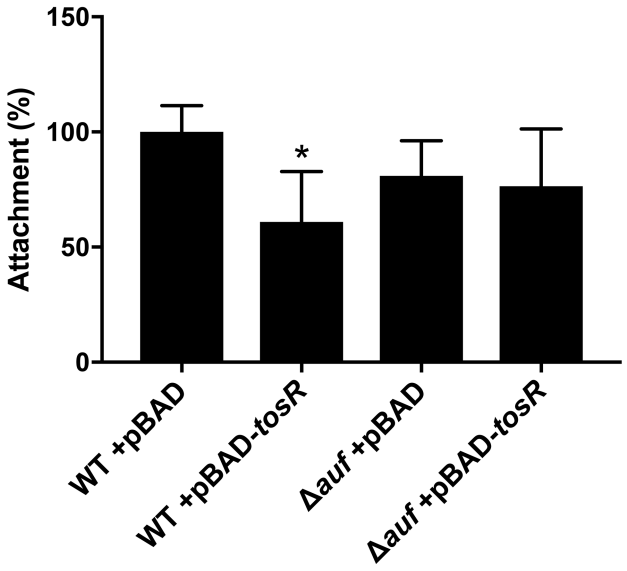

Figure 4.9 Overexpression of *tosR* decreases attachment to T24 bladder epithelial cells
Attachment of CFT073 pBAD-*tosR*-His_6 or Δ*auf* carrying either pBAD or pBAD-*tosR*-His_6 to T24 human bladder epithelial cells. Bacteria were grown until mid-logarithmic growth, induced with 10mM L-Arabinose, and then incubated with confluent bladder epithelial cells for 1hr at 37°C with 5% CO_2. After incubation, bladder cells were washed three times with sterile PBS, lysed with 0.04% Triton-X 100 for 20 min, and bacterial cells were enumerated on LB agar. Attachment levels of wild type CFT073 +pBAD was set to 100%. Each bar represents the mean (N=6). Error bars represent the standard deviation, and statistical significance was determined using Dunnett's multiple comparisons test; *: $P < 0.05$

***tosR* overexpression increases Congo red and Calcofluor white binding**

Bacteria producing curli and/or cellulose will bind Congo red on YESCA plates, which can result in a RDAR (red, dry, and rough) phenotype (333, 334). Previous studies have shown that expression of the *auf* operon was elevated in *E. coli* during biofilm formation, although a function for Auf in biofilm formation has not yet been determined (277, 335). Since overproduction of TosR resulted in an increase in *auf* expression, as well as *csgD,* a known regulator of curli biosynthesis, we investigated the contribution of TosR and Auf to Congo red binding. We did not observe any phenotypic differences between *ΔtosR* and wild type, but induction of *tosR* in CFT073 wild type, *ΔtosR,* and *ΔaufABCDEFG* led to an increase in Congo red binding compared to an empty vector control **(Figure 4.11)**. Interestingly, when TosR was overproduced in the Δ*aufABCDEFG* background, we observed a more pronounced RDAR phenotype compared to *tosR* overexpression in wild type or in the *tosR* mutant, suggesting that Auf fimbriae are interfering with RDAR formation in the presence of high levels of TosR. Furthermore, deletion or overexpression of the *auf* operon did not have any apparent effect on Congo red binding. Loss of *csg*D abrogated Congo red binding and the RDAR phenotype, supporting that TosR-mediated regulation of *csgD* is contributing to increased amyloid formation by a pathway independent of the *auf* locus.

CsgD also positively regulates the *bcsGE* and *bcsQABZC* operons involved in the production and export of cellulose, a secreted polysaccharide that functions as a structural component in the formation of biofilms (330, 336). Additionally, the amyloid-binding Congo red dye can bind both curli and cellolose. Therefore to better assess cellulose production, we performed an additional binding assay using the fluorescent cellulose-binding dye, Calcofluor white. We did not observe any difference in Calcofluor white binding between the *tosR* mutant

and wild type. However, induction of *tosR* in CFT073 wild type, Δ*tosR,* and Δ*aufABCDEFG* increased Calcofluor white binding, observed as an increase in fluorescence **(Figure 4.11)**. Additionally, overexpression of *tosR* in a *csgD* mutant did not increase binding of Calcofluor white, suggesting that the presence of both CsgD and TosR is necessary for elevated binding of Calcofluor white. Our RNA-Seq analysis did not identify any *bcs* genes to be differentially regulated in response to induction of *tosR* **(Figure 4.10)**.

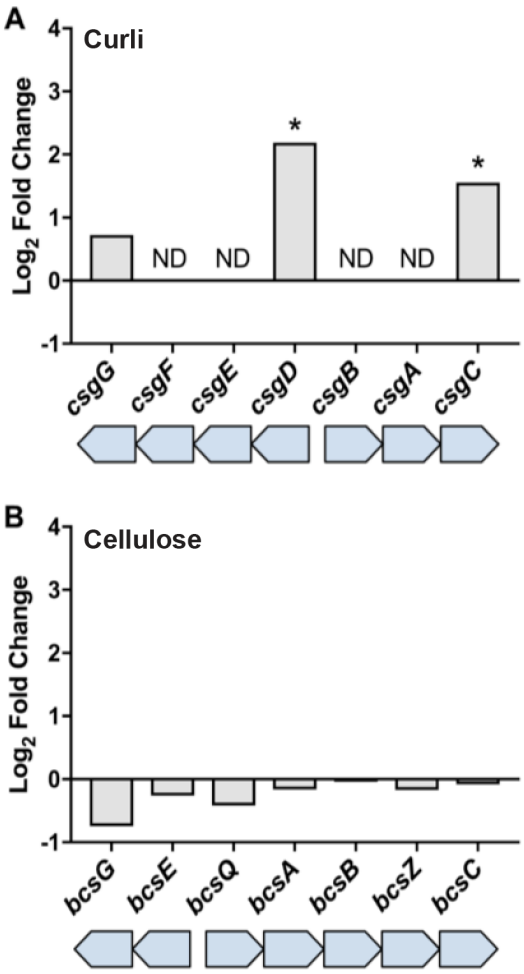

Figure 4.10 TosR increases expression of genes encoding curli, but not genes for cellulose production.
Data from RNA-Seq show the $\log_2$ fold change in abundance of mRNA transcript levels compared between CFT073 carrying either pBAD or pBAD-*tosR*-His_6 for each gene within the *csgD* and *bcsA* gene clusters. ND, no data (i.e. genes did not return a sufficient number of sequencing reads for analysis). *, $\log_2$ FC $\geq |\pm 1.5|$ and a false discovery rate (FDR) < 0.05.

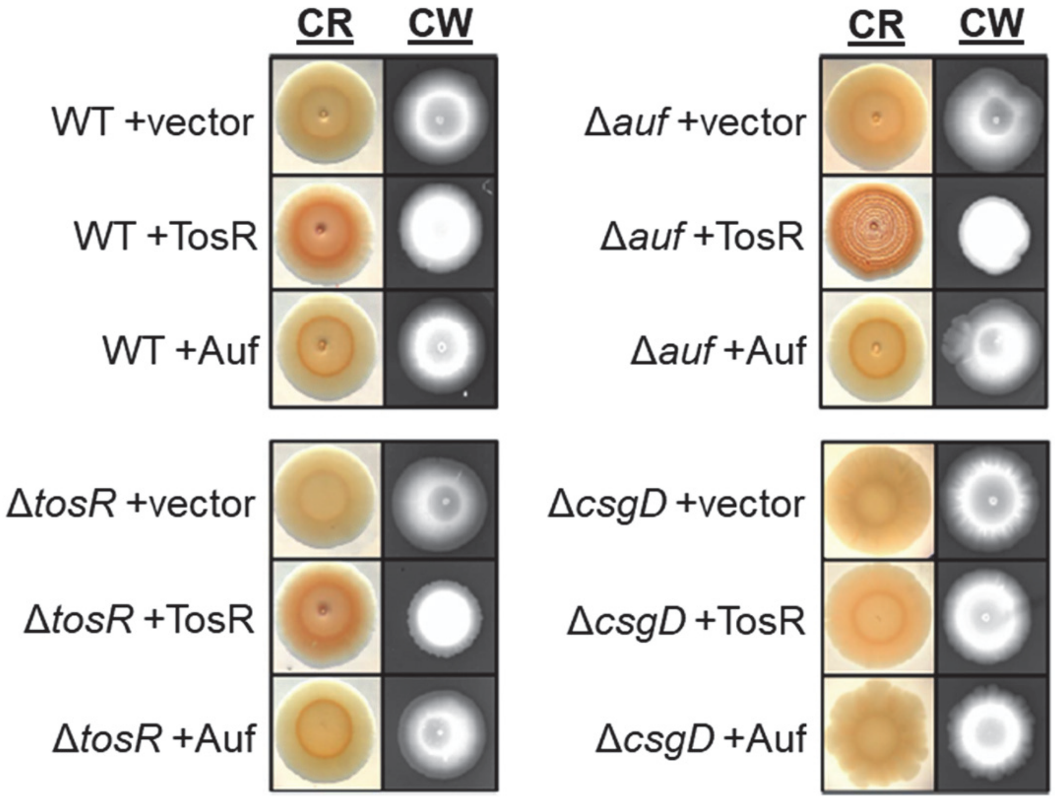

Figure 4.11 TosR overproduction increases binding to Congo red and Calcofluor white. Data from Congo red (CR) and Calcofluor white (CW) binding assays are shown comparing the CFT073 wild type and Δ*tosR*, Δ*auf*, and Δ*csgD* mutant strains harboring either pBAD (+vector), pBAD-*tosR*-His_6 (+TosR), or pBAD-*aufABCDEFG* (+Auf) after 48 h of incubation at 30°C. CR binding was visually determined as an increase in RDAR (rough, dry, and red) morphology, and CW binding was determined as an increase in fluorescence in the presence of UV light. Representative images from three independent experiments are shown.

TosR overproduction promotes biofilm formation in LB and human urine

Biofilms are sessile bacterial communities that mediate cell-cell adherence as well as attachment to biotic and abiotic surfaces (337-339). Amyloid fibers and cellulose are two components that contribute to the complex formation of biofilms. Since production of TosR resulted in increased Congo Red and Cellulose binding, which are markers for the presence of amyloid fibers and cellulose, we next investigated if increased expression of *tosR* would translate to increased biofilm formation. Therefore, we compared biofilm formation between CFT073, Δ*tosR*, and Δ*aufABCDEFG* harboring pBAD, pBAD-*tosR*-His_6, or pBAD-*aufABCDEFG*. We did not observe any differences in biofilm formation between the *tosR* mutant and wild type. However, we did observe a significant increase in biofilm formation, determined by increased retention of crystal violet, when *tosR* was overexpressed in both salt-free LB **(Figure 4.12A)** and human urine **(Figure 4.12B)** that was not due to an increase in biofilm inhabitants **(Figure 4.13).** We did not see any significant change in biofilm formation upon deletion or overexpression of the *auf* operon. Additionally, overexpression of *tosR* in the Δ*tosR* and Δ*csgD* mutants did not result in a statistically significant change in biofilm formation in salt-free LB but did increase biofilm formation in human urine.

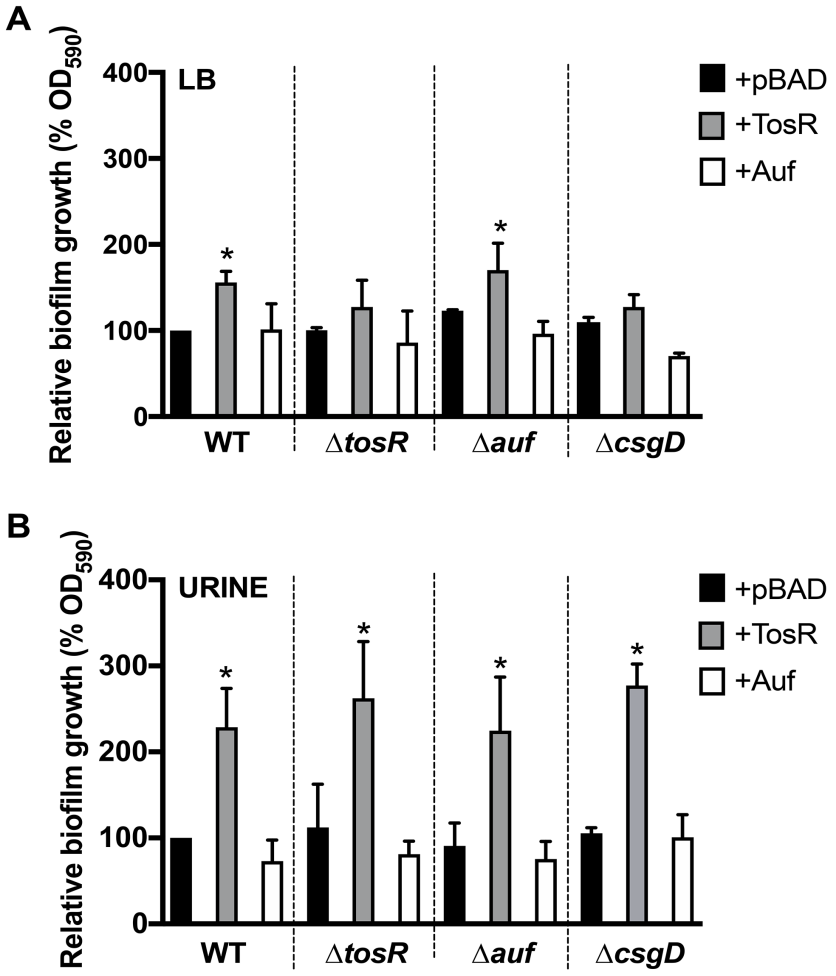

Figure 4.12 Overexpression of *tosR* increases biofilm formation in salt-free LB and human urine.
Biofilm formation was measured in **(A)** salt-free LB or **(B)** pooled human urine in the CFT073 wild type and Δ*tosR*, Δ*auf*, and Δ*csgD* mutants harboring either pBAD (empty vector control [+pBAD]), pBAD-*tosR*-His_6 (+TosR), or pBAD-*aufABCDEFG* (+Auf). Biofilm growth was assessed using crystal violet and normalized to the induced wild type carrying pBAD (WT +pBAD). Each bar represents the mean absorbance from three biological replicates, with error bars showing standard deviation. Statistically significant differences between strains were determined using Dunnett's multiple-comparison test. *, $P < 0.05$.

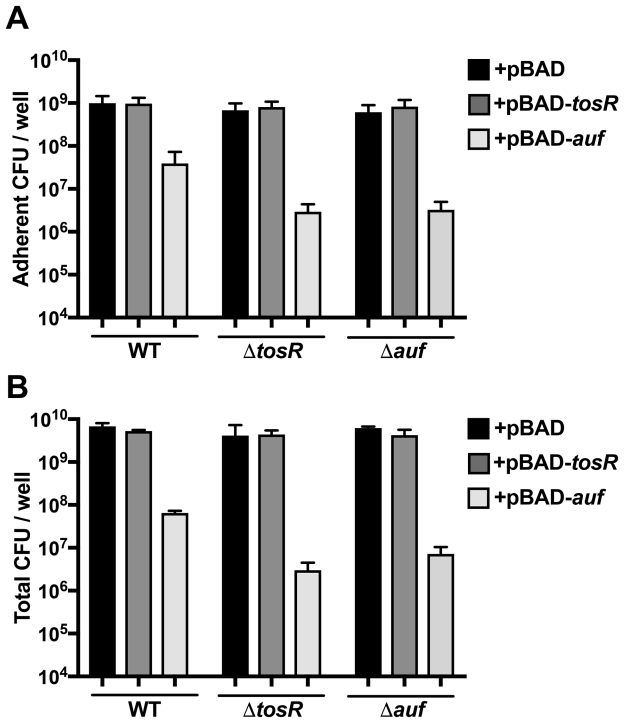

Figure 4.13 TosR does not affect levels of biofilm inhabitants
(A) Colony forming units (CFU) of adherent or **(B)** total (adherent and nonadherent) bacteria incubated statically in LB medium for 24 hrs at 37°C. To enumerate adherent bacteria, unbound cells were removed by washing twice with sterile 1x PBS. The remaining bacteria and matrix components were resuspended in sterile PBS using vigorous pipetting and then plated on LB agar with ampicillin and incubated at 37°C to enumerate viable counts. Removal of bacteria and matrix components were confirmed by crystal violet staining compared to an empty control well.

Discussion

Using RNA-Seq, our study further characterizes the function of the transcriptional regulator TosR in UPEC. In total when TosR was overproduced, we identified 200 genes that were differentially expressed (123 upregulated and 77 downregulated). Based on structural homology to members of the PapB protein family, TosR is predicted to bind AT-rich sequences and mediate regulation by modulating the local nucleoid structure, similar to the mechanism of the nucleoid-structuring proteins Lrp and H-NS (133, 299, 340-342). Indeed, PapB has been shown to compete against H-NS and Lrp transcriptional silencing of the *pap* operon, and TosR is predicted to similarly antagonize the H-NS and Lrp-mediated regulation of the *tos* operon (133, 299, 343). Overproduction of TosR resulted in elevated expression of *tosCDB* of the *tos* operon, but we did not see any significant upregulation of *tosAEF*. Previous work has shown via immunoblotting that expression of *tosR in trans* in the strain CFT073 results in a significant increase in TosA production compared to an empty vector control (133). However, high concentrations of TosR, as was also used in our study, resulted in only a slight increase in TosA production compared to wild type and may explain why *tosA* gene expression trended towards upregulation but was not statistically significant.

PapB family members frequently participate in regulatory cross-talk between fimbrial operons, and our previous work identified TosR as a negative regulator of the *pap* operon (133, 134, 224, 305). Our current RNA-Seq study supports these conclusions as we observed downregulation of the *foc, pap1*, and *pap2* operons, as well as, upregulation of the *auf* operon in response to overexpression of *tosR*. The *auf* operon is more prevalent in uropathogenic than fecal *E. coli* strains (115). However, co-challenge infections between wild type CFT073 and an isogenic mutant lacking the *auf* operon did not demonstrate Auf fimbriae as an important UPEC

fitness factor during murine UTI (139). Interestingly, *aufA* is poorly expressed in urine samples collected from human UTI, but *aufDEG* was previously shown to be upregulated (1.8-2.5 fold) in the asymptomatic bacteriuria *E. coli* isolate 83972 and CFT073 during culture in biofilm-promoting conditions in human urine (150, 277). Therefore, Auf fimbriae may contribute more towards UPEC pathogenesis during catheter-associated UTIs where biofilm formation on urinary catheters promotes a more persistent and severe infection (29, 344). As there is little information regarding regulation of the *auf* operon, to our knowledge, TosR is the first known regulator associated with this operon. While it is unclear whether TosR directly or indirectly promotes *auf* expression, we were able to identify a shared AT-rich motif that was enriched in the upstream regions of genes differentially regulated following *tosR* overexpression and may represent putative TosR binding sites (345-347).

The *tos* operon is more prevalent in UPEC isolates (~25-30%) compared to fecal *E. coli* strains (11%) (131, 134). As we have shown that induction of *tosR* affects the expression of multiple UPEC-associated fitness factors in CFT073, these results are likely broadly applicable to other UPEC strains carrying the *tos* operon. However, our RNA-Seq results represent genes affected by TosR induction during *in vitro* culture in LB, which may not comprehensively identify the genes regulated by TosR during infection. Therefore, additional gene expression studies in other growth conditions, such as human urine or *in vivo* studies, would add to our understanding of the impact of TosR on gene expression during pathogenesis.

Our study reveals that overproduction of TosR increases Congo red and Calcofluor white binding, as well as biofilm formation in salt-free LB and human urine. We were able to show that Congo red and Calcofluor white binding was dependent on the presence of *csgD*, encoding a transcriptional regulator of curli and cellulose production (327, 334, 348). We found that the loss

of *tosR* did not increase Congo red binding, Calcofluor white binding, or biofilm formation compared to wild type. This may be due to limited native expression of *tosR* or indicate the presence of a compensatory regulatory mechanism. Interestingly, deletion of the *auf* operon promoted a more robust RDAR phenotype when TosR was overproduced in the Congo red binding assay but did not have any effect on TosR-mediated biofilm formation. We also found that overexpression of *tosR* decreased attachment to T24 human bladder epithelial cells, and this phenotype was abrogated in the *auf* mutant. Therefore, it may be that Auf fimbriae sterically inhibit the function of other adhesins. For example, the production of Auf fimbriae may affect the formation, secretion, or localization of biofilm components and the contribution of Auf to biofilm formation may be context-dependent or require additional factors not present in our tested *in vitro* conditions. Indeed, overproduction of type 1, P, and F1C fimbriae prevents autoaggregation by the autotransporter protein Ag43, which is involved in cell-to-cell adhesion (349, 350). Additionally, the deletion of *auf* may affect the expression of genes encoding other adhesins or biofilm-related genes. Therefore, deletion of the *auf* operon may impact biofilm development through an unknown mechanism.

Additionally, the absence of CsgD did not affect TosR-mediated biofilm formation when cultured in human urine, suggesting that additional regulatory or structural factors account for TosR-mediated biofilm formation, which is not surprising considering construction of biofilms is a complex association of curli, cellulose, fimbrial and non-fimbrial adhesins, flagella, colonic acids, and other exopolysaccharides (351-354). Therefore, expanded testing of these phenotypes under different culture conditions would improve our understanding of TosR-mediated regulation of *csgD*. Nevertheless, our results reveal for the first time that TosR-mediated gene regulation is part of a global gene network linking the regulation of adhesins and biofilm

formation, and future studies should be designed to investigate TosR-mediated gene regulation during murine UTI.

Materials and Methods

Bacterial strains and media

E. coli CFT073 was isolated from the blood and urine of a patient with acute pyelonephritis (285). Strains were cultured at 37°C with aeration in either lysogeny broth (LB; 10 g/L tryptone, 5 g/L yeast extract, 0.5 g/L NaCl), LB without NaCl (salt-free LB; 10 g/L tryptone, 5 g/L yeast extract) or in filter-sterilized pooled human urine. Urine was collected from at least 3 healthy female volunteers, pooled, filter sterilized, and stored at -20°C. Urine collection was performed as approved by the University of Michigan Institutional Review Board (HUM00004949). The following antibiotic concentrations were used when appropriate: ampicillin (100 μg/ml) and kanamycin (25 μg/ml). 10mM L-arabinose was added to the medium to induce expression from the pBAD promoter.

Construction of mutants and complementation

Strains and plasmids used for this study are listed in **Table 4.6**, while primers used are listed in **Table B.2**. *E. coli* CFT073 mutants were constructed using recombineering (286). In brief, to construct the Δ*aufABCDEFG* mutant a kanamycin resistance cassette was PCR amplified from pKD4 using EasyA polymerase (Agilent) and primers Δ*auf*KO_f and Δ*auf*KO_r and transformed into CFT073 expressing the λ Red recombinase system genes on the temperature-sensitive plasmid, pKD46. Transformants were plated on LB agar with kanamycin and incubated overnight at 37°C. Deletion of the *aufABCDEFG* operon was confirmed by PCR

using primers *auf*_screen_f and *auf*_screen_r. The Δ*csgD* mutant was constructed in a similar manner but using the primers Δ*csgD*KO_f /Δ*csgD*KO_r, and the Δ*tosR* mutant was previously constructed (134).

pBAD-*tosR*-His_6 harboring *tosR* under the control of the arabinose-inducible *ara*BAD promoter was previously engineered (134). To generate pBAD-*auf*, the *aufABCDEFG* operon was PCR amplified using EasyA polymerase (Agilent) and the primers pBAD_auf_f and pBAD_auf_r. The resulting PCR product was digested by NcoI and KpnI (New England BioLabs), and ligated into pBAD-*myc*-HisA using T4 DNA Ligase (New England Biolabs). The resulting construct was transformed into TOP10 *E. coli* and transformants were selected on LB agar containing ampicillin and verified by DNA sequencing. Plasmids were isolated and transformed into electrocompetent CFT073 or isogenic mutants and selected on LB agar with ampicillin.

Table 4.5. Bacterial strains and plasmids used in this study

Strain	**Genotype/Resistance/Use**[a]	**Source**
CFT073	Wild-type pyelonephritis isolate (O6:K2:H1)	(11)
Δ*tosR*	CFT073 *tosR::kan*	(20)
Δ*csgD*	CFT073 *csgD::kan*	This Study
Δ*aufABCDEFG*	CFT073 *aufABCDEFG::kan*	This Study
Plasmid	**Relevant Characteristics**	**References**
pBAD-*myc*-HisA	Vector carrying arabinose inducible *ara*BAD promoter, amp^R	Invitrogen
pBAD::*aufABCDEFG*	*aufABCDEFG* cloned into the NcoI and HindIII sites of pBAD-*myc*-HisA	This Study
pBAD-*tosR*-His_6	*tosR* cloned into NcoI and HindIII sites of pBAD-*myc*-HisA	(20)
pKD4	Vector carrying a FRT-flanked *kan* gene (amp^R, kan^R)	(99)
pKD46	Vector carrying phage λ Red recombinase, amp^R	(99)

a: kan-kanamycin, amp-ampicillin, R-resistant

RNA isolation and sequencing

E. coli CFT073 carrying either pBAD or pBAD-*tosR*-His_6 were cultured overnight in biological triplicates in LB medium containing ampicillin. Cultures were diluted 1:100 into fresh LB medium containing 10 mM L-arabinose and ampicillin and cultured at 37°C with aeration. A 400 µL sample was collected between OD_{600} 0.46-0.96, and stabilized by the immediate addition of 800 µl of RNAprotect (Qiagen). Cells were then lysed with 0.2 µM of lysozyme in TE (10 mM Tris-Cl, 1 mM EDTA, pH 8.0) for 5 min at room temperature, and total RNA was extracted using the RNeasy Mini Kit (Qiagen). DNA contamination was eliminated by treatment with TURBO DNase (Thermo Fisher). Depletion of ribosomal RNA was accomplished with the Ribominus Transcriptome Isolation Kit (Thermo Fisher) followed by ethanol precipitation. A stranded library was prepared using a ScriptSeq kit (Illumina) using manufacturer's recommended protocols. Each sample was tagged with a unique six-nucleotide barcode for multiplexing. The products were purified and enriched by PCR to create the final cDNA library,

which were checked for quality and quantity by TapeStation (Agilent) and qPCR using Kapa's library quantification kit for Illumina Sequencing platforms (Kapa Biosystems). Six samples were sequenced per lane on a 50 cycle single end run on a HiSeq 2500 (Illumina) in high output mode using version 4 reagents. cDNA reads were aligned to the CFT073 genome (NCBI accession number NC_004431.1) by the Bioinformatics Core of the University of Michigan Medical School and the program SPARTA was used for quality control analysis and calculation of differential gene expression presented as $\log_2$ fold change (FC) (142, 355). Compositional biases between libraries were eliminated using Trimmed Means of *M*-values (TMM) normalization. Genes were identified as differentially expressed if they had a $\log_2$ FC greater than or equal to ± 1.5, compared to the empty vector, and a false discovery rate (FDR) < 0.05. Additionally, we excluded genes with low expression by requiring at least 3 of the six individual counts per million (CPM) mapped reads for a given gene to be greater than 2.

qPCR

E. coli CFT073 strains harboring pBAD or pBAD-*tosR*-His_6 were cultured overnight in LB with ampicillin and then diluted 1:100 into fresh LB medium containing ampicillin and cultured to an OD_{600} of 0.15 at which point 10 mM L-arabinose was added to the cultures to induce gene expression. Samples were collected at an OD_{600} of 0.5-0.6 and stabilized in phenol-ethanol (95% phenol, 5% ethanol, 4°C). RNA was extracted and TURBO DNase (Thermo Fisher) was used to eliminate genomic DNA. Removal of genomic DNA was verified by PCR using gapA_f and gapA_r. RNA was converted into cDNA using SuperScript III (Thermo Fisher), and GenCatch PCR Cleanup Kit (Epoch Life Science) was used to purify cDNA. qPCR was performed using Brilliant III SYBR Green master mix (Agilent) with 12 ng of total cDNA.

Primers used to detect *papA1*, *papA2*, *aufA*, and *gapA* are listed in **Table A.4**. *gapA* expression was used for normalization of gene expression between samples and data were analyzed using the $2^{-\Delta\Delta CT}$ method (287). Data are shown as the $\log_2$ FC in gene expression compared to CFT073 carrying the empty vector pBAD of three biological replicates.

Congo red binding assay

Congo red binding was determined by spotting 5 µl of bacteria cultured overnight in LB medium onto YESCA plates (1 g/L yeast extract, 10 g/L casamino acids, 20 g/L agar, 50 µg/ml Congo red (Sigma), 1 µg/ml Coomassie Brilliant Blue G-250 (Bio-Rad) with 100 µg/ml ampicillin and 10 mM L-arabinose (356). YESCA plates were incubated at 30°C for 48 hours. Congo red binding and RDAR (red, dry, and rough) phenotypes were visually determined using an Olympus SZX16 microscope.

Calcofluor white binding assay

To detect cellulose production, 5 µl of overnight culture was spotted onto YESCA plates (1 g/L yeast extract, 10 g/L casamino acids, 20 g/L agar, 50 µg/ml Fluorescent Brightener 28 (calcofluor white, Sigma) with 100 µg/ml ampicillin and 10 mM L-arabinose. Inoculated plates were incubated in the dark at 30°C for 48 hours (357). The level of calcofluor white binding to cellulose was visualized using ultraviolet light and images were recorded using a ChemiDoc Touch Imaging System (Bio-Rad).

Biofilm Formation

Levels of biofilm formation were quantitatively assessed using crystal violet, modified from (358). Briefly, overnight cultures of CFT073 wild type, Δ*tosR*, and Δ*auf* harboring either pBAD, pBAD-*tosR*-His_6 or pBAD-*aufABCDEFG* were diluted 1:100 into 2 ml salt-free LB medium or human urine with ampicillin and 10 mM L-arabinose in 6 well plates (CELLSTAR, BioExpress). Plates were incubated statically at 37°C for 24 hours. After incubation, unbound cells were removed by washing with water and the remaining material was stained with 0.1% crystal violet (Fisher) for 15 min. Excess crystal violet was removed by rinsing with phosphate buffered saline (137 mM NaCl, 2.7 mM KCl, 10 mM Na_2HPO_4, 1.8 KH_2PO_4, pH 7.4) three times followed by resuspension of the retained crystal violet (80:20 ethanol to acetone). OD_{590} was measured with a μQuant plate reader (BioTek).

Data Availability

The RNA-Seq data discussed in this publication have been deposited in NCBI's Gene Expression Omnibus repository with the accession number GSE112878.

Chapter V: Discussion

While both motility and adherence are important for the ascension and colonization of the urinary tract, it is not fully understood what signals within the urinary tract influence the transition between motility and adherence or what the consequences are for regulatory mistiming on the production of these traits during infection. Therefore, deconstruction of the complex regulatory network coordinating the expression of multiple adherence factors and flagella in UPEC will ultimately aid in the development of therapeutic strategies to reduce colonization of the urinary tract. The primary focus of this dissertation was to characterize the function of the transcriptional regulators, PapX, FocX, and TosR, encoded within the fimbrial (*pap* and *foc*) and nonfimbrial (*tos*) adhesin operons, respectively, and their involvement with cross-talk between genes encoding adherence factors and flagella. Specifically, P fimbriae were confirmed as a virulence factor during ascending UTI in the murine model. Additionally, *papX* and *focX* were found to both function as repressors of *flhDC* expression. Lastly, TosR was demonstrated to be involved in the regulation of fimbrial operons, motility, adherence to human bladder cells, and biofilm formation.

Chapter Summaries

Chapter II described the investigation of fitness and virulence factors in the cystitis *E. coli* isolate F11 that contribute to colonization in the ascending murine model of UTI. To accomplish this goal, signature-tagged mutagenesis was used to generate 1334 mutants, which were assembled into a total of 29 screening pools and independently transurethrally inoculated

into CBA mice. Mutants displaying a fitness defect in colonization of the bladder or kidneys were confirmed for attenuation by *in vivo* competitive cochallenge against wild type F11. Ultimately, 19 fitness factors were identified in F11, including genes involved with the production of P (*papC*) and type 1 fimbriae (*fimA*), colanic acid biosynthesis, potassium and nitrate transport, and nicotinamide adenine dinucleotide (NAD+) biosynthesis **(Table 2.2)**.

Since both type 1 and P fimbriae were identified as putative fitness factors, we investigated the cross-talk between these fimbrial types in *E. coli* F11 and determined that constitutive *fim* expression, generated by locking the orientation of a regulatory invertible element within the *fim* promoter, did not affect *pap* expression **(Figure 2.1)**. Finally, Molecular Koch postulates were fulfilled and the role of P fimbriae as a virulence factor was confirmed in UPEC CFT073 by cochallenge infections in CBA mice inoculated with a 1:1 mixture of CFT073 and a mutant unable to produce P fimbriae **(Figure 2.2)**.

The findings presented in Chapter III represent an extensive characterization of the effects of the MarR-like proteins FocX and PapX, encoded by the *foc* and *pap* operons, respectively, on flagellar gene expression and motility in the UPEC strain CFT073. A multidimensional experimental approach was performed using swimming motility assays, qPCR and immunoblots to demonstrate that FocX and PapX when overexpressed share the same function as repressors of *flhD* expression, which results in reduced flagella production and motility **(Figure 3.4)**. Intriguingly, single gene deletions of *papX* and *focX* had different effects on motility compared to wild type, with the loss of *papX* resulting in hypermotility and the loss of *focX* having no effect on motility **(Figure 3.2)**. These swimming data indicated the existence of cross-talk between *focX* and *papX*, which resulted in the discovery that FocX represses the expression of *papX* **(Figure 3.8)**. Additionally, a shared independent promoter was identified

upstream of *focX* and *papX,* suggesting that these genes could also be independently regulated in addition to being expressed by the fimbrial operon promoter **(Figure 3.6)**. However, the expression of *focX* and *papX* positively correlated with *focA* and *papA* expression when cultured in human urine or on LB agar plates compared to LB medium **(Figure 3.7)**. The contribution of *papX* to UPEC fitness was assessed in the murine model of ascending UTI following intraurethral inoculation, but a statistically significant fitness defect was not observed in the *papX* mutant when compared to wild type **(Figure 3.9)**. Furthermore, *in vivo* competition infection between wild type and the double Δ*focXpapX* mutant did not show a significant fitness defect in the colonization of the murine bladder or kidneys **(Figure 3.9)**.

The findings from Chapter IV detail the effects of overexpression of *tosR* in the UPEC strain CFT073 on global gene expression as well as the contribution of TosR to adherence and biofilm formation. RNA-Seq was performed on CFT073 carrying either pBAD or pBAD-*tosR*. In summary, 200 genes were differentially regulated following overexpression of *tosR* with a significant portion of these genes being enriched on genomic islands **(Figure 4.1)**. A number of the differentially regulated genes encoded for adhesins; specifically, the overexpression of *tosR* resulted in the upregulation of the *auf* and *tos* operons and the downregulation of the *foc, pap1*, and *pap*2 operons **(Figure 4.3, Figure 4.4, Figure 4.5)**. Interestingly, we found no change in the expression of *papX* or *focX*, which may indicate a compensatory regulatory mechanism affecting the independent proximal promoter upstream of *papX* and *focX* **(Figure 4.5)**. Using a bioinformatics approach, a putative TosR AT-rich binding motif was identified and found to be more prevalent upstream of differentially regulated genes compared to non-differentially regulated genes **(Figure 4.2 and Figure 4.3)**. In addition to affecting adhesin production, the overexpression of *tosR* resulted in increased Congo red binding, cellulose binding, and biofilm

production, and the increase in biofilm formation was more pronounced when bacteria were cultured to stationary phase in human urine as compared to salt-free LB medium **(Figure 4.11 and Figure 4.12)**. Intriguingly, the increase in Congo red binding was more robust in a CFT073 mutant lacking the *auf* operon, encoding Auf fimbriae. Additionally, overproduction of TosR reduced bacterial association with T24 bladder transitional epithelial cells, and the deletion of the *auf* operon restored binding **(Figure 4.9)**. Thus, Auf fimbriae may sterically inhibit TosR-mediating biofilm formation and adherence.

Regulatory framework for transitioning between motility and adherence in UPEC

Since it is counterproductive for a bacterium to attach to a surface while being highly motile, the expression of genes encoding adhesins and flagella must be coordinated to efficiently transition between adherent and motile states. However, the regulatory network linking motility and adherence is highly complex, in part since *E. coli* strains typically encode 8-16 different fimbrial types. Additionally, cross-talk between fimbrial operons limits production to a single fimbrial type on a bacterium (112, 224, 359). Also, the regulation of *flhDC*, which controls the expression of > 50 flagellar genes, is itself regulated by numerous transcription factors that can compete for binding sites within the *flhD* promoter (74, 75). Thus, transcription factors mediating the cross-talk between motility and adherence, including PapX, FocX and TosR, function within a complex regulatory framework. The findings presented in this dissertation fill a gap in our understanding of the cross-talk between adhesin operons and predicts a model of the regulatory network linking adherence and motility in the *E. coli* strain CFT073 **(Figure 5.1)**.

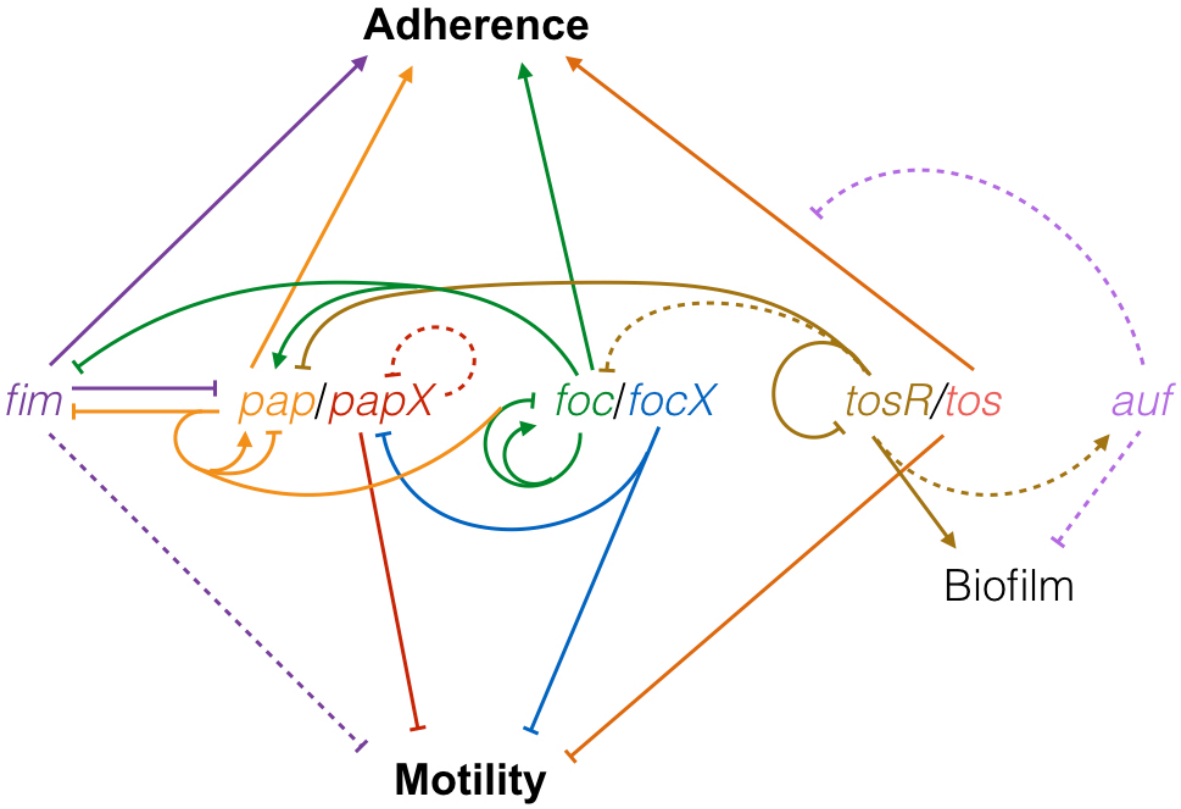

Figure 5.1 Regulatory network coordinating adherence and motility in CFT073
Cross-talk between the adhesin operons *fim, pap, foc, tos,* and *auf* can occur through direct binding interactions (solid lines) or through indirect effects (dashed lines). The transcriptional regulators PapB and FocB, encoded by the *pap* and *foc* operons respectively, mediate extensive cross-talk between *pap, foc,* and *fim*, and function as dual regulators of the *pap* and *foc* operons depending on protein concentration. *papX* and *focX* are transcribed with the fimbrial operon promoter as well as with an independent proximal promoter. Therefore, *papX* and *focX* can also be independently regulated. While Auf fimbriae likely promote adherence, a specific cell type has not been identified and the expression of *auf* inhibited TosR-mediated adherence to human T24 bladder transitional cells.

There have been multiple studies elucidating cross-talk between fimbrial operons, which provided a number of assumptions used in the construction of this regulatory model. For example, the production of type 1 and P fimbriae are coordinated in the *E. coli* isolate J96 such that only one fimbrial type is expressed at a time. This mechanism of phase variable regulation is presumed to also extend to other fimbrial types in other UPEC strains (137, 224, 359). Indeed, in CFT073 the expression of *fim* genes is correlated with a decrease in *pap* expression, and likewise, the deletion of both the *fim* and *pap* operons induced the production of F1C fimbriae (216). However, fimbrial expression can be stochastic as well as influenced by numerous environmental conditions. Additionally, the mechanism responsible for the repression of *pap* genes in response to *fim* expression is not well understood. For example, in the *E. coli* strain F11 when the phase variable *fim* promoter was locked-on for type 1 expression (*fim* L-ON) there was no effect on *pap* expression **(Figure 2.1)** (279). Thus, the strain background can influence fimbrial regulation, which is in part influenced by the diversity of encoded fimbriae types and regulators among UPEC isolates. As a consequence, the assumptions of the regulatory model in CFT073 presented here may vary between UPEC isolates.

The *pap* and *foc*-encoded transcriptional regulators, PapB and FocB, respectively, have been extensively characterized in CFT073 and shown to coordinate the expression of the *fim, pap,* and *foc* operons. Specifically, PapB can repress *fim* transcription by inhibiting the transcription *fimB*, encoding a site-specific recombinase responsible for switching the invertible element within the *fim* promoter to either the on or off orientation (224, 300). Concurrently, PapB promotes the expression of *fimE*, encoded another site-specific recombinase that switches the *fim* invertible element from on to off (163, 223, 224, 300). Similarly, FocB also acts a

negative regulator of *fim* expression; however, the mechanism of regulation is not as well characterized (305).

PapB can also function as a dual regulator of the *pap* operon and repressor of the *foc* operon. Specifically, at low protein concentrations PapB binds with high affinity to DNA sites within the *pap* promoter and promotes expression of the *pap* operon. However, high protein concentrations induce PapB to bind with lower affinity to alternative sites within the *pap* promoter, resulting in decreased *pap* expression (305, 306). FocB performs a similar function as a dual regulator of the *foc* operon and a positive regulator of the *pap* operon (305).

TosR is also part of the PapB protein family and is involved in cross-talk between multiple adhesin operons (134). Findings presented in this dissertation demonstrated that overproduction of TosR repressed the expression of the *tos*, *pap,* and *foc* operons and induced the expression of the *auf* operon **(Figure 4.5)**. The direct binding of TosR to the *pap* and *tos* promoters was previously confirmed by EMSA (133, 134). Similar to PapB and FocB, TosR-mediated regulation is focused on cross-talk between adhesins, as overexpression of *tosR* does not affect flagellar genes or motility (134). However, expression of the *tosEF* genes repress swimming motility in CFT073 through an unknown mechanism (134).

Conversely, the expression of the *fim, pap,* and *foc* operons have all been linked to the repression of motility. For example, Simms *et al.* demonstrated that constitutive expression of *fim* genes (*fim* L-ON) in *E. coli* CFT073 resulted in decreased motility, and a number of genes, including *papX*, were found to mediate the repression of motility (273). Additionally, the findings presented in this dissertation, as well as previous work by others, demonstrated that PapX directly binds within the *flhDC* promoter and represses motility **(Figure 3.2 and Figure**

3.4). Futhermore, FocX was also found to share the same function as a repressor of motility **(Figure 3.4)** (169, 170, 176, 273).

Intriguingly, ectopic expression of *sfaX* in the NMEC strain IHE3034 was shown to decrease *fim* expression by decreasing the expression of *fimB* (360). However, microarray analysis in *E. coli* CFT073 following the overproduction or loss of *papX* did not identify any *fim* genes to be differentially expressed. These microarray results were consistent with microarray analysis I performed comparing the differentially regulated genes in the double Δ*focXpapX* mutant compared to wild type CFT073 **(Table A.1)**(176). Therefore, the function of SfaX on *fim* expression may be specific to SfaX or the NMEC IHE3034 genetic background. PapX and FocX may be unable to affect *fim* expression in CFT073 due to functional differences, an inhibitory mechanism, or the absence of a required additional regulator.

Approximately 25-30% of UPEC isolates carry both *papX* and *focX* compared to only 8% of fecal *E. coli* isolates (169). The identification of an independent promoter upstream of *focX* and *papX* adds additional complexity into the model. The loss of *focX* resulted in increased *papX* expression **(Figure 3.6 and 3.8)**. Yet, the loss of *papX* had no effect on *focX* expression **(Figure 3.8)**. FocX-mediated repression of *papX* is presumed to occur at the *papX* promoter, since the loss or overexpression of *focX* did not affect the transcription of *papA* **(Figure 3.8)**. Since PapX and FocX share high structural and sequence homology, these proteins are presumed to bind to the same DNA sequences. Therefore, the regulation of *papX* is likely autoregulatory. However, there are no binding motifs upstream of *papX* or *focX* that match with high sequence identity to the PapX binding site identified upstream of *flhDC*. Therefore, PapX may bind to a degenerate DNA sequence within the proximal promoter and additional investigations by EMSA are necessary to confirm the binding specificity of PapX. For example, the MarR-like protein PecS

found in the Gram-negative phytopathogen *Dickeya dadantii* interacts with degenerate DNA sequences that have little sequence conservation with its originally defined DNA binding site (361, 362). Additionally, *Staphylococcus aureus* MepR binds both to a specific DNA sequence within the promoter of *mepRA*, encoding a multidrug efflux pump, and also binds nonspecifically to different DNA sites through interactions with the DNA backbone (363). Therefore, one possible regulatory model is that when PapX protein levels cross a concentration threshold, PapX may then be able to bind to DNA binding sites with lower affinity within the *papX* promoter and thereby repress its own transcription and consequently relieving the repression of motility. This mechanism may allow UPEC to limit the attachment time mediated by P fimbriae to host cells and act as a signal to transition from an adherent to a motile state. Thus, cross-talk between "X" genes may allow for continuous repression of motility while permitting transient expression between fimbrial types.

One gap in the presented regulatory model is a better understanding of the regulation of the independent "X" promoter. An investigation of the transcription factors affecting the independent expression of *papX* or *focX* will provide insight on how various environmental signals stimulate the repression of motility. Another caveat of this model is that the additional fimbrial and nonfimbrial operons encoded by CFT073 are not incorporated into the final model, including the second *pap* operon lacking *papX*. However, the regulation of many fimbrial operons is poorly studied and cross-talk between all fimbrial types is not clearly defined. Additionally, UPEC strains encode a heterogeneous combination of *fim, pap, foc,* and *tos* operons, which would likely affect the outcomes on motility and adherence in different strain backgrounds.

Interestingly, while there are multiple mechanisms linking the production of adhesins to repression of motility, there is not the same level of regulatory sophistication linking the production of flagella to the repression of adhesins. For example, a deletion of *fliC* in the AIEC strain LF82, isolated from a patient with Crohn's disease, resulted in decreased *fim* expression, but it is unclear what factors mediate this interaction and whether this also occurs in UPEC (364). Therefore, it seems that more resources are invested in the regulation between fimbriae, which may be indicative of greater selective pressure to coordinate heterogeneous fimbrial expression. Indeed, many fimbrial types, especially type 1, P, and F1C, are immunogenic and sequential production of fimbriae may improve evasion of the host immune system during infection (154).

A model of coordinated regulation of adherence and motility during ascending UTI

Additionally, the findings presented in this dissertation can be built into a proposed model for the regulation of adherence and motility during UTI **(Figure 5.2)**. Increased voiding is an effective host defense mechanism to remove bacteria from the urinary tract; however, UPEC strains encode fimbrial types that adhere to cells within the urinary tract and improve resistance to the powerful shear forces produced by voiding (116, 117). Additionally, reducing motility improves the success of attachment to host cells by granting more time for bacteria to attach to host cell moieties and minimizing the risk of fimbrial breakage once attached (365). However, a premature stop in flagella production may be detrimental for colonization, if bacteria become nonmotile within the bladder lumen and are either voided from the urinary tract or neutralized by host immune defenses (366). Thus, the precise timing of the regulation between adherence and motility likely contributes to UPEC pathogenesis.

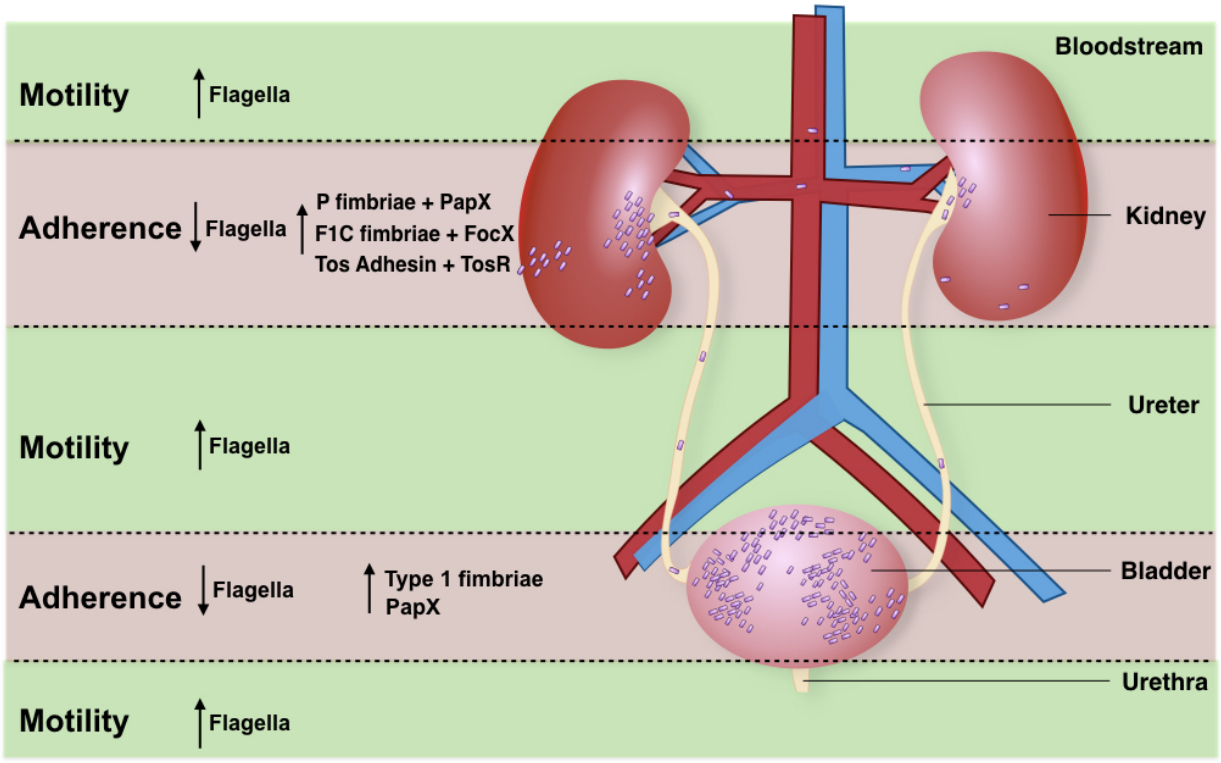

Figure 5.2 Schematic of the coordinated regulation of adherence and motility during murine UTI

Multiple transitions between adherence and motility occur as UPEC ascend the urinary tract. Motility increases during ascencion of the urethra, ureters, and presumably when bacteria cross the endothelium and epithelium barriers of the kidneys and enter the bloodstream. This model focuses on the dynamics of the fimbrial adheins type 1, P, F1C fimbriae and the non-fimbrial adhesin TosA. In the murine bladder, type 1 fimbriae have been shown to the most dominant fimbrial type contributing to colonization. PapX can be produced from an independent proximal promoter and can mediate type 1 repression of motility through an unknown mechanism. In the kidneys, the P, F1C and Tos adhesins all promote binding to renal cells and their expression will produce the transcriptional regulators TosR as well as PapX and FocX, which repress motility.

Infection of the urinary tract can be defined into spatially and temporally distinct stages as bacteria initially colonize the lower urinary tract and then ascend in multiple rounds to the kidneys via the ureters (367). While the expression of flagellar genes is evident during initial ascension of the urethra into the bladder in the murine ascending model of UTI, upon reaching the bladder, flagellar gene expression is rapidly downregulated (101). Therefore, the early stages of bladder colonization represent a transition point were bacteria switch from motile to adherent states. Type 1 fimbriae are strongly associated with adherence to mannosylated uroplakin Ia glycoprotein receptors on the bladder epithelium, and accordingly, *fim* genes are highly expressed during murine UTI (140, 150, 226, 368). Thus, the expression of type 1 fimbriae is likely coordinated *in vivo* with the down-regulation of flagellar genes. *Simms et al.* identified a number of genes, including *papX*, that mediated the repression of motility in the UPEC CFT073 L-ON mutant, a variant that is phase-locked ON for constitutive *fim* expression (273). Therefore, PapX, and possibly FocX based on shared amino acid identity and the presence of an independent promoter, may be involved in the repression of flagellar genes within the bladder. Since *pap* and *foc* genes are only moderately expressed in the urine of infected mice, the production of PapX and FocX may occur through transcription at the independent "X" promoter and be independent of transcription of the *pap* and *foc* fimbrial operons, respectively (150).

Since fimbriae bind irreversibly to host cells, detachment of bacteria from the bladder epithelium is often due to shearing of the fimbriae or as a consequence of bacterial replication, which can alter the total concentration of transcriptional regulators mediating phase variation between fimbrial types (113, 369). Therefore, ascension from the bladder to the kidneys represents a second transition point where bacteria switch from adherent to motile subpopulations. Differences in the environmental conditions (e.g. osmolarity) between the

kidneys and the bladder may signal for the production of P, F1C, or TosA to mediate adherence within the kidneys (132, 157, 182, 370). Therefore within the kidneys, expression of either the *pap* or *foc* operon would lead to the production of PapX or FocX, respectively, and result in the repression of motility. Reduced motility may improve bacterial adherence to the renal epithelium or endothelium and thereby promote colonization of the upper urinary tract. Indeed, *in vivo* competitive cochallenges demonstrated that the loss of *papX* in UPEC CFT073 compared to wild type resulted in a subtle fitness defect ($P = 0.06$) in the colonization of the kidneys after 24 hrs, and the loss of both *focX* and *papX* had a slight fitness defect ($P = 0.06$) in colonization of the kidneys after 48 hrs.

An alternative explanation for these findings is that increased flagella production in the single Δ*papX* and double Δ*focX*Δ*papX* mutants stimulates the host innate immune defenses resulting in increased bacterial clearance. The detection of pathogen-associated molecular patterns (PAMPs) by host TLRs is one of the primary immune defense mechanisms within humans. The detection of monomeric flagellin via TLR5 or adhesins via TLR4 can result in the rapid release (~ 1-7 h post inoculation) of inflammatory chemokines, cytokines, and the recruitment of neutrophils to the site of infection (371, 372). However, a statistically significant fitness defect for the Δ*papX* and Δ*focX*Δ*papX* constructs compared to wild type was not observed in independent colonization of the bladder, kidneys and spleen. Therefore in mice, the contribution of "X" proteins to pathogenesis is subtle. A limitation of this model is that the dependency of type 1 and P fimbriae for colonization of the urinary tract may differ between murine and human UTIs. For instance, while the *fim* genes are highly expressed in bacteria collected from murine UTI, *fim* expression is minimal in bacteria collected from the urine of women experiencing cystitis (150). Additionally, P fimbriae may play larger role in humans than

mice, as P fimbriae were also shown to mediate *in vitro* adherence to human T24 bladder cells (373). Therefore, PapX and FocX may have a greater contribution to fitness during human compared to murine UTI.

Considering the role of PapX and FocX as repressors of motility, the ability to decrease flagellar gene expression following ascension into the kidneys would likely be advantageous for colonization. Concurrently, bacteria may express the *tos* genes, which through TosR-mediated regulation would result in the down-regulation of the *pap* and *foc* operons but not *papX* or *focX* **(Figure 4.5)**. Therefore, PapX or FocX may also be repressing motility in bacteria expressing the TosA adhesin and function in a broader capacity in the regulation of motility during UTI.Yet, approximately 20% of UPEC strains isolated from women experiencing pyelonephritis were found to be nonmotile. Vesicoureteral reflux occurs when urine flows retrograde from the bladder into the kidneys, and increased vesicoureteral reflux promotes more rapid development of pyelonephritis in mice (374). However, the majority of healthy women experiencing uncomplicated acute pyelonephritis do not show significant levels of vesicoureteral reflux (375). Thus, it is not well understood how nonmotile bacteria ascend the ureters during uncomplicated UTI, and there are likely additional mechanisms independent of motility during uropathogenesis that contribute to the ascension of the urinary tract. In conclusion, the findings presented in this thesis have expanded the regulatory network linking key virulence factors, including adhesins, motility, and biofilm production, and presented models investigating their contribution to uropathogenesis.

Future Directions

The work presented in this dissertation addressed multiple facets of the transcriptional regulation of adherence and motility in UPEC. However, there remain many unanswered mechanistic details that should be further investigated.

PapX and FocX

A key area of future research should be focused on investigating the transcriptional regulation of *papX* and *focX*. There are limited data demonstrating the advantages of having an independent promoter upstream of *papX* and *focX*. Indeed, qPCR data showed that the expression of *papX* and *focX* was consistent with transcription from the the preceeding *pap* and *foc* operons, respectively. Thus, the most straight-forward mechanism is that the production of P or F1C fimbriae results in the production of PapX and FocX, respectively, and thereby the repression of motility. Yet, UPEC strains also encode orphan X genes, which are either *papX*, *focX*, or a homolog (>90% DNA sequence identity) that are not located at the 3' terminal end of a fimbrial operon. Preliminary work characterizing the prevalence and expression of orphan "X" genes is presented in **Appendix A.** Orphan "X" genes also share with *papX* and *focX* high DNA sequence identity up to 200-bp upstream of the ATG translational start site. Therefore, orphan "X" genes are presumed to also be transcribed from their own promoter. However, additional testing using 5'RACE should be performed to confirm this assumption. That the function of orphan "X" genes on motility has not been characterized, the environmental cues that induce their expression may not be obvious. Performing swimming motility assays with orphan "X" deletions would begin addressing their role in regulating motility. As UPEC strains frequently

encode (60%) orphan "X" genes, they represent a significant piece in the regulatory model linking adherence and motility.

The presence of an independent "X" promoter as well as orphan X genes suggest that there are situtations, potentially unrelated to fimbrial production, that induce "X" expression. Thus, future work should characterize the expression of *papX* and *focX* independently from their fimbrial promoters. The transcription of *papX* and *focX* could be quantified by qPCR in a CFT073 mutant carrying deletions of the preceeding *pap* and *foc* genes. Additionally, it would be worthwhile to screen the effects on *papX* and *focX* expression in the CFT073 Δ*papA-H*Δ*focA-c1246* mutant cultured in various environmental conditions (i.e. temperature, osmolarity, pH, urea concentrations). Two approaches for quantification of "X" expression include using qPCR with primers specific for *papX* or *focX* or using a transcriptional reporter for *papX* and *focX* expression. Identifying a condition that affects "X" expression would likely identify novel transcriptional regulators of "X" genes and may provide an explanation for why independent "X" gene expression has arisen. Currently, it is not clear if orphan "X" genes are contributing to *in vivo* fitness during UTI. Defining the environmental cues responsible for "X" expression would increase our understanding of the contribution of "X" genes to colonization of different niches.

Preliminary work has been done on characterizing the transcriptional regulators affecting *papX* **(Appendix B).** To identify genes affecting the expression of *papX*, I constructed a chromosomal transcriptional reporter consisting of *gfp* under the control of the *papX* promoter and inserted this construct into the CFT073 genome at the attTn7 site. This *papX* reporter strain was used to generate a Tn5 transposon mutant library to identify genes that when disrupted affected the expression of *papX*. Future research should focus on identifying the disrupted gene within a subset of transposon mutants demonstrating the highest and lowest fluorescence levels.

Disrupted genes that result in high levels of fluorescence may indicate that these genes encode transcriptional repressors of *papX*. Conversely, disrupted genes that result in low levels of fluorescence indicate that this gene encodes for a transcriptional activator of *papX* or has disrupted the *gfp* reporter gene. Since the upstream regions of "X" genes are highly similar, transcriptional regulators identified through this screen may also affect the expression of *focX* or other orphan X genes. Yet, despite similarities in upstream DNA sequences, only FocX was shown to repress PapX expression. Therefore, future research should independently assess the function of putative transcription factors of "X" genes on *papX*, *focX*, and orphan X genes.

In addition to flagellar genes, PapX has been shown to affect the expression of a number of non-flagellar genes including a number of putative transposases **(Appendix A).** The function of these genes is unknown. However, mobile and insertional elements can influence gene regulation, including flagellar gene expression. For example, there are multiple sites within the *flhD* promoter that are known to be amenable for the targeted placement of insertional elements, resulting in changes to the downstream accessibility of binding sites for other transcription factors (89). Therefore, the role of these putative transposases in the regulation of motility and the mobility of "X" genes in the genome should be further explored. Additionally, there is limited data on non-flagellar genes specifically affected by FocX. RNA-seq assays between CFT073 wild type and Δ*focX*, as well as, wild type and Δ*papX*, would allow for comparisons between genes affected by FocX and PapX at a resolution that is not possible with previous microarray studies. Futhermore, an RNA-seq assay between Δ*papX* and the double mutant Δ*papX*Δ*focX* may identify the factors reponsible for decreased motility in the double mutant. These experiments would provide substantial insight to the genes regulated by "X" genes and identify contrasting any differences between the mechanisms of FocX and PapX.

Much of the work presented in this dissertation focuses on the regulation of adherence and motility at the transcriptional level. Therefore, future research should also incude a characterization of dimerization and ligand binding of PapX and FocX. The presence of cross-talk between *papX* and *focX* provided a rationale for why the deletion of *focX* does not affect motility. However, the mechanism responsible for "X" cross-talk is not clear. One hypothesis is that FocX is directly binding upstream of *papX* and functioning as a transcriptional repressor. To test this hypothesis, the presence of a binding site for FocX needs to be confirmed. Electrophoretic mobility Shift Assays (EMSA) have been successful in identifying the PapX binding site upstream of *flhDC*. Therefore, a follow-up experiment should include an EMSA investigating the ability of FocX or PapX to bind to labeled DNA fragments of the *papX* and *focX* promoter. Intriguingly, an "X" binding motif was not identified near the ATG start site of *papX* or *focX*. Therefore, conducting an EMSA on the binding of papX and focX to each "X" promoters would clarify if these proteins directly bind to a site within this region as well as the the presence of autoregulation. Additionally, using nested DNA probes of the *papX* promoter would narrow down the location of a FocX binding site within the *papX* promoter. The inability to identify an X binding site may indicate that crosstalk occurs through an indirect mechanism (i.e. regulation of another transcription factor). One caveat with this approach is that PapX and FocX have been difficult to purify due to poor protein solubility. Optimization of the binding conditions, including fresh protein samples and minimal processing time, improves the consistency of the binding reaction but limits the ability to manipulate the testing conditions.

Overall, there are limited data on the dimerization interactions of PapX and FocX. Since PapX and FocX are highly homologous in amino acid sequence and structure, it is assumed that they are able to form heterodimers with each other with no impact on overall protein function.

However, heterodimerization between FocX and PapX has never been tested. Additionally, there is some evidence that site-directed mutants in PapX may be capable of forming dominant negative heterodimers **(Appendix C)**. Affinity purification between uniquely tagged PapX-Myc and FocX-His proteins would address the presence of heterodimer formation. This experimental design would include binding FocX-His proteins to a nickel column, passaging PapX-Myc proteins through the column to allow for protein-protein binding to occur, followed by elution of bound proteins. Heterodimer formation would be present if a dimer was formed carrying both the Myc and His tags. Since UPEC isolates frequently contain multiple "X" genes, a better understanding of heterodimerization will clarify if different combinations of "X" genes have different effects on gene regulation.

tosR

Investigation of the genes regulated by TosR demonstrated the broad involvement of this transcriptional regulator in adherence, biofilm formation and virulence. Likewise, there a number of future experiments that would greatly improve our understanding of the function of TosR. For example, the fimbrial *auf* operon was the most highly expressed adherence-associated operon in response to TosR overproduction. However, the function of Auf in host colonization is not well understood. Our work demonstrated that the presence of the *auf* operon inhibited robust RDAR formation and adherence of CFT073 to T24 bladder transitional epithelial cells. Our leading hypothesis was that Auf fimbriae sterically occluded the binding of other extracellular factors involved with adherence and biofilm formation. Based on this work, it appears that production of Auf fimbriae would be counterproductive for the development of adherence and biofilm formation, both important virulence traits during UTIs. Thus, future work should include a

detailed visual evaluation of the effects of overproduction of TosR and Auf on the bacterial cell surface. Additionally, the role of TosR in regulating adherence factors should be evaluated on a more diverse panel of cell types to detemine if our observed adherence phenotype was cell-specific. Results from these experiments will provide a better understanding of how the production of Auf fimbriae and TosR affect the organization of fimbrial and biofilm components at the extracellular surface.

Since *tos* genes are poorly expressed *in vitro*, our RNA-seq assay was limited to investigating conditions of high TosR production. Therefore, results using this experimental approach may include regulatory pathways that are not relevant during infection. It would be worthwhile to compare the function of TosR on gene regulation in CFT073 grown in sterile human urine, which more closely mimics the host urinary tract than LB. Additionally, we observed a higher level of biofilm formation in a strain overexpression *tosR* cultured in human urine compared to LB, and the deletion of *csgD* did not affect biofilm formation. Therefore, the environmental growth conditions provided by human urine may be influencing different TosR-mediated regulatory pathways than what was identified by RNA-seq in LB. Results from this approach may identity biofilm-associated genes that are more highly expressed in human urine and regulated by TosR.

Biofilm formation promotes bacterial persistence within the urinary tract, and the overproduction of TosR resulted in elevated bilfilm formation in LB and human urine (307). Specifically, overexpression of *tosR* resulted in a significant increase in the expression of the curli-associated genes CsgDC. However, additional curli and cellulose-associated genes were not differentially expressed. One explanation for limited supporting transcriptional data is that the mRNA for the RNA-seq was collected under growth conditions that are not optimized to induce

curli and cellulose production. Taking this into account, one future experiment should be to conduct a qPCR analysis of curli and cellulose-associated genes in a strain overexpressing *tosR* cultured under curli-inducing conditions (e.g. growth on agar plates at $\leq$ 30ºC). The quantification of additional differentially regulated curli and cellulose-associated genes will better clarify if TosR regulates curli and/or cellulose-associated gene expression. While direct binding of TosR has been demonstrated for the *tos* and *pap* promoters, the accuracy of the predicted TosR binding site has not been vetted. Thus, the predicted TosR binding motif should be experimentally confirmed using an EMSA with purified TosR protein. Validation of TosR binding sites within the promoters of differentially regulated genes identified by RNA-seq will broaded our understanding of direct and indirect TosR-mediated regulation. Defining the binding sites of TosR will improve our prediction of additional TosR-regulated genes in other UPEC isolates.

Appendix A: A brief characterization of orphan "X" genes in UPEC

While the majority of *foc* (90%) and *pap* (60%) operons carry a 3' terminal "X" gene, a bioinformatics screen of the genomes of UPEC isolates revealed that most UPEC genomes carry additional "X" genes that share > 90% DNA sequence identity with *papX* and *focX* but are not associated with a fimbrial operon **(Figure A.1A)** (169). Overall, UPEC genomes encoded as many as 4 "X" genes, and an orphan "X" gene was more prevalent (60%) than either *papX* or *focX* when only one "X" gene was present within a genome. Furthermore, many of these orphan genes are located near mobile elements, which may be involved in the transposition of these genes into various regions in the genome. Additionally, orphan "X" genes share high DNA sequence identity up to 200 bp upstream of the ATG start site **(Figure A.1B)**. Since "X" genes can be transcribed from an independent promoter, orphan "X" genes may be regulated by transcription factors that also regulate the expression of *papX* or *focX*. Therefore, orphan "X" genes represent a significant portion of "X" genes carried by UPEC genomes, yet their contribution to the repression of motility and cross-talk between adherence and motility has not been well investigated. Additional work characterizing the effects on motility in a UPEC mutant with a deleted orphan "X" gene would address whether orphan "X" genes are also capable of repressing motility.

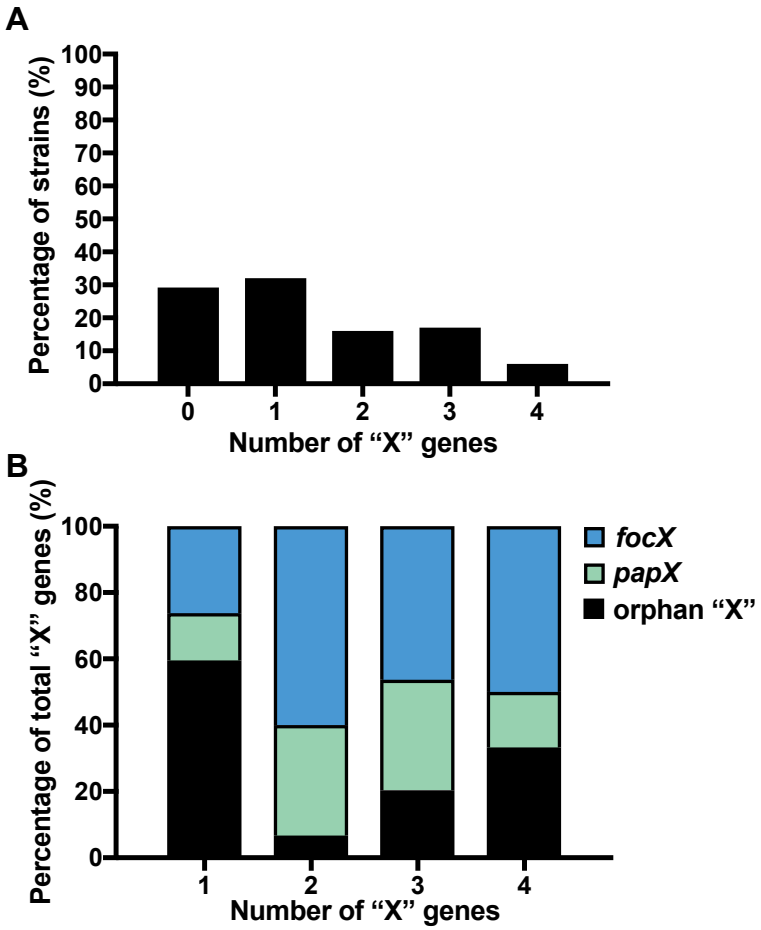

Figure A.1 The majority of UPEC isolates carry at least one "X" gene.
(A) Percentage of UPEC *E. coli* strains (Total N = 107) carrying *papX* homologs (>90% DNA sequence identity). Strains were obtained from the UMEÅ database representing UPEC isolates collected from the urine of female patients experiencing uncomplicated UTI made available by the *E. coli* UTI Bacteremia initiative, Broad Institute (broadinstitute.org). **(B)** The total number of all (%) of *focX, papX* or non-fimbrial associated *papX* or *focX*, termed orphan "X", in individual *E. coli* strains.

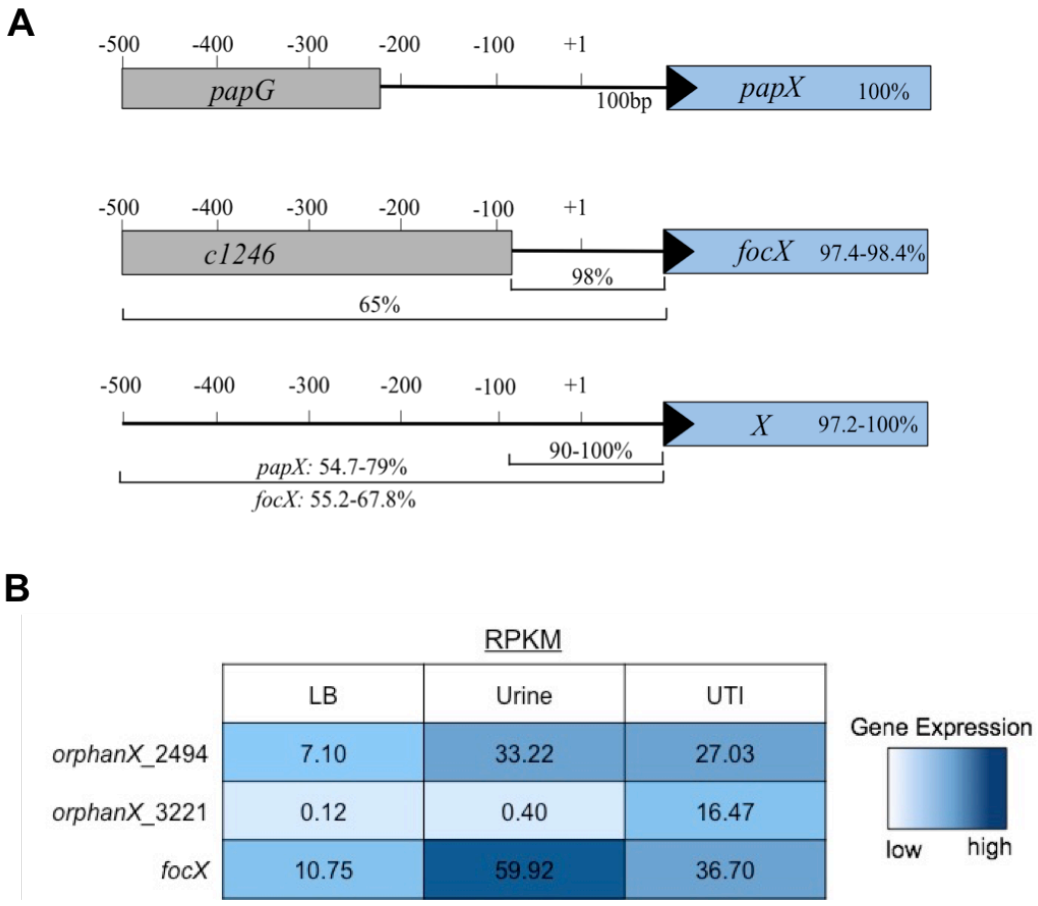

Figure A.2 "X" genes share a conserved upstream DNA sequence but are differentially expressed

(A) A BLAST search of UPEC genomes was performed to identify all genes that shared >90% sequence identity to *papX*. UPEC genomes were all isolated from female UTI patients with uncomplicated UTI as part of the in the UMEÅ database (broadinstitute.org). Gene sequences for *focX*, *papX* and non-fimbrial associated *papX* or *focX*, termed orphan "X" were aligned by the Clustal W method and the sequence identity is indicated as the percentage compared to *papX*. **(B)** An analysis of RNAseq performed by Subashchandrabose *et al* of the UPEC cystitis strain, HM27, isolated from the urine of a woman experiencing cystitis (246). RNA was immediately isolated from voided urine (UTI), and compared to *in vitro* growth in LB or in sterile pooled human urine. Data are presented as Reads per Kilobase of transcripts per Million mapped reads (RPKM) in the different growth conditions

Similar to PapX and FocX, the uropathogen *Proteus mirabilis* strain HI4320 encodes a helix-turn-helix xenobiotic response element (XRE) transcription factor MrpJ that is located at the 3' terminal end of the *mrp* operon, encoding the mannose-resistant *Proteus*-like MR/P fimbriae (170, 376). MrpJ represses both swimming and swarming motility in *P. mirabilis*, and while MrpJ differs structurally from MarR-like proteins, PapX and MrpJ are considered functional homologs. Additionally, ectopic expression of *papX* represses motility in *P. mirabilis* (170, 377, 378). Intriguingly, the *P. mirabilis* strain HI4320 encodes 17 chaperone-usher fimbriae with 15 MrpJ variants, including 4 paralogs that are not encoded within a fimbrial operon and are therefore considered to be orphan genes (378). Thus, uropathogens appear to encode redundant mechanisms to regulate motility and the role of orphan genes may be important in the mechanism of regulating motility independent of fimbrial expression.

"X" genes share a low G+C content (<40%) compared to the *E. coli* CFT073 genome (50.5%), which is a common feature of genes that have been horizontally acquired. Therefore, it is possible that orphan "X" genes are acquired through transposition events within a genome from different UPEC strains (64, 169, 178). An analysis of the DNA sequences surrounding "X" genes, including *papX* and *focX*, revealed that in the majority of cases an upstream or downstream mobile genetic element is located nearby. The *pap* and *foc* operons are located on PAIs and therefore are already associated with horizontally transferred DNA elements. Yet, downstream of *papX* and *focX* is a 150 bp DNA sequence that shares sequence homology to IS66 family transposase. Thus "X" genes may be carried on regions of DNA that are prone to recombination, resulting in the transposition of *papX* or *focX* to different sites within the genome (142, 379).

Additionally, there is a tantalizing relationship between the presence of PapX and the expression of transposases. Previous work reported that the overexpression of *papX* resulted in the repression of multiple flagellar, as well as, a number of nonflagellar genes, including genes encoding phage-related proteins (176). Further investigation by microarray in *E. coli* CFT073 found that the top genes upregulated following the loss of *papX* encoded phage-related proteins, hypothetical proteins, or transposases **(Table A.1)**. Similar microarray results were observed when comparing gene expression between *E. coli* CFT073 and the double mutant Δ*focXpapX*. Of these genes, four of them are found within the same gene cluster c3190:c3186 which is predicted to encode a cryptic prophage (380, 381). While these genes do not have a defined role in the literature, ectopic expression of c3192:c3186 in a Δ*papX* mutant resulted in a slight but statistically significant increase in motility **(Figure A.3B).** An increase in motility was not observed following ectopic expression of c3190:86 in wild type CFT073, which may be due to native levels of PapX affecting the expression of genes within the c3192:86 gene cluster or the presence of an indirect mechanism. The integration of insertion sequences within the *flhDC* promoter can enhance *flhDC* expression and promote flagella production. Indeed in the *E. coli* K-12 MG1655 strain, multiple insertions of IS1 and IS5 elements upstream of *flhDC* enhanced *flhDC* expression and subsequently increased motility (89, 382). Thus, additional investigation of the association of "X" genes, both fimbrial and nonfimbrial associated, would provide insight into the association between "X" genes and mobile DNA elements.

A

Gene	Annotation	Fold change in: CFT073 Δ*papX*	CFT073 Δ*focX*Δ*papX*
c3581	Hypothetical protein	25.52	13.77
c3187	Hypothetical protein *ydfU*	6.58	4.34
c3188	Hypothetical protein	8.61	5.98
c3189	Hypothetical protein/ putative crossover junction endodeoxyribonuclease	12.44	3.96
c3190	Hypothetical protein/ LexA transcription factor	7.28	3.74
c3645	Putative transposase	18.87	8.54
c3646	Hypothetical protein/ Putative transposase	8.55	2.83
c3576	Hypothetical protein/Putative transposase	6.51	3.92

B

Gene	Annotation	Fold change in: CFT073 Δ*papX*	CFT073 Δ*focX*Δ*papX*
flhD	Flagellar transcriptional activator	2.23	1.78
flhC	Flagellar transcriptional activator	1.83	1.82
fliL	Flagellar biosynthesis protein	1.85	1.43
flgB	Flagellar basal body rod protein	2.34	1.58
flgC	Flagellar basal body rod protein	2.28	1.49
flgE	Flagellar hook protein	1.89	1.42
flgF	Flagellar basal body rod protein	1.79	1.43
flgG	Flagellar basal body rod protein	1.75	1.28
flgH	Flagellar L-ring protein precursor	2.38	1.48
flgI	Flagellar P-ring protein precursor	1.69	1.34
fliA	RNA polymerase sigma factor	1.94	1.39

Table A.1. The loss of *papX* and *focX* results in an increase in the relative gene expression of multiple flagellar and nonflagellar genes compared to wild type
Microarray assays were used to assess the gene expression in *E. coli* CFT073 *ΔpapX* and *ΔpapXΔfocX* compared to wild type. RNA was extracted from strains cultured in lysogeny broth (LB) to mid-logarithmic growth. Results show a sample of the highest upregulated **(A)** non-flagellar and **(B)** flagellar genes identified from the microarray.

A

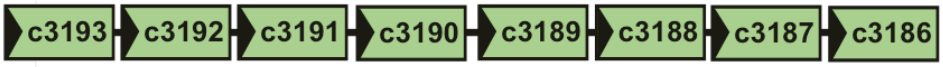

Gene Name	Predicted Protein Function
c3190	Uncharacterized
c3192	HTH Transcriptional regulator
c3191	PerC family transcriptional regulator
c3190	LexA family transcriptional regulator
c3189	RusA family crossover junction endodeoxyribonuclease
c3188	KilA-N domain-containing protein
c3187	Uncharacterized
c3186	λ prophage Qin antitermination protein

B

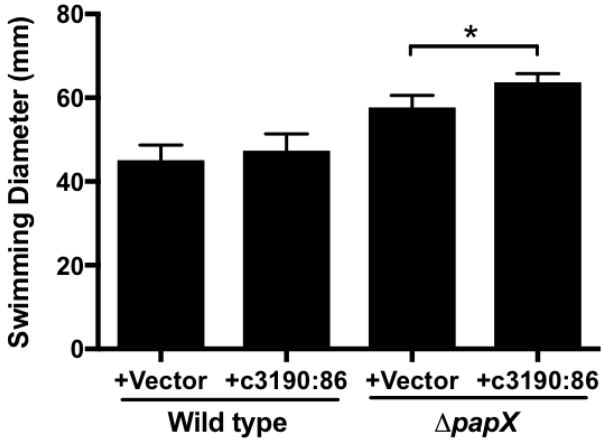

Figure A.3 Expression of the c3190:86 gene cluster promotes motility of the Δ*papX* mutant **(A)** Gene organization of the c3190:86 gene cluster contains multiple transcriptional regulators of unknown function and is predicted to represent a cryptic prophage based on the presence of c3186 encoding the λ prophage Q antiterminator protein. **(B)** Bars represent the average diameter (mm) of swimming motility of CFT073 carrying either pLX3607 (+Vector) or pLXc3190-86 (+c3190:86) encoding the c3190:86 gene cluster, following 16-18 hr incubation at 30°C. Data represent three biological replicates with the error bars showing the standard deviation. An unpaired *t*-test was used for statistical analysis. *, $P < 0.05$

Methods

Bioinformatics Screen.

The prevalence of *papX*, *focX*, and nonfimbrial-associated *papX* homologs, referred to as orphan "X" genes, were calculated from the Umeå collection of *E. coli* UPEC genomes provided as part of the *E. coli* UTI Bacteremia initiative, Broad Institute (broadinstitute.org). The Umeå collection represents 106 isolates collected from female UTI patients with uncomplicated UTI, including both acute and recurrent infections. For each UPEC genome, the presence of *papX* and *focX* was determined by BLAST using the *papX* and *focX* sequences from CFT073. Positive matches were defined by sequence identity >90% and 3' proximity to the *pap* or *foc* operons, respectively. Orphan "X" genes were characterized as any *papX* or *focX* homologs that were not located at the 3' terminal end of a fimbrial operon and sequence identity >90%. The total number of any identified "X" gene per strain, which includes *papX*, *focX*, and orphan "X" genes, are shown in **Fig. A.1A**, and the relative distributions of *papX*, *focX*, and orphan "X" genes is quantified in **Fig. A.1B**. To compare sequence homology, we used MegAlign (DNASTAR) to align and calculate the sequence identity of the gene and upstream DNA sequences of *papX* (N=38), *focX* (N=66), and orphan "X" (N=48) identified from the Umeå collection (**Figure A.2A)**.

Microarray analysis

CFT073 wild type and the Δ*papX* and Δf*ocX*Δ*papX* mutants were grown in LB medium to an OD_{600} of ~0.5. Triplicate cultures of each strain were treated with RNAprotect (Qiagen) to stabilize RNA according to the manufacturer's protocol. Total RNA from bacterial samples was extracted by using ribopure RNA Purification kit (Thermo Fisher Scientific) as described by the manufacturer. cDNA was synthesized and the FairPlay III Microarray labeling kit (Agilent) was

used to fluorescently label cDNA with either the Cy3 or Cy5 dye. RNA was then hybribized and scanned using Affymetrix *E. coli* Genome 2.0 GeneChips. Data analysis were performed by Gary Moran at the Dublin Dental University Hospital, Trinity College, Ireland.

Construction of pLX-c3190:86

The c3190:86 gene cluster was cloned into the vector pLX3607 under the control of an IPTG-inducible promoter to induce expression, referred to as pLX-*c3190:86* (170). In brief, the c3190:86 gene cluster was amplified by PCR using EasyA polymerase and the primers pLX-c3190:86-F/pLX-c3190:86-R from *E. coli* CFT073 **(Table B.4)**. The resulting PCR product and pLX3607 were both digested by NcoI and HindIII, ligated together using T4 DNA Ligase (New England BioLabs) to generate pLX-*c3190:86*, and transformed into competent Top10 *E. coli*. Transformants were plated on LB with ampicillin and the resulting colonies were screened by PCR and sequencing to verify plasmid construction.

Appendix B: Investigation of the transcription factors involved in regulating "X" genes

Summary

papX and *focX* are members of a 17-kDa family of "X" genes carried in *E. coli*, which includes *sfaX, prfX, prsX* and fotX (169). The findings presented in Chapter III identified an independent proximal reporter upstream of *papX* and *focX*. Based on high DNA sequence identity in the 200 bp proceeding *papX* and *focX*, it is likely that *papX* and *focX* share a similar mechanism of regulation. However, it is unclear what transcription factors can regulate *papX* and/or *focX* at the shared "X" promoter. Therefore, to identify genes affecting the expression of *papX*, I constructed a chromosomal transcriptional reporter consisting of *gfp* under the control of the *papX* promoter that was inserted into the CFT073 genome at the attTn7 site. Culture of the *papX* transcriptional reporter and a positive control carrying the empty vector pSLC284 in LB medium demonstrated that *gfp* expression could be detected from both reporters, but the strongest and most consistent fluorescence signal occurred at later time points **(Figure B.1)**. Consequently, a CFT073 construct encoding the chromosomal *papX* transcriptional reporter was used to generate a Tn5 transposon mutant library to identify genes that when impaired affected the cumulative level of fluorescence. Overall, a total of 12,904 transposon mutants were generated and assessed for fluorescence at 24 hr following static incubation at 37°C **(Figure B.2)**. A subset of 50 transposon mutants demonstrating the highest and lowest levels of fluorescence compared to the control CFT073 (attTn7 P_{papX}-*gfp*) were further evaluated. From this secondary screen, 25 Transposon mutants were confirmed for significantly higher or lower

levels of fluorescence and are being currently investigated to determine the transposon insertion site and association to the *papX* promoter.

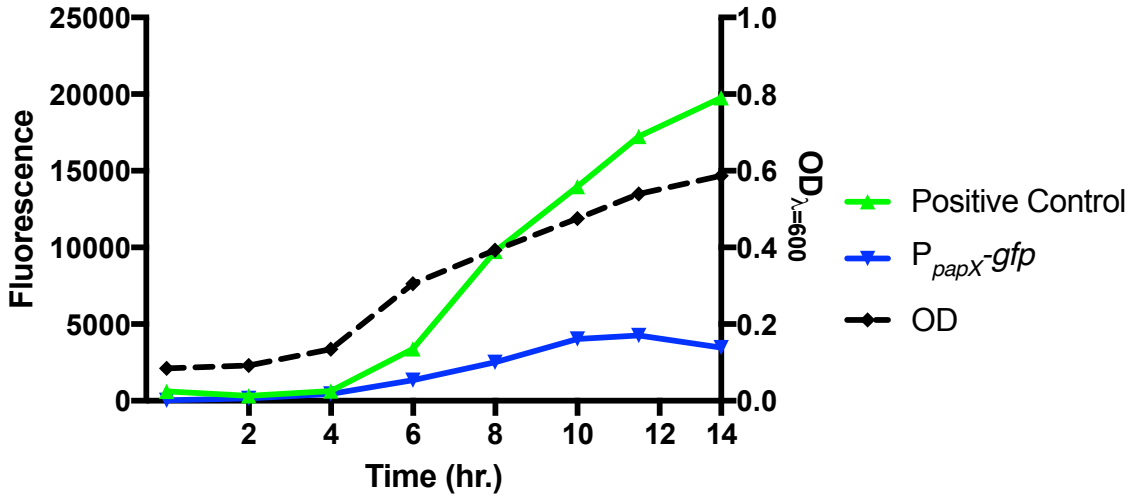

Figure B.1 GFP expression increases over time in CFT073 encoding P_{papX}-*gfp*
CFT073 carrying either P_{papX}-*gfp* (blue line) or the positive control (P_{tac}-*gfp*) (green line) were cultured statically in 200µL of LB medium and fluorescence reading were taken every two hours. The OD_{600} is plotted on the right Y-axis and was comparable in both strains.

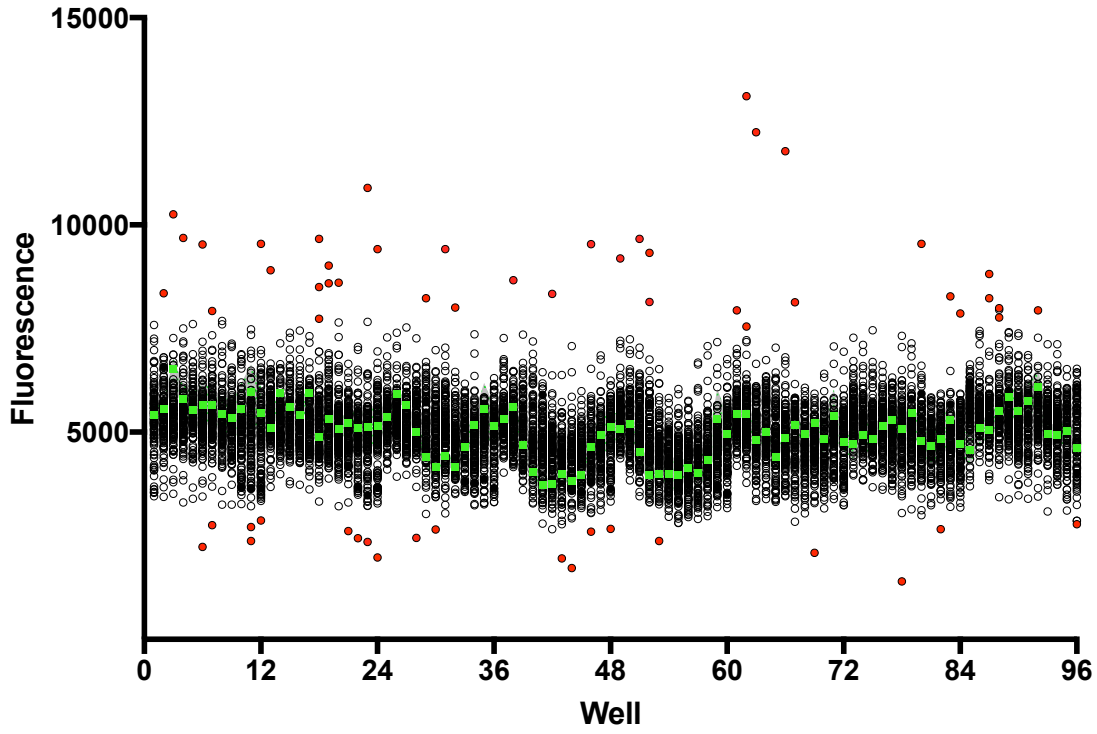

Figure B.2 Measurement of fluorescence of 12,904 transposon mutants in CFT073 carrying P_{papX}-*gfp* at the attTn7 Site

Transposon mutants in CFT073 carrying P_{papX}-*gfp* were cultured statically in 200µL of LB medium in a 90-well plate, and fluorescence was measured after 24 hr. Each dot represents an individual fluorescence reading from a well. In total, 12,904 transformants are plotted with the X-axis representing the well location within the 96-well plate. The fluorescence reading has been normalized to the OD_{600} to account for difference in growth. The green dots are the average fluorescence reading per well location, the red dots signify transposon mutants whose produced with significantly higher or lower fluorescence reading compared to the average fluorescence and were thus selected for secondary screening. Culture in the central wells of the 96-well plate resulted in a predictable dip in fluoresence and is presumable due to decreased oxygen saturation.

Methods

Construct of the CFT073 chromosomal P_{papX}-*gfp* transcriptional reporter

The *papX* promoter was cloned upstream of the *vsfGFP-9* to generate a transcriptional GFP reporter. The *E. coli* strain DH5α carrying the vector pSLC-284 encoding vsfGFP-9 was generously provided by Dr. Melanie Pearson (383). The *papX* promoter was generated by PCR using the EasyA polymerase (Agilent) and the primers papXF-slc and papXR-slc, and the final PCR product included 500 bp upstream of the ATG translational start site of *papX* **(Table B.4)**. The pSLC-284 plasmid was linearized using the primers pSLC_284R/pSLX_284F, assembled with the *papX* PCR product using the NEBuilder HiFi DNA Assembly Cloning Kit (New England Biolabs), and transformed into Top10 *E. coli*. The pSLC284 P_{papX}-*gfp* plasmid was isolated by miniprep and linearized by the primers F-apaI and R-speI. The linearized plasmid and the mini-Tn7 vector pMCL2868 were both subjected to restriction digest by ApaI and SpeI, ligated, and transformed into S17 λ *pir*. Confirmed transformants were triparentally mated with CFT073 (rifampin resistance-Rif^R) and *E. coli* WAM2817 for 24 hr at 30°C on LB medium. After 24 hr, bacteria were plated onto LB agar plates containing rifampin and ampicillin and cultured at 37°C to isolate CFT073 carrying the chromosomal *papX* transcriptional reporter at the attTn7 site.

Identifying regulators of *papX*

A transposon mutant library was generated using the EZ-Tn5 transposome kit (Lucigen) in the CFT07t attTn7 P_{papX}-*gfp* construct following the manufacturer's guidelines. A total of 12,904 transposon mutants were generated and harvested using a QPix Colony Picker. To measure the expression of *gfp,* bacteria were statically cultured to stationary phase in 200 µL of

LB medium at 37°C in 96-well clear flat bottom costar plates (Corning). Bacteria were diluted 1:100 in fresh LB medium and cultured under the same conditions. Fluorescence was measured using a Synergy HT plate reader at an excitation wavelength of 480 and emission wavelength of 510 using a top-view reading. Fluorescence was normalized to OD_{600} and well location using a standard 96 plate inoculated with only the parent strain.

Appendix C: Insights on heterodimerization and ligand binding of PapX and FocX

A number of MarR-like proteins bind small molecular ligands at sites located between the protein dimer interface and the DNA-binding domain (171, 384). Ligand binding can result in conformational changes and alter the dynamics of the DNA-binding domains, frequently resulting in attenuation of DNA binding (385). The canonical example was characterized for the *E. coli* MarR protein that is encoded with the *marRAB* operon, encoding the transcriptional regulator MarA associated with antibiotic resistance and the production of a multidrug efflux pump (386, 387). MarR binds to two DNA palindromic sequences within the *mar* promoter and inhibits the recruitment of RNA polymerase, resulting in reduced transcription of *marRAB* and the divergently transcribed *marC* (388). The ligands associated with MarR-like proteins are often substrates related to regulatory targets. For example, exposure to the phenolic compound salicylate (SAL) promotes expression of the *marRAB* operon, and MarR co-crystallized in the presence of salicylate. Specifically, salicylate was bound at two ligand-binding pockets within the protein dimer and SAL-bound MarR was unable to bind DNA (172, 266, 271). More recently, MarR was characterized as a copper sensor in *E. coli* as copper-mediated oxidation of the Cys80 residue resulted in disulfide bond formation between two MarR dimers and abrogated DNA binding (389). Thus, there are alternatives to ligand binding that can affect the structure and function of MarR-like proteins.

A ligand has not been identified for PapX or FocX and represents a gap in an understanding of the timing of PapX-mediated repression of motility. The purification of PapX

has been challenging as PapX proteins are poorly stabilized under *in vitro* conditions. Intriguingly, a site-directed mutant the PapX homolog SfaX demonstrated that the alteration of a cysteine to a serine within the wing domain (C70S) dramatically improved protein stability, presumably due to decreased intermolecular interactions (390). Additionally, a C70S PapX protein is also more stable, and therefore the effect of this cysteine on protein stability is shared between these two "X" proteins. Furthermore, wild type PapX and C70S PapX repress motility to the same extant in CFT073, and therefore the mutation did not initially appear to affect protein function. However, in the Δ*papX* mutant, ectopic expression of C70S PapX results in a substantially greater repression of motility **(Figure C.1)**. Intriguingly, this effect on repression appears to be dependent on the presence of FocX and the simultaneous absence of PapX. It is not readily apparent the explanation for these effect on motility. While FocX and PapX have not been confirmed to form heterodimers, due to their sequence similarities a heterodimer FocX-PapX would likely perform the same function as homodimers. However, these data suggest that there may be additional interactions between FocX and PapX that are not fully accounted for in the regulatory mechanism of "X" genes. Indeed, protein turnover may be a strategy to relieve PapX repression of motility, and the C70S mutant, which has significantly increased *in vitro* protein stability, may bind longer or with greater affinity to DNA, resulting in greater repression of *flhDC*. Future experiments exploring the effects of oxidation on PapX function may identify an alternative strategy to modulate the DNA binding of "X" genes.

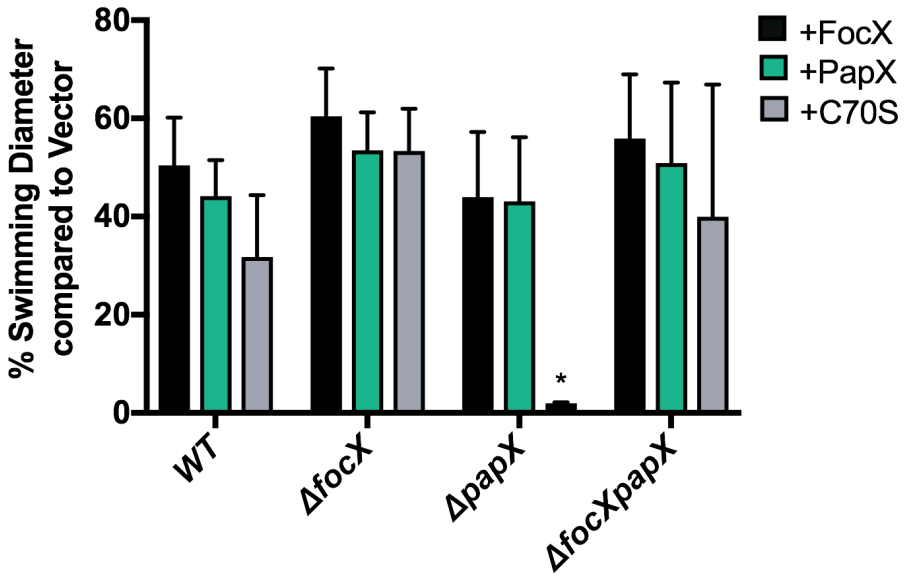

Figure C.1 Expression of C70S PapX results in robust repression of motility in the Δ*papX* mutant

Bars represent the average diameter (mm) of swimming motility of CFT073 carrying either pLX-*focX,* pLX-*papX*, or pLX-*papX*-C70S following 16-18 hr incubation at 30°C. Data represent three biological replicates with the error bars showing the standard deviation. A Student's *t*-test was used for statistical analysis. *, $P < 0.05$

Methods

Construction of C70S PapX

The site-directed mutant C70S PapX was constructed in pLX3607 using the QuikChange II kit (Stratagene) according to the manufacturer's guidelines. Briefly, overlapping primers (pLX-C70SF/pLX-C70SR) were used for rolling PCR of pLX3607 **(Table B.4)**. PCR products were treated for 2 hr with DpnI at 37°C, transformed into electrocompetent CFT073, and plated onto LB agar containing ampicillin (100 μg/ml). Site-directed mutagenesis was confirmed by sequencing the extracted pLX-C70S plasmid by miniprep.

Appendix D: Supplementary Information for Chapters II-IV

Table B.1. Oligonucleotide primers used in Chapter II

Primer	Direction of primer	Purpose	Sequence (5'-3')
Donne340	Forward	Amplification of variable region of DNA signature tags	GGCCACGCGTCGACTAGTC ANNNNNNNNNACGCC
Donne341	Reverse		GGCCACGCGTCGACTAGTC ANNNNNNNNNNGATAT
Donne298	Forward	Amplification of DNA adjacent to transposon junction for sequencing	AAAGCTTGCTCAATCAATC
Donne299	Reverse		AGCATAAAGCTTGCTCAAT C
Donne646	Forward	PCR screening for presence of *pap* operon	CGGTAGCTATGGCAGTGGT GTCTTTTG
Donne792	Reverse		CCCAGATATCCACAACACT CTATCC

Table B.2. Oligonucleotide primers used in Chapter III

Strain	**Genotype/Resistance/Use**[a]	**Source**
CFT073	Pyelonephritis isolate (O6:K2:H1)	[Mobley, 1990]
ΔfocX	CFT073 *ΔfocX::cat* (Cam^R)	This Study
ΔpapX	CFT073 *ΔpapX::kan* (Kan^R)	(273)
ΔfocXΔpapX	CFT073 *ΔfocX::cat ΔpapX::kan* (Cam^R, Kan^R)	This Study
E. coli F11	Cystitis isolate (O6:K2:H31)	(206)
E. coli F11 *ΔpapX*	F11 *ΔpapX::kan* (Kan^R)	This Study
E. coli HM69	Cystitis isolate	(65)
E. coli HM69 *ΔpapX*	HM69 *ΔpapX::kan* (Kan^R)	This Study
Top10 *E. coli*	Used for cloning	ThermoFisher Scientific
Plasmid	**Relevant Characteristics**	**References**
pLX3607	IPTG-inducible vector (Amp^R)	(170)
pLX-*focX*	pLX3607+*focX* (Amp^R)	This Study
pLX-*papX*	pLX3607+*papX,* also known as pDRM001 (Amp^R)	(170)
pKD4	Vector carrying a FRT-flanked *kan* gene (Amp^R, Kan^R)	(286)

pKD3	Vector carrying a FRT-flanked *cat* gene (Amp^R, Cam^R)	(286)
pKD46	Vector carrying phage λ Red recombinase (Amp^R)	(286)

a: cam-chloramphenicol, kan-kanamycin, amp-ampicillin, R-resistant

Table B.3. Oligonucleotide primers used in Chapter IV

Primer	Purpose	Sequence (5'-3')
ΔaufKO_f	Amplification of kanamycin cassette from pKD4 for λ Red recombineering with *aufABCDEFG*	GCTTGGATTTTTTAACAAAAGG AAAGGTATAAATGGTGTAGGCT GGAGCTGCTTC
ΔaufKO_r	Amplification of kanamycin cassette from pKD4 for λ Red recombineering with *aufABCDEFG*	TGCGCAGAAGCAGCCTAGTTTT CCACCAATCTGAAATGGGAATT AGCCATGGTCC
ΔaufKO_f	Amplification of kanamycin cassette from pKD4 for λ Red recombineering with csgD	TGTGCGATCAATAAAAAAAGC GGGGTTTCATCATGGTGTAGGC TGGAGCTGCTTC
ΔcsgDKO_r	Amplification of kanamycin cassette from pKD4 for λ Red recombineering with csgD	AACGTTTCATGGCTTTATCGCC TGAGGTTATCGTTATGGGAATT AGCCATGGTCC
auf_screen_f	Screening for deletion of *auf* operon	AAGAACCTTCTGGAATTAGC
auf_screen_r	Screening for deletion of *auf* operon	AGCCAGTGCATTATAACGAC
csgD_screen_f	Screening for deletion of *csgD*	GCAACATCTGTCAGTACTTC
csgD_screen_r	Screening for deletion of *csgD*	GAAATTCTGCCGCCACAATC
pBAD Screen_f	Screening for insertion into pBAD-*myc*-HisA	TGCCATAGCATTTTTATCC
pBAD Screen_r	Screening for insertion into pBAD-*myc*-HisA	CTGATTTAATCTGTATCAGG
pBAD_auf_f	Amplification of *aufABCDEFG* with 5' NcoI restriction site for cloning into pBAD-*myc*-HisA	NNNNCCATGGCCAAATTCAATT TATCTAATTTATCCGCAG
pBAD_auf_r	Amplification of *aufABCDEFG* with 5' KpnI restriction site for cloning into pBAD-*myc*-HisA	NNNNGGTACCCAGGTAAAGTC AGAAAAGTAAC
gapA_f	qPCR	CGTTAAAGGCGCTAACTTCG
gapA_r	qPCR	ACGGTGGTCATCAGACCTTC
papA1_f	qPCR	ATTTGATGGTGCGACAGCAACA GG
papA1_r	qPCR	TCTGTTACAGGGTTGCCACTAC CA
papA2_f	qPCR	CGGGTGAAATTTGATGGAGCCA CT
papA2_r	qPCR	AGGCACCTTCAGCTACATTCTT GC
aufA_f	qPCR	GAATCGGTTGCGACCTTACA
aufA_r	qPCR	CAGGCTCACTGATATGGATGAC

Table B.4. Oligonucleotide primers used in Appendix A, B, and C

pLX-C70SF	CAGCGGAGAGTCATT**CC**CTGTCACCTTCAGAG
pLX-C70SR	CTCTGAAGGTGACAGGGAATGACTCTCCGCTG
pLX-c3186:92	NNNNCCATGGCAAGCACTAAATTAACCGG
pLX-c3186:	NNNNAAGCTTTTATCTCGTCACTTTTCTTAATTGC
pslc_284r	TTGCCAGAACCGTTATGATG
pslc_284f	CAGAATTCGAGCTCGGTACC
papxf-slc	CATCATAACGGTTCTGGCAA
papxr-slc	GTACCGGGCCCAAGCTTCTCGAAGCTTGCATGCC TGCAGGAG
slc284_f_apai	NNNNGGGCCCGACATCATAACGGTTCTGGC
slc284_r_spei	NNNNACTAGTGTTTCACTTCTGAGTTCGGC

References

1. Berg RD. 1996. The indigenous gastrointestinal microflora. Trends Microbiol 4:430-5.

2. Tenaillon O, Skurnik D, Picard B, Denamur E. 2010. The population genetics of commensal Escherichia coli. Nat Rev Microbiol 8:207-17.

3. Eisenstein BI, Jones GW. 1988. The spectrum of infections and pathogenic mechanisms of Escherichia coli. Adv Intern Med 33:231-52.

4. Orskov I, Orskov F. 1985. Escherichia coli in extra-intestinal infections. J Hyg (Lond) 95:551-75.

5. Palaniappan RU, Zhang Y, Chiu D, Torres A, Debroy C, Whittam TS, Chang YF. 2006. Differentiation of Escherichia coli pathotypes by oligonucleotide spotted array. J Clin Microbiol 44:1495-501.

6. Pupo GM, Karaolis DK, Lan R, Reeves PR. 1997. Evolutionary relationships among pathogenic and nonpathogenic Escherichia coli strains inferred from multilocus enzyme electrophoresis and mdh sequence studies. Infect Immun 65:2685-92.

7. Kaper JB, Nataro JP, Mobley HL. 2004. Pathogenic Escherichia coli. Nat Rev Microbiol 2:123-40.

8. Johnson JR, Russo TA. 2002. Extraintestinal pathogenic Escherichia coli: "the other bad E coli". J Lab Clin Med 139:155-62.

9. Moriel DG, Rosini R, Seib KL, Serino L, Pizza M, Rappuoli R. 2012. Escherichia coli: great diversity around a common core. MBio 3.

10. Johnson JR. 1991. Virulence factors in Escherichia coli urinary tract infection. Clin Microbiol Rev 4:80-128.

11. Russo TA, Johnson JR. 2000. Proposal for a new inclusive designation for extraintestinal pathogenic isolates of Escherichia coli: ExPEC. J Infect Dis 181:1753-4.

12. Dobrindt U, Hacker J. 2001. Whole genome plasticity in pathogenic bacteria. Curr Opin Microbiol 4:550-7.

13. Johnson JR, Delavari P, O'Bryan TT. 2001. Escherichia coli O18:K1:H7 isolates from patients with acute cystitis and neonatal meningitis exhibit common phylogenetic origins and virulence factor profiles. J Infect Dis 183:425-34.

14. Spurbeck RR, Dinh PC, Jr., Walk ST, Stapleton AE, Hooton TM, Nolan LK, Kim KS, Johnson JR, Mobley HL. 2012. Escherichia coli isolates that carry vat, fyuA, chuA, and yfcV efficiently colonize the urinary tract. Infect Immun 80:4115-22.

15. Toval F, Kohler CD, Vogel U, Wagenlehner F, Mellmann A, Fruth A, Schmidt MA, Karch H, Bielaszewska M, Dobrindt U. 2014. Characterization of Escherichia coli isolates from hospital inpatients or outpatients with urinary tract infection. J Clin Microbiol 52:407-18.

16. Ratledge C, Dover LG. 2000. Iron metabolism in pathogenic bacteria. Annu Rev Microbiol 54:881-941.

17. Skaar EP. 2010. The battle for iron between bacterial pathogens and their vertebrate hosts. PLoS Pathog 6:e1000949.

18. Touati D. 2000. Iron and oxidative stress in bacteria. Arch Biochem Biophys 373:1-6.

19. Cotter PA, Darie S, Gunsalus RP. 1992. The effect of iron limitation on expression of the aerobic and anaerobic electron transport pathway genes in Escherichia coli. FEMS Microbiol Lett 100:227-32.

20. Nicholson BA, West AC, Mangiamele P, Barbieri N, Wannemuehler Y, Nolan LK, Logue CM, Li G. 2016. Genetic Characterization of ExPEC-Like Virulence Plasmids among a Subset of NMEC. PLoS One 11:e0147757.

21. Subashchandrabose S, Smith SN, Spurbeck RR, Kole MM, Mobley HL. 2013. Genome-wide detection of fitness genes in uropathogenic Escherichia coli during systemic infection. PLoS Pathog 9:e1003788.

22. Brumbaugh AR, Smith SN, Subashchandrabose S, Himpsl SD, Hazen TH, Rasko DA, Mobley HL. 2015. Blocking yersiniabactin import attenuates extraintestinal pathogenic Escherichia coli in cystitis and pyelonephritis and represents a novel target to prevent urinary tract infection. Infect Immun 83:1443-50.

23. Ranjan A, Shaik S, Nandanwar N, Hussain A, Tiwari SK, Semmler T, Jadhav S, Wieler LH, Alam M, Colwell RR, Ahmed N. 2017. Comparative Genomics of Escherichia coli Isolated from Skin and Soft Tissue and Other Extraintestinal Infections. MBio 8.

24. Wijetunge DS, Gongati S, DebRoy C, Kim KS, Couraud PO, Romero IA, Weksler B, Kariyawasam S. 2015. Characterizing the pathotype of neonatal meningitis causing Escherichia coli (NMEC). BMC Microbiol 15:211.

25. Robins-Browne RM, Holt KE, Ingle DJ, Hocking DM, Yang J, Tauschek M. 2016. Are Escherichia coli Pathotypes Still Relevant in the Era of Whole-Genome Sequencing? Front Cell Infect Microbiol 6:141.

26. Foxman B. 2010. The epidemiology of urinary tract infection. Nat Rev Urol 7:653-60.

27. Stamm WE, Norrby SR. 2001. Urinary tract infections: disease panorama and challenges. J Infect Dis 183 Suppl 1:S1-4.

28. Schappert SM, Rechtsteiner EA. 2011. Ambulatory medical care utilization estimates for 2007. Vital Health Stat 13:1-38.

29. Flores-Mireles AL, Walker JN, Caparon M, Hultgren SJ. 2015. Urinary tract infections: epidemiology, mechanisms of infection and treatment options. Nat Rev Microbiol 13:269-84.

30. Tabibian JH, Gornbein J, Heidari A, Dien SL, Lau VH, Chahal P, Churchill BM, Haake DA. 2008. Uropathogens and host characteristics. J Clin Microbiol 46:3980-6.

31. Zhao L, Chen X, Zhu X, Yang W, Dong L, Xu X, Gao S, Liu X. 2009. Prevalence of virulence factors and antimicrobial resistance of uropathogenic Escherichia coli in Jiangsu province (China). Urology 74:702-7.

32. Kazemnia A, Ahmadi M, Dilmaghani M. 2014. Antibiotic resistance pattern of different Escherichia coli phylogenetic groups isolated from human urinary tract infection and avian colibacillosis. Iran Biomed J 18:219-24.

33. Foxman B. 2014. Urinary tract infection syndromes: occurrence, recurrence, bacteriology, risk factors, and disease burden. Infect Dis Clin North Am 28:1-13.

34. Shariff VAA, Shenoy MS, Yadav T, M R. 2013. The antibiotic susceptibility patterns of uropathogenic Escherichia coli, with special reference to the fluoroquinolones. J Clin Diagn Res 7:1027-30.

35. Johnson CC. 1991. Definitions, classification, and clinical presentation of urinary tract infections. Med Clin North Am 75:241-52.

36. Geerlings SE. 2016. Clinical Presentations and Epidemiology of Urinary Tract Infections. Microbiol Spectr 4.

37. Hooton TM, Bradley SF, Cardenas DD, Colgan R, Geerlings SE, Rice JC, Saint S, Schaeffer AJ, Tambayh PA, Tenke P, Nicolle LE, Infectious Diseases Society of A. 2010. Diagnosis, prevention, and treatment of catheter-associated urinary tract infection in adults: 2009 International Clinical Practice Guidelines from the Infectious Diseases Society of America. Clin Infect Dis 50:625-63.

38. Nicolle LE, Committee* ACG. 2005. Complicated urinary tract infection in adults. Can J Infect Dis Med Microbiol 16:349-60.

39. Foxman B. 2002. Epidemiology of urinary tract infections: incidence, morbidity, and economic costs. Am J Med 113 Suppl 1A:5S-13S.

40. Foxman B, Gillespie B, Koopman J, Zhang L, Palin K, Tallman P, Marsh JV, Spear S, Sobel JD, Marty MJ, Marrs CF. 2000. Risk factors for second urinary tract infection among college women. Am J Epidemiol 151:1194-205.

41. Hooton TM, Stamm WE. 1997. Diagnosis and treatment of uncomplicated urinary tract infection. Infect Dis Clin North Am 11:551-81.

42. Laupland KB, Ross T, Pitout JD, Church DL, Gregson DB. 2007. Community-onset urinary tract infections: a population-based assessment. Infection 35:150-3.

43. Yamamoto S, Tsukamoto T, Terai A, Kurazono H, Takeda Y, Yoshida O. 1997. Genetic evidence supporting the fecal-perineal-urethral hypothesis in cystitis caused by Escherichia coli. J Urol 157:1127-9.

44. McLellan LK, Hunstad DA. 2016. Urinary Tract Infection: Pathogenesis and Outlook. Trends Mol Med 22:946-957.

45. Little P, Merriman R, Turner S, Rumsby K, Warner G, Lowes JA, Smith H, Hawke C, Leydon G, Mullee M, Moore MV. 2010. Presentation, pattern, and natural course of severe symptoms, and role of antibiotics and antibiotic resistance among patients presenting with suspected uncomplicated urinary tract infection in primary care: observational study. BMJ 340:b5633.

46. Hooton TM. 2001. Recurrent urinary tract infection in women. Int J Antimicrob Agents 17:259-68.

47. Foxman B, Barlow R, D'Arcy H, Gillespie B, Sobel JD. 2000. Urinary tract infection: self-reported incidence and associated costs. Ann Epidemiol 10:509-15.

48. Christiaens TC, De Meyere M, Verschraegen G, Peersman W, Heytens S, De Maeseneer JM. 2002. Randomised controlled trial of nitrofurantoin versus placebo in the treatment of uncomplicated urinary tract infection in adult women. Br J Gen Pract 52:729-34.

49. Brown P, Ki M, Foxman B. 2005. Acute pyelonephritis among adults: cost of illness and considerations for the economic evaluation of therapy. Pharmacoeconomics 23:1123-42.

50. Schneeberger C, Holleman F, Geerlings SE. 2016. Febrile urinary tract infections: pyelonephritis and urosepsis. Curr Opin Infect Dis 29:80-5.

51. Mann R, Mediati DG, Duggin IG, Harry EJ, Bottomley AL. 2017. Metabolic Adaptations of Uropathogenic E. coli in the Urinary Tract. Front Cell Infect Microbiol 7:241.

52. Kaye D. 1968. Antibacterial activity of human urine. J Clin Invest 47:2374-90.

53. Sobel JD. 1997. Pathogenesis of urinary tract infection. Role of host defenses. Infect Dis Clin North Am 11:531-49.

54. Mulvey MA, Lopez-Boado YS, Wilson CL, Roth R, Parks WC, Heuser J, Hultgren SJ. 1998. Induction and evasion of host defenses by type 1-piliated uropathogenic Escherichia coli. Science 282:1494-7.

55. Cox CE, Hinman F, Jr. 1961. Experiments with induced bacteriuria, vesical emptying and bacterial growth on the mechanism of bladder defense to infection. J Urol 86:739-48.

56. Carlson KV, Rome S, Nitti VW. 2001. Dysfunctional voiding in women. J Urol 165:143-7; discussion 147-8.

57. Blumenthal I. 2006. Vesicoureteric reflux and urinary tract infection in children. Postgrad Med J 82:31-5.

58. Haraoka M, Hang L, Frendeus B, Godaly G, Burdick M, Strieter R, Svanborg C. 1999. Neutrophil recruitment and resistance to urinary tract infection. J Infect Dis 180:1220-9.

59. Spencer JD, Schwaderer AL, Becknell B, Watson J, Hains DS. 2014. The innate immune response during urinary tract infection and pyelonephritis. Pediatr Nephrol 29:1139-49.

60. Song J, Abraham SN. 2008. Innate and adaptive immune responses in the urinary tract. Eur J Clin Invest 38 Suppl 2:21-8.

61. Blanco M, Blanco JE, Alonso MP, Mora A, Balsalobre C, Munoa F, Juarez A, Blanco J. 1997. Detection of pap, sfa and afa adhesin-encoding operons in uropathogenic

Escherichia coli strains: relationship with expression of adhesins and production of toxins. Res Microbiol 148:745-55.

62. Lloyd AL, Henderson TA, Vigil PD, Mobley HL. 2009. Genomic islands of uropathogenic Escherichia coli contribute to virulence. J Bacteriol 191:3469-81.

63. Hacker J, Blum-Oehler G, Muhldorfer I, Tschape H. 1997. Pathogenicity islands of virulent bacteria: structure, function and impact on microbial evolution. Mol Microbiol 23:1089-97.

64. Lloyd AL, Rasko DA, Mobley HL. 2007. Defining genomic islands and uropathogen-specific genes in uropathogenic Escherichia coli. J Bacteriol 189:3532-46.

65. Subashchandrabose S, Hazen TH, Rasko DA, Mobley HL. 2013. Draft genome sequences of five recent human uropathogenic Escherichia coli isolates. Pathog Dis 69:66-70.

66. Amsler CD, Cho M, Matsumura P. 1993. Multiple factors underlying the maximum motility of Escherichia coli as cultures enter post-exponential growth. J Bacteriol 175:6238-44.

67. Lauffenburger DA. 1991. Quantitative studies of bacterial chemotaxis and microbial population dynamics. Microb Ecol 22:175-85.

68. Hansen CH, Endres RG, Wingreen NS. 2008. Chemotaxis in Escherichia coli: a molecular model for robust precise adaptation. PLoS Comput Biol 4:e1.

69. Kearns DB. 2010. A field guide to bacterial swarming motility. Nat Rev Microbiol 8:634-44.

70. Swiecicki JM, Sliusarenko O, Weibel DB. 2013. From swimming to swarming: Escherichia coli cell motility in two-dimensions. Integr Biol (Camb) 5:1490-4.

71. Armitage JP. 1992. Bacterial motility and chemotaxis. Sci Prog 76:451-77.

72. Harshey RM, Matsuyama T. 1994. Dimorphic transition in Escherichia coli and Salmonella typhimurium: surface-induced differentiation into hyperflagellate swarmer cells. Proc Natl Acad Sci U S A 91:8631-5.

73. Berg HC, Anderson RA. 1973. Bacteria swim by rotating their flagellar filaments. Nature 245:380-2.

74. Macnab RM. 1992. Genetics and biogenesis of bacterial flagella. Annu Rev Genet 26:131-58.

75. Chilcott GS, Hughes KT. 2000. Coupling of flagellar gene expression to flagellar assembly in Salmonella enterica serovar typhimurium and Escherichia coli. Microbiol Mol Biol Rev 64:694-708.

76. Soutourina OA, Bertin PN. 2003. Regulation cascade of flagellar expression in Gram-negative bacteria. FEMS Microbiol Rev 27:505-23.

77. Wang S, Fleming RT, Westbrook EM, Matsumura P, McKay DB. 2006. Structure of the Escherichia coli FlhDC complex, a prokaryotic heteromeric regulator of transcription. J Mol Biol 355:798-808.

78. Fitzgerald DM, Bonocora RP, Wade JT. 2014. Comprehensive mapping of the Escherichia coli flagellar regulatory network. PLoS Genet 10:e1004649.

79. Liu X, Fujita N, Ishihama A, Matsumura P. 1995. The C-terminal region of the alpha subunit of Escherichia coli RNA polymerase is required for transcriptional activation of the flagellar level II operons by the FlhD/FlhC complex. J Bacteriol 177:5186-8.

80. Silverman M, Simon M. 1977. Chemotaxis in Escherichia coli: methylation of che gene products. Proc Natl Acad Sci U S A 74:3317-21.

81. Helmann JD, Chamberlin MJ. 1987. DNA sequence analysis suggests that expression of flagellar and chemotaxis genes in Escherichia coli and Salmonella typhimurium is controlled by an alternative sigma factor. Proc Natl Acad Sci U S A 84:6422-4.

82. Manson MD, Tedesco P, Berg HC, Harold FM, Van der Drift C. 1977. A protonmotive force drives bacterial flagella. Proc Natl Acad Sci U S A 74:3060-4.

83. Guttenplan SB, Shaw S, Kearns DB. 2013. The cell biology of peritrichous flagella in Bacillus subtilis. Mol Microbiol 87:211-29.

84. Scharf BE, Fahrner KA, Turner L, Berg HC. 1998. Control of direction of flagellar rotation in bacterial chemotaxis. Proc Natl Acad Sci U S A 95:201-6.

85. Zaslaver A, Mayo AE, Rosenberg R, Bashkin P, Sberro H, Tsalyuk M, Surette MG, Alon U. 2004. Just-in-time transcription program in metabolic pathways. Nat Genet 36:486-91.

86. Zhao K, Liu M, Burgess RR. 2007. Adaptation in bacterial flagellar and motility systems: from regulon members to 'foraging'-like behavior in E. coli. Nucleic Acids Res 35:4441-52.

87. Paradis G, Chevance FFV, Liou W, Renault TT, Hughes KT, Rainville S, Erhardt M. 2017. Variability in bacterial flagella re-growth patterns after breakage. Sci Rep 7:1282.

88. Yoon SI, Kurnasov O, Natarajan V, Hong M, Gudkov AV, Osterman AL, Wilson IA. 2012. Structural basis of TLR5-flagellin recognition and signaling. Science 335:859-64.

89. Barker CS, Pruss BM, Matsumura P. 2004. Increased motility of Escherichia coli by insertion sequence element integration into the regulatory region of the flhD operon. J Bacteriol 186:7529-37.

90. Yakhnin AV, Baker CS, Vakulskas CA, Yakhnin H, Berezin I, Romeo T, Babitzke P. 2013. CsrA activates flhDC expression by protecting flhDC mRNA from RNase E-mediated cleavage. Mol Microbiol 87:851-66.

91. Li C, Louise CJ, Shi W, Adler J. 1993. Adverse conditions which cause lack of flagella in Escherichia coli. J Bacteriol 175:2229-35.

92. Shin S, Park C. 1995. Modulation of flagellar expression in Escherichia coli by acetyl phosphate and the osmoregulator OmpR. J Bacteriol 177:4696-702.

93. Lehnen D, Blumer C, Polen T, Wackwitz B, Wendisch VF, Unden G. 2002. LrhA as a new transcriptional key regulator of flagella, motility and chemotaxis genes in Escherichia coli. Mol Microbiol 45:521-32.

94. Thomason MK, Fontaine F, De Lay N, Storz G. 2012. A small RNA that regulates motility and biofilm formation in response to changes in nutrient availability in Escherichia coli. Mol Microbiol 84:17-35.

95. Sperandio V, Torres AG, Kaper JB. 2002. Quorum sensing Escherichia coli regulators B and C (QseBC): a novel two-component regulatory system involved in the regulation of flagella and motility by quorum sensing in E. coli. Mol Microbiol 43:809-21.

96. Soutourina O, Kolb A, Krin E, Laurent-Winter C, Rimsky S, Danchin A, Bertin P. 1999. Multiple control of flagellum biosynthesis in Escherichia coli: role of H-NS protein and the cyclic AMP-catabolite activator protein complex in transcription of the flhDC master operon. J Bacteriol 181:7500-8.

97. Tipton KA, Rather PN. 2016. An ompR/envZ Two-Component System Ortholog Regulates Phase Variation, Osmotic Tolerance, Motility, and Virulence in Acinetobacter baumannii strain AB5075. J Bacteriol doi:10.1128/JB.00705-16.

98. Cai SJ, Inouye M. 2002. EnvZ-OmpR interaction and osmoregulation in Escherichia coli. J Biol Chem 277:24155-61.

99. Pruss BM. 1998. Acetyl phosphate and the phosphorylation of OmpR are involved in the regulation of the cell division rate in Escherichia coli. Arch Microbiol 170:141-6.

100. Lane MC, Lockatell V, Monterosso G, Lamphier D, Weinert J, Hebel JR, Johnson DE, Mobley HL. 2005. Role of motility in the colonization of uropathogenic Escherichia coli in the urinary tract. Infect Immun 73:7644-56.

101. Lane MC, Alteri CJ, Smith SN, Mobley HL. 2007. Expression of flagella is coincident with uropathogenic Escherichia coli ascension to the upper urinary tract. Proc Natl Acad Sci U S A 104:16669-74.

102. Wright KJ, Seed PC, Hultgren SJ. 2005. Uropathogenic Escherichia coli flagella aid in efficient urinary tract colonization. Infect Immun 73:7657-68.

103. Schwan WR. 2008. Flagella allow uropathogenic Escherichia coli ascension into murine kidneys. Int J Med Microbiol 298:441-7.

104. Lane MC, Simms AN, Mobley HL. 2007. complex interplay between type 1 fimbrial expression and flagellum-mediated motility of uropathogenic Escherichia coli. J Bacteriol 189:5523-33.

105. Herrmann B, Burman LG. 1985. Pathogenesis of Escherichia coli cystitis and pyelonephritis: apparent lack of significance of bacterial motility and chemotaxis towards human urine. Infection 13:4-7.

106. Snyder JA, Haugen BJ, Buckles EL, Lockatell CV, Johnson DE, Donnenberg MS, Welch RA, Mobley HL. 2004. Transcriptome of uropathogenic Escherichia coli during urinary tract infection. Infect Immun 72:6373-81.

107. Smith KD, Andersen-Nissen E, Hayashi F, Strobe K, Bergman MA, Barrett SL, Cookson BT, Aderem A. 2003. Toll-like receptor 5 recognizes a conserved site on flagellin required for protofilament formation and bacterial motility. Nat Immunol 4:1247-53.

108. Smith DR, Chapman MR. 2010. Economical evolution: microbes reduce the synthetic cost of extracellular proteins. MBio 1.

109. Kakkanat A, Totsika M, Schaale K, Duell BL, Lo AW, Phan MD, Moriel DG, Beatson SA, Sweet MJ, Ulett GC, Schembri MA. 2015. The role of H4 flagella in Escherichia coli ST131 virulence. Sci Rep 5:16149.

110. Sharon N, Eshdat Y, Silverblatt FJ, Ofek I. 1981. Bacterial adherence to cell surface sugars. Ciba Found Symp 80:119-41.

111. Berne C, Ducret A, Hardy GG, Brun YV. 2015. Adhesins Involved in Attachment to Abiotic Surfaces by Gram-Negative Bacteria. Microbiol Spectr 3.

112. Wurpel DJ, Beatson SA, Totsika M, Petty NK, Schembri MA. 2013. Chaperone-usher fimbriae of Escherichia coli. PLoS One 8:e52835.

113. Sjollema J, van der Mei HC, Hall CL, Peterson BW, de Vries J, Song L, Jong ED, Busscher HJ, Swartjes J. 2017. Detachment and successive re-attachment of multiple, reversibly-binding tethers result in irreversible bacterial adhesion to surfaces. Sci Rep 7:4369.

114. Vigil PD, Stapleton AE, Johnson JR, Hooton TM, Hodges AP, He Y, Mobley HL. 2011. Presence of putative repeat-in-toxin gene tosA in Escherichia coli predicts successful colonization of the urinary tract. MBio 2:e00066-11.

115. Spurbeck RR, Stapleton AE, Johnson JR, Walk ST, Hooton TM, Mobley HL. 2011. Fimbrial profiles predict virulence of uropathogenic Escherichia coli strains: contribution of ygi and yad fimbriae. Infect Immun 79:4753-63.

116. Kaye D. 1975. Host defense mechanisms in the urinary tract. Urol Clin North Am 2:407-22.

117. Thomas WE, Trintchina E, Forero M, Vogel V, Sokurenko EV. 2002. Bacterial adhesion to target cells enhanced by shear force. Cell 109:913-23.

118. Song J, Bishop BL, Li G, Duncan MJ, Abraham SN. 2007. TLR4-initiated and cAMP-mediated abrogation of bacterial invasion of the bladder. Cell Host Microbe 1:287-98.

119. Herwald H, Morgelin M, Olsen A, Rhen M, Dahlback B, Muller-Esterl W, Bjorck L. 1998. Activation of the contact-phase system on bacterial surfaces--a clue to serious complications in infectious diseases. Nat Med 4:298-302.

120. Frendeus B, Wachtler C, Hedlund M, Fischer H, Samuelsson P, Svensson M, Svanborg C. 2001. Escherichia coli P fimbriae utilize the Toll-like receptor 4 pathway for cell activation. Mol Microbiol 40:37-51.

121. Kansal R, Rasko DA, Sahl JW, Munson GP, Roy K, Luo Q, Sheikh A, Kuhne KJ, Fleckenstein JM. 2013. Transcriptional modulation of enterotoxigenic Escherichia coli virulence genes in response to epithelial cell interactions. Infect Immun 81:259-70.

122. Baorto DM, Gao Z, Malaviya R, Dustin ML, van der Merwe A, Lublin DM, Abraham SN. 1997. Survival of FimH-expressing enterobacteria in macrophages relies on glycolipid traffic. Nature 389:636-9.

123. Fexby S, Bjarnsholt T, Jensen PO, Roos V, Hoiby N, Givskov M, Klemm P. 2007. Biological Trojan horse: Antigen 43 provides specific bacterial uptake and survival in human neutrophils. Infect Immun 75:30-4.

124. Kenny B, DeVinney R, Stein M, Reinscheid DJ, Frey EA, Finlay BB. 1997. Enteropathogenic E. coli (EPEC) transfers its receptor for intimate adherence into mammalian cells. Cell 91:511-20.

125. Watarai M, Tobe T, Yoshikawa M, Sasakawa C. 1995. Contact of Shigella with host cells triggers release of Ipa invasins and is an essential function of invasiveness. EMBO J 14:2461-70.

126. Sjolinder H, Eriksson J, Maudsdotter L, Aro H, Jonsson AB. 2008. Meningococcal outer membrane protein NhhA is essential for colonization and disease by preventing phagocytosis and complement attack. Infect Immun 76:5412-20.

127. Kirjavainen V, Jarva H, Biedzka-Sarek M, Blom AM, Skurnik M, Meri S. 2008. Yersinia enterocolitica serum resistance proteins YadA and ail bind the complement regulator C4b-binding protein. PLoS Pathog 4:e1000140.

128. Mikaty G, Soyer M, Mairey E, Henry N, Dyer D, Forest KT, Morand P, Guadagnini S, Prevost MC, Nassif X, Dumenil G. 2009. Extracellular bacterial pathogen induces host cell surface reorganization to resist shear stress. PLoS Pathog 5:e1000314.

129. Chahales P, Thanassi DG. 2015. Structure, Function, and Assembly of Adhesive Organelles by Uropathogenic Bacteria. Microbiol Spectr 3.

130. Linhartova I, Bumba L, Masin J, Basler M, Osicka R, Kamanova J, Prochazkova K, Adkins I, Hejnova-Holubova J, Sadilkova L, Morova J, Sebo P. 2010. RTX proteins: a highly diverse family secreted by a common mechanism. FEMS Microbiol Rev 34:1076-112.

131. Vigil PD, Alteri CJ, Mobley HL. 2011. Identification of in vivo-induced antigens including an RTX family exoprotein required for uropathogenic Escherichia coli virulence. Infect Immun 79:2335-44.

132. Vigil PD, Wiles TJ, Engstrom MD, Prasov L, Mulvey MA, Mobley HL. 2012. The repeat-in-toxin family member TosA mediates adherence of uropathogenic Escherichia coli and survival during bacteremia. Infect Immun 80:493-505.

133. Engstrom MD, Mobley HL. 2016. Regulation of Expression of Uropathogenic Escherichia coli Nonfimbrial Adhesin TosA by PapB Homolog TosR in Conjunction with H-NS and Lrp. Infect Immun 84:811-21.

134. Engstrom MD, Alteri CJ, Mobley HL. 2014. A conserved PapB family member, TosR, regulates expression of the uropathogenic Escherichia coli RTX nonfimbrial adhesin TosA while conserved LuxR family members TosE and TosF suppress motility. Infect Immun 82:3644-56.

135. Busch A, Waksman G. 2012. Chaperone-usher pathways: diversity and pilus assembly mechanism. Philos Trans R Soc Lond B Biol Sci 367:1112-22.

136. Hultgren SJ, Porter TN, Schaeffer AJ, Duncan JL. 1985. Role of type 1 pili and effects of phase variation on lower urinary tract infections produced by Escherichia coli. Infect Immun 50:370-7.

137. Nowicki B, Rhen M, Vaisanen-Rhen V, Pere A, Korhonen TK. 1984. Immunofluorescence study of fimbrial phase variation in Escherichia coli KS71. J Bacteriol 160:691-5.

138. Mitsumori K, Terai A, Yamamoto S, Yoshida O. 1998. Identification of S, F1C and three PapG fimbrial adhesins in uropathogenic Escherichia coli by polymerase chain reaction. FEMS Immunol Med Microbiol 21:261-8.

139. Buckles EL, Bahrani-Mougeot FK, Molina A, Lockatell CV, Johnson DE, Drachenberg CB, Burland V, Blattner FR, Donnenberg MS. 2004. Identification and characterization of a novel uropathogenic Escherichia coli-associated fimbrial gene cluster. Infect Immun 72:3890-901.

140. Connell I, Agace W, Klemm P, Schembri M, Marild S, Svanborg C. 1996. Type 1 fimbrial expression enhances Escherichia coli virulence for the urinary tract. Proc Natl Acad Sci U S A 93:9827-32.

141. Giampapa CS, Abraham SN, Chiang TM, Beachey EH. 1988. Isolation and characterization of a receptor for type 1 fimbriae of Escherichia coli from guinea pig erythrocytes. J Biol Chem 263:5362-7.

142. Welch RA, Burland V, Plunkett G, 3rd, Redford P, Roesch P, Rasko D, Buckles EL, Liou SR, Boutin A, Hackett J, Stroud D, Mayhew GF, Rose DJ, Zhou S, Schwartz DC, Perna NT, Mobley HL, Donnenberg MS, Blattner FR. 2002. Extensive mosaic structure revealed by the complete genome sequence of uropathogenic Escherichia coli. Proc Natl Acad Sci U S A 99:17020-4.

143. Klemm P, Jorgensen BJ, van Die I, de Ree H, Bergmans H. 1985. The fim genes responsible for synthesis of type 1 fimbriae in Escherichia coli, cloning and genetic organization. Mol Gen Genet 199:410-4.

144. Hamrick TS, Harris SL, Spears PA, Havell EA, Horton JR, Russell PW, Orndorff PE. 2000. Genetic characterization of Escherichia coli type 1 pilus adhesin mutants and identification of a novel binding phenotype. J Bacteriol 182:4012-21.

145. Wu XR, Sun TT, Medina JJ. 1996. In vitro binding of type 1-fimbriated Escherichia coli to uroplakins Ia and Ib: relation to urinary tract infections. Proc Natl Acad Sci U S A 93:9630-5.

146. Xie B, Zhou G, Chan SY, Shapiro E, Kong XP, Wu XR, Sun TT, Costello CE. 2006. Distinct glycan structures of uroplakins Ia and Ib: structural basis for the selective binding of FimH adhesin to uroplakin Ia. J Biol Chem 281:14644-53.

147. Hull RA, Donovan WH, Del Terzo M, Stewart C, Rogers M, Darouiche RO. 2002. Role of type 1 fimbria- and P fimbria-specific adherence in colonization of the neurogenic human bladder by Escherichia coli. Infect Immun 70:6481-4.

148. Lim JK, Gunther NWt, Zhao H, Johnson DE, Keay SK, Mobley HL. 1998. In vivo phase variation of Escherichia coli type 1 fimbrial genes in women with urinary tract infection. Infect Immun 66:3303-10.

149. Gunther NWt, Lockatell V, Johnson DE, Mobley HL. 2001. In vivo dynamics of type 1 fimbria regulation in uropathogenic Escherichia coli during experimental urinary tract infection. Infect Immun 69:2838-46.

150. Hagan EC, Lloyd AL, Rasko DA, Faerber GJ, Mobley HL. 2010. Escherichia coli global gene expression in urine from women with urinary tract infection. PLoS Pathog 6:e1001187.

151. Otto G, Sandberg T, Marklund BI, Ulleryd P, Svanborg C. 1993. Virulence factors and pap genotype in Escherichia coli isolates from women with acute pyelonephritis, with or without bacteremia. Clin Infect Dis 17:448-56.

152. Johnson JR. 1998. papG alleles among Escherichia coli strains causing urosepsis: associations with other bacterial characteristics and host compromise. Infect Immun 66:4568-71.

153. Mobley HL, Jarvis KG, Elwood JP, Whittle DI, Lockatell CV, Russell RG, Johnson DE, Donnenberg MS, Warren JW. 1993. Isogenic P-fimbrial deletion mutants of pyelonephritogenic Escherichia coli: the role of alpha Gal(1-4) beta Gal binding in virulence of a wild-type strain. Mol Microbiol 10:143-55.

154. Totsika M, Beatson SA, Holden N, Gally DL. 2008. Regulatory interplay between pap operons in uropathogenic Escherichia coli. Mol Microbiol 67:996-1011.

155. Vaisanen V, Elo J, Tallgren LG, Siitonen A, Makela PH, Svanborg-Eden C, Kallenius G, Svenson SB, Hultberg H, Korhonen T. 1981. Mannose-resistant haemagglutination and P antigen recognition are characteristic of Escherichia coli causing primary pyelonephritis. Lancet 2:1366-9.

156. van der Bosch JF, Verboom-Sohmer U, Postma P, de Graaff J, MacLaren DM. 1980. Mannose-sensitive and mannose-resistant adherence to human uroepithelial cells and urinary virulence of Escherichia coli. Infect Immun 29:226-33.

157. Roberts JA, Marklund BI, Ilver D, Haslam D, Kaack MB, Baskin G, Louis M, Mollby R, Winberg J, Normark S. 1994. The Gal(alpha 1-4)Gal-specific tip adhesin of Escherichia coli P-fimbriae is needed for pyelonephritis to occur in the normal urinary tract. Proc Natl Acad Sci U S A 91:11889-93.

158. Wullt B, Bergsten G, Connell H, Rollano P, Gebretsadik N, Hull R, Svanborg C. 2000. P fimbriae enhance the early establishment of Escherichia coli in the human urinary tract. Mol Microbiol 38:456-64.

159. Sivick KE, Mobley HL. 2010. Waging war against uropathogenic Escherichia coli: winning back the urinary tract. Infect Immun 78:568-85.

160. Hedlund M, Svensson M, Nilsson A, Duan RD, Svanborg C. 1996. Role of the ceramide-signaling pathway in cytokine responses to P-fimbriated Escherichia coli. J Exp Med 183:1037-44.

161. Wullt B. 2003. The role of P fimbriae for Escherichia coli establishment and mucosal inflammation in the human urinary tract. Int J Antimicrob Agents 21:605-21.

162. Wullt B, Bergsten G, Samuelsson M, Gebretsadik N, Hull R, Svanborg C. 2001. The role of P fimbriae for colonization and host response induction in the human urinary tract. J Infect Dis 183 Suppl 1:S43-6.

163. Holden NJ, Totsika M, Mahler E, Roe AJ, Catherwood K, Lindner K, Dobrindt U, Gally DL. 2006. Demonstration of regulatory cross-talk between P fimbriae and type 1 fimbriae in uropathogenic Escherichia coli. Microbiology 152:1143-53.

164. Arthur M, Campanelli C, Arbeit RD, Kim C, Steinbach S, Johnson CE, Rubin RH, Goldstein R. 1989. Structure and copy number of gene clusters related to the pap P-adhesin operon of uropathogenic Escherichia coli. Infect Immun 57:314-21.

165. Dodson KW, Jacob-Dubuisson F, Striker RT, Hultgren SJ. 1993. Outer-membrane PapC molecular usher discriminately recognizes periplasmic chaperone-pilus subunit complexes. Proc Natl Acad Sci U S A 90:3670-4.

166. Blyn LB, Braaten BA, Low DA. 1990. Regulation of pap pilin phase variation by a mechanism involving differential dam methylation states. EMBO J 9:4045-54.

167. Kaltenbach LS, Braaten BA, Low DA. 1995. Specific binding of PapI to Lrp-pap DNA complexes. J Bacteriol 177:6449-55.

168. Hernday AD, Braaten BA, Low DA. 2003. The mechanism by which DNA adenine methylase and PapI activate the pap epigenetic switch. Mol Cell 12:947-57.

169. Reiss DJ, Mobley HL. 2011. Determination of target sequence bound by PapX, repressor of bacterial motility, in flhD promoter using systematic evolution of ligands by exponential enrichment (SELEX) and high throughput sequencing. J Biol Chem 286:44726-38.

170. Li X, Rasko DA, Lockatell CV, Johnson DE, Mobley HL. 2001. Repression of bacterial motility by a novel fimbrial gene product. EMBO J 20:4854-62.

171. Grove A. 2013. MarR family transcription factors. Curr Biol 23:R142-3.

172. Alekshun MN, Levy SB, Mealy TR, Seaton BA, Head JF. 2001. The crystal structure of MarR, a regulator of multiple antibiotic resistance, at 2.3 A resolution. Nat Struct Biol 8:710-4.

173. Seoane AS, Levy SB. 1995. Characterization of MarR, the repressor of the multiple antibiotic resistance (mar) operon in Escherichia coli. J Bacteriol 177:3414-9.

174. Grove A. 2017. Regulation of Metabolic Pathways by MarR Family Transcription Factors. Comput Struct Biotechnol J 15:366-371.

175. Wilkinson SP, Grove A. 2004. HucR, a novel uric acid-responsive member of the MarR family of transcriptional regulators from Deinococcus radiodurans. J Biol Chem 279:51442-50.

176. Simms AN, Mobley HL. 2008. PapX, a P fimbrial operon-encoded inhibitor of motility in uropathogenic Escherichia coli. Infect Immun 76:4833-41.

177. Reiss DJ, Howard FM, Mobley HL. 2012. A novel approach for transcription factor analysis using SELEX with high-throughput sequencing (TFAST). PLoS One 7:e42761.

178. Marklund BI, Tennent JM, Garcia E, Hamers A, Baga M, Lindberg F, Gaastra W, Normark S. 1992. Horizontal gene transfer of the Escherichia coli pap and prs pili operons as a mechanism for the development of tissue-specific adhesive properties. Mol Microbiol 6:2225-42.

179. Siitonen A, Martikainen R, Ikaheimo R, Palmgren J, Makela PH. 1993. Virulence-associated characteristics of Escherichia coli in urinary tract infection: a statistical analysis with special attention to type 1C fimbriation. Microb Pathog 15:65-75.

180. Orskov I, Orskov F, Birch-Andersen A. 1980. Comparison of Escherichia coli fimbrial antigen F7 with type 1 fimbriae. Infect Immun 27:657-66.

181. Klemm P, Orskov I, Orskov F. 1982. F7 and type 1-like fimbriae from three Escherichia coli strains isolated from urinary tract infections: protein chemical and immunological aspects. Infect Immun 36:462-8.

182. Backhed F, Alsen B, Roche N, Angstrom J, von Euler A, Breimer ME, Westerlund-Wikstrom B, Teneberg S, Richter-Dahlfors A. 2002. Identification of target tissue glycosphingolipid receptors for uropathogenic, F1C-fimbriated Escherichia coli and its role in mucosal inflammation. J Biol Chem 277:18198-205.

183. Khan AS, Kniep B, Oelschlaeger TA, Van Die I, Korhonen T, Hacker J. 2000. Receptor structure for F1C fimbriae of uropathogenic Escherichia coli. Infect Immun 68:3541-7.

184. Ko YC, Mukaida N, Ishiyama S, Tokue A, Kawai T, Matsushima K, Kasahara T. 1993. Elevated interleukin-8 levels in the urine of patients with urinary tract infections. Infect Immun 61:1307-14.

185. Riegman N, Kusters R, Van Veggel H, Bergmans H, Van Bergen en Henegouwen P, Hacker J, Van Die I. 1990. F1C fimbriae of a uropathogenic Escherichia coli strain: genetic and functional organization of the foc gene cluster and identification of minor subunits. J Bacteriol 172:1114-20.

186. Hultdin UW, Lindberg S, Grundstrom C, Huang S, Uhlin BE, Sauer-Eriksson AE. 2010. Structure of FocB--a member of a family of transcription factors regulating fimbrial adhesin expression in uropathogenic Escherichia coli. FEBS J 277:3368-81.

187. Spurbeck RR, Tarrien RJ, Mobley HL. 2012. Enzymatically active and inactive phosphodiesterases and diguanylate cyclases are involved in regulation of Motility or sessility in Escherichia coli CFT073. MBio 3.

188. Lasaro MA, Salinger N, Zhang J, Wang Y, Zhong Z, Goulian M, Zhu J. 2009. F1C fimbriae play an important role in biofilm formation and intestinal colonization by the Escherichia coli commensal strain Nissle 1917. Appl Environ Microbiol 75:246-51.

189. Litwin MS, Saigal CS, Yano EM, Avila C, Geschwind SA, Hanley JM, Joyce GF, Madison R, Pace J, Polich SM, Wang M. 2005. Urologic diseases in America Project: analytical methods and principal findings. J Urol 173:933-7.

190. DeBusscher J, Zhang L, Buxton M, Foxman B, Barbosa-Cesnik C. 2009. Persistent extended-spectrum beta-lactamase urinary tract infection. Emerg Infect Dis 15:1862-4.

191. Schito GC, Naber KG, Botto H, Palou J, Mazzei T, Gualco L, Marchese A. 2009. The ARESC study: an international survey on the antimicrobial resistance of pathogens involved in uncomplicated urinary tract infections. Int J Antimicrob Agents 34:407-13.

192. Eden CS, Hansson HA. 1978. Escherichia coli pili as possible mediators of attachment to human urinary tract epithelial cells. Infect Immun 21:229-37.

193. Hung CS, Bouckaert J, Hung D, Pinkner J, Widberg C, DeFusco A, Auguste CG, Strouse R, Langermann S, Waksman G, Hultgren SJ. 2002. Structural basis of tropism of Escherichia coli to the bladder during urinary tract infection. Mol Microbiol 44:903-15.

194. O'Hanley P, Low D, Romero I, Lark D, Vosti K, Falkow S, Schoolnik G. 1985. Gal-Gal binding and hemolysin phenotypes and genotypes associated with uropathogenic Escherichia coli. N Engl J Med 313:414-20.

195. Ott M, Hacker J, Schmoll T, Jarchau T, Korhonen TK, Goebel W. 1986. Analysis of the genetic determinants coding for the S-fimbrial adhesin (sfa) in different Escherichia coli strains causing meningitis or urinary tract infections. Infect Immun 54:646-53.

196. Nowicki B, Svanborg-Eden C, Hull R, Hull S. 1989. Molecular analysis and epidemiology of the Dr hemagglutinin of uropathogenic Escherichia coli. Infect Immun 57:446-51.

197. Kallenius G, Dornbusch K, Hallander HO, Jakobsson K. 1981. Comparison of direct and standardized antibiotic susceptibility testing in bacteriuria. Chemotherapy 27:99-105.

198. Kallenius G, Mollby R, Svenson SB, Helin I, Hultberg H, Cedergren B, Winberg J. 1981. Occurrence of P-fimbriated Escherichia coli in urinary tract infections. Lancet 2:1369-72.

199. Johnson DE, Lockatell CV, Russell RG, Hebel JR, Island MD, Stapleton A, Stamm WE, Warren JW. 1998. Comparison of Escherichia coli strains recovered from human cystitis and pyelonephritis infections in transurethrally challenged mice. Infect Immun 66:3059-65.

200. Falkow S. 1988. Molecular Koch's postulates applied to microbial pathogenicity. Rev Infect Dis 10 Suppl 2:S274-6.

201. Hensel M, Shea JE, Gleeson C, Jones MD, Dalton E, Holden DW. 1995. Simultaneous identification of bacterial virulence genes by negative selection. Science 269:400-3.

202. Mei JM, Nourbakhsh F, Ford CW, Holden DW. 1997. Identification of Staphylococcus aureus virulence genes in a murine model of bacteraemia using signature-tagged mutagenesis. Mol Microbiol 26:399-407.

203. Chiang SL, Mekalanos JJ. 1998. Use of signature-tagged transposon mutagenesis to identify Vibrio cholerae genes critical for colonization. Mol Microbiol 27:797-805.

204. Sanschagrin F, Kukavica-Ibrulj I, Levesque RC. 2008. Essential genes in the infection model of Pseudomonas aeruginosa PCR-based signature-tagged mutagenesis. Methods Mol Biol 416:61-82.

205. Bahrani-Mougeot FK, Buckles EL, Lockatell CV, Hebel JR, Johnson DE, Tang CM, Donnenberg MS. 2002. Type 1 fimbriae and extracellular polysaccharides are preeminent uropathogenic Escherichia coli virulence determinants in the murine urinary tract. Mol Microbiol 45:1079-93.

206. Stapleton A, Moseley S, Stamm WE. 1991. Urovirulence determinants in Escherichia coli isolates causing first-episode and recurrent cystitis in women. J Infect Dis 163:773-9.

207. de Lorenzo V, Herrero M, Jakubzik U, Timmis KN. 1990. Mini-Tn5 transposon derivatives for insertion mutagenesis, promoter probing, and chromosomal insertion of cloned DNA in gram-negative eubacteria. J Bacteriol 172:6568-72.

208. Herrero M, de Lorenzo V, Timmis KN. 1990. Transposon vectors containing non-antibiotic resistance selection markers for cloning and stable chromosomal insertion of foreign genes in gram-negative bacteria. J Bacteriol 172:6557-67.

209. Blyn LB, Braaten BA, White-Ziegler CA, Rolfson DH, Low DA. 1989. Phase-variation of pyelonephritis-associated pili in Escherichia coli: evidence for transcriptional regulation. EMBO J 8:613-20.

210. Snyder JA, Lloyd AL, Lockatell CV, Johnson DE, Mobley HL. 2006. Role of phase variation of type 1 fimbriae in a uropathogenic Escherichia coli cystitis isolate during urinary tract infection. Infect Immun 74:1387-93.

211. Miller VL, Mekalanos JJ. 1988. A novel suicide vector and its use in construction of insertion mutations: osmoregulation of outer membrane proteins and virulence determinants in Vibrio cholerae requires toxR. J Bacteriol 170:2575-83.

212. Hanahan D. 1985. Techniques for transformation of *E. coli*. Oxford University Press, Washington DC.

213. Wang RF, Kushner SR. 1991. Construction of versatile low-copy-number vectors for cloning, sequencing and gene expression in Escherichia coli. Gene 100:195-9.

214. Hagberg L, Engberg I, Freter R, Lam J, Olling S, Svanborg Eden C. 1983. Ascending, unobstructed urinary tract infection in mice caused by pyelonephritogenic Escherichia coli of human origin. Infect Immun 40:273-83.

215. Johnson DE, Lockatell CV, Hall-Craigs M, Mobley HL, Warren JW. 1987. Uropathogenicity in rats and mice of Providencia stuartii from long-term catheterized patients. J Urol 138:632-5.

216. Snyder JA, Haugen BJ, Lockatell CV, Maroncle N, Hagan EC, Johnson DE, Welch RA, Mobley HL. 2005. Coordinate expression of fimbriae in uropathogenic Escherichia coli. Infect Immun 73:7588-96.

217. Welch RA, Dellinger EP, Minshew B, Falkow S. 1981. Haemolysin contributes to virulence of extra-intestinal E. coli infections. Nature 294:665-7.

218. Burall LS, Harro JM, Li X, Lockatell CV, Himpsl SD, Hebel JR, Johnson DE, Mobley HL. 2004. Proteus mirabilis genes that contribute to pathogenesis of urinary tract infection: identification of 25 signature-tagged mutants attenuated at least 100-fold. Infect Immun 72:2922-38.

219. Zhao H, Li X, Johnson DE, Mobley HL. 1999. Identification of protease and rpoN-associated genes of uropathogenic Proteus mirabilis by negative selection in a mouse model of ascending urinary tract infection. Microbiology 145 (Pt 1):185-95.

220. Himpsl SD, Lockatell CV, Hebel JR, Johnson DE, Mobley HL. 2008. Identification of virulence determinants in uropathogenic Proteus mirabilis using signature-tagged mutagenesis. J Med Microbiol 57:1068-78.

221. Kallenius G, Mollby R, Svenson SB, Winberg J, Hultberg H. 1980. Identification of a carbohydrate receptor recognized by uropathogenic Escherichia coli. Infection 8 Suppl 3:288-93.

222. Abraham JM, Freitag CS, Clements JR, Eisenstein BI. 1985. An invertible element of DNA controls phase variation of type 1 fimbriae of Escherichia coli. Proc Natl Acad Sci U S A 82:5724-7.

223. Gally DL, Leathart J, Blomfield IC. 1996. Interaction of FimB and FimE with the fim switch that controls the phase variation of type 1 fimbriae in Escherichia coli K-12. Mol Microbiol 21:725-38.

224. Xia Y, Gally D, Forsman-Semb K, Uhlin BE. 2000. Regulatory cross-talk between adhesin operons in Escherichia coli: inhibition of type 1 fimbriae expression by the PapB protein. EMBO J 19:1450-7.

225. Beuzon CR, Holden DW. 2001. Use of mixed infections with Salmonella strains to study virulence genes and their interactions in vivo. Microbes Infect 3:1345-52.

226. Keith BR, Maurer L, Spears PA, Orndorff PE. 1986. Receptor-binding function of type 1 pili effects bladder colonization by a clinical isolate of Escherichia coli. Infect Immun 53:693-6.

227. Gunther NWt, Snyder JA, Lockatell V, Blomfield I, Johnson DE, Mobley HL. 2002. Assessment of virulence of uropathogenic Escherichia coli type 1 fimbrial mutants in which the invertible element is phase-locked on or off. Infect Immun 70:3344-54.

228. Brooks T, Keevil CW. 1997. A simple artificial urine for the growth of urinary pathogens. Lett Appl Microbiol 24:203-6.

229. Jones SA, Jorgensen M, Chowdhury FZ, Rodgers R, Hartline J, Leatham MP, Struve C, Krogfelt KA, Cohen PS, Conway T. 2008. Glycogen and maltose utilization by Escherichia coli O157:H7 in the mouse intestine. Infect Immun 76:2531-40.

230. Anfora AT, Haugen BJ, Roesch P, Redford P, Welch RA. 2007. Roles of serine accumulation and catabolism in the colonization of the murine urinary tract by Escherichia coli CFT073. Infect Immun 75:5298-304.

231. Alteri CJ, Smith SN, Mobley HL. 2009. Fitness of Escherichia coli during urinary tract infection requires gluconeogenesis and the TCA cycle. PLoS Pathog 5:e1000448.

232. Novel M, Novel G. 1976. Regulation of beta-glucuronidase synthesis in Escherichia coli K-12: pleiotropic constitutive mutations affecting uxu and uidA expression. J Bacteriol 127:418-32.

233. Rodionov DA, Mironov AA, Rakhmaninova AB, Gelfand MS. 2000. Transcriptional regulation of transport and utilization systems for hexuronides, hexuronates and hexonates in gamma purple bacteria. Mol Microbiol 38:673-83.

234. Chang DE, Smalley DJ, Tucker DL, Leatham MP, Norris WE, Stevenson SJ, Anderson AB, Grissom JE, Laux DC, Cohen PS, Conway T. 2004. Carbon nutrition of Escherichia coli in the mouse intestine. Proc Natl Acad Sci U S A 101:7427-32.

235. Silverman R. 2000. The Organic Chemistry of Enzyme-catalyzed Reactions. Academic Press, San Diego.

236. Li Z, Bouckaert J, Deboeck F, De Greve H, Hernalsteens JP. 2012. Nicotinamide dependence of uropathogenic Escherichia coli UTI89 and application of nadB as a neutral insertion site. Microbiology 158:736-45.

237. Stewart V. 1993. Nitrate regulation of anaerobic respiratory gene expression in Escherichia coli. Mol Microbiol 9:425-34.

238. Clegg S, Yu F, Griffiths L, Cole JA. 2002. The roles of the polytopic membrane proteins NarK, NarU and NirC in Escherichia coli K-12: two nitrate and three nitrite transporters. Mol Microbiol 44:143-55.

239. Domenech-Sanchez A, Benedi VJ, Martinez-Martinez L, Alberti S. 2006. Evaluation of differential gene expression in susceptible and resistant clinical isolates of Klebsiella pneumoniae by DNA microarray analysis. Clin Microbiol Infect 12:936-40.

240. Culham DE, Lu A, Jishage M, Krogfelt KA, Ishihama A, Wood JM. 2001. The osmotic stress response and virulence in pyelonephritis isolates of Escherichia coli: contributions of RpoS, ProP, ProU and other systems. Microbiology 147:1657-70.

241. Schwan WR. 2009. Survival of uropathogenic Escherichia coli in the murine urinary tract is dependent on OmpR. Microbiology 155:1832-9.

242. Laimins LA, Rhoads DB, Altendorf K, Epstein W. 1978. Identification of the structural proteins of an ATP-driven potassium transport system in Escherichia coli. Proc Natl Acad Sci U S A 75:3216-9.

243. Gassel M, Siebers A, Epstein W, Altendorf K. 1998. Assembly of the Kdp complex, the multi-subunit K+-transport ATPase of Escherichia coli. Biochim Biophys Acta 1415:77-84.

244. Booth IR. 1985. Regulation of cytoplasmic pH in bacteria. Microbiol Rev 49:359-78.

245. Laimins LA, Rhoads DB, Epstein W. 1981. Osmotic control of kdp operon expression in Escherichia coli. Proc Natl Acad Sci U S A 78:464-8.

246. Subashchandrabose S, Hazen TH, Brumbaugh AR, Himpsl SD, Smith SN, Ernst RD, Rasko DA, Mobley HL. 2014. Host-specific induction of Escherichia coli fitness genes during human urinary tract infection. Proc Natl Acad Sci U S A 111:18327-32.

247. Utsumi R, Katayama S, Ikeda M, Igaki S, Nakagawa H, Miwa A, Taniguchi M, Noda M. 1992. Cloning and sequence analysis of the evgAS genes involved in signal transduction of Escherichia coli K-12. Nucleic Acids Symp Ser:149-50.

248. Eguchi Y, Utsumi R. 2014. Alkali metals in addition to acidic pH activate the EvgS histidine kinase sensor in Escherichia coli. J Bacteriol 196:3140-9.

249. Eguchi Y, Okada T, Minagawa S, Oshima T, Mori H, Yamamoto K, Ishihama A, Utsumi R. 2004. Signal transduction cascade between EvgA/EvgS and PhoP/PhoQ two-component systems of Escherichia coli. J Bacteriol 186:3006-14.

250. Nishino K, Inazumi Y, Yamaguchi A. 2003. Global analysis of genes regulated by EvgA of the two-component regulatory system in Escherichia coli. J Bacteriol 185:2667-72.

251. Ma Z, Masuda N, Foster JW. 2004. Characterization of EvgAS-YdeO-GadE branched regulatory circuit governing glutamate-dependent acid resistance in Escherichia coli. J Bacteriol 186:7378-89.

252. Cosma CL, Danese PN, Carlson JH, Silhavy TJ, Snyder WB. 1995. Mutational activation of the Cpx signal transduction pathway of Escherichia coli suppresses the toxicity conferred by certain envelope-associated stresses. Mol Microbiol 18:491-505.

253. Danese PN, Silhavy TJ. 1998. CpxP, a stress-combative member of the Cpx regulon. J Bacteriol 180:831-9.

254. Otto K, Silhavy TJ. 2002. Surface sensing and adhesion of Escherichia coli controlled by the Cpx-signaling pathway. Proc Natl Acad Sci U S A 99:2287-92.

255. Jubelin G, Vianney A, Beloin C, Ghigo JM, Lazzaroni JC, Lejeune P, Dorel C. 2005. CpxR/OmpR interplay regulates curli gene expression in response to osmolarity in Escherichia coli. J Bacteriol 187:2038-49.

256. Duguay AR, Silhavy TJ. 2004. Quality control in the bacterial periplasm. Biochim Biophys Acta 1694:121-34.

257. Batchelor E, Walthers D, Kenney LJ, Goulian M. 2005. The Escherichia coli CpxA-CpxR envelope stress response system regulates expression of the porins ompF and ompC. J Bacteriol 187:5723-31.

258. Debnath I, Norton JP, Barber AE, Ott EM, Dhakal BK, Kulesus RR, Mulvey MA. 2013. The Cpx stress response system potentiates the fitness and virulence of uropathogenic Escherichia coli. Infect Immun 81:1450-9.

259. Palmer C, Bik EM, DiGiulio DB, Relman DA, Brown PO. 2007. Development of the human infant intestinal microbiota. PLoS Biol 5:e177.

260. Bettelheim KA, Bushrod FM, Chandler ME, Cooke EM, O'Farrell S, Shooter RA. 1974. Escherichia coli serotype distribution in man and animals. J Hyg (Lond) 73:467-71.

261. Foxman B, Brown P. 2003. Epidemiology of urinary tract infections: transmission and risk factors, incidence, and costs. Infect Dis Clin North Am 17:227-41.

262. Ronald A. 2003. The etiology of urinary tract infection: traditional and emerging pathogens. Dis Mon 49:71-82.

263. Harshey RM. 2003. Bacterial motility on a surface: many ways to a common goal. Annu Rev Microbiol 57:249-73.

264. Yamamoto S, Tsukamoto T, Terai A, Kurazono H, Takeda Y, Yoshida O. 1995. Distribution of virulence factors in Escherichia coli isolated from urine of cystitis patients. Microbiol Immunol 39:401-4.

265. Korhonen TK, Virkola R, Holthofer H. 1986. Localization of binding sites for purified Escherichia coli P fimbriae in the human kidney. Infect Immun 54:328-32.

266. Sulavik MC, Gambino LF, Miller PF. 1995. The MarR repressor of the multiple antibiotic resistance (mar) operon in Escherichia coli: prototypic member of a family of bacterial regulatory proteins involved in sensing phenolic compounds. Mol Med 1:436-46.

267. Deochand DK, Grove A. 2017. MarR family transcription factors: dynamic variations on a common scaffold. Crit Rev Biochem Mol Biol 52:595-613.

268. Deochand DK, Meariman JK, Grove A. 2016. pH-Dependent DNA Distortion and Repression of Gene Expression by Pectobacterium atrosepticum PecS. ACS Chem Biol 11:2049-56.

269. Kakkanat A, Phan MD, Lo AW, Beatson SA, Schembri MA. 2017. Novel genes associated with enhanced motility of Escherichia coli ST131. PLoS One 12:e0176290.

270. Deochand DK, Perera IC, Crochet RB, Gilbert NC, Newcomer ME, Grove A. 2016. Histidine switch controlling pH-dependent protein folding and DNA binding in a transcription factor at the core of synthetic network devices. Mol Biosyst 12:2417-26.

271. Duval V, McMurry LM, Foster K, Head JF, Levy SB. 2013. Mutational analysis of the multiple-antibiotic resistance regulator MarR reveals a ligand binding pocket at the interface between the dimerization and DNA binding domains. J Bacteriol 195:3341-51.

272. Bordelon T, Wilkinson SP, Grove A, Newcomer ME. 2006. The crystal structure of the transcriptional regulator HucR from Deinococcus radiodurans reveals a repressor preconfigured for DNA binding. J Mol Biol 360:168-77.

273. Simms AN, Mobley HL. 2008. Multiple genes repress motility in uropathogenic Escherichia coli constitutively expressing type 1 fimbriae. J Bacteriol 190:3747-56.

274. Girgis HS, Liu Y, Ryu WS, Tavazoie S. 2007. A comprehensive genetic characterization of bacterial motility. PLoS Genet 3:1644-60.

275. Fahrner KA, Berg HC. 2015. Mutations That Stimulate flhDC Expression in Escherichia coli K-12. J Bacteriol 197:3087-96.

276. Sjostrom AE, Sonden B, Muller C, Rydstrom A, Dobrindt U, Wai SN, Uhlin BE. 2009. Analysis of the sfaX(II) locus in the Escherichia coli meningitis isolate IHE3034 reveals two novel regulatory genes within the promoter-distal region of the main S fimbrial operon. Microb Pathog 46:150-8.

277. Hancock V, Vejborg RM, Klemm P. 2010. Functional genomics of probiotic Escherichia coli Nissle 1917 and 83972, and UPEC strain CFT073: comparison of transcriptomes, growth and biofilm formation. Mol Genet Genomics 284:437-54.

278. Roberts JA, Hardaway K, Kaack B, Fussell EN, Baskin G. 1984. Prevention of pyelonephritis by immunization with P-fimbriae. J Urol 131:602-7.

279. Buckles EL, Luterbach CL, Wang X, Lockatell CV, Johnson DE, Mobley HL, Donnenberg MS. 2015. Signature-tagged mutagenesis and co-infection studies demonstrate the importance of P fimbriae in a murine model of urinary tract infection. Pathog Dis 73.

280. Hopkins WJ, Hall JA, Conway BP, Uehling DT. 1995. Induction of urinary tract infection by intraurethral inoculation with Escherichia coli: refining the murine model. J Infect Dis 171:462-5.

281. Parreira VR, Gyles CL. 2003. A novel pathogenicity island integrated adjacent to the thrW tRNA gene of avian pathogenic Escherichia coli encodes a vacuolating autotransporter toxin. Infect Immun 71:5087-96.

282. Nichols KB, Totsika M, Moriel DG, Lo AW, Yang J, Wurpel DJ, Rossiter AE, Strugnell RA, Henderson IR, Ulett GC, Beatson SA, Schembri MA. 2016. Molecular Characterization of the Vacuolating Autotransporter Toxin in Uropathogenic Escherichia coli. J Bacteriol 198:1487-98.

283. Alekshun MN, Levy SB. 1997. Regulation of chromosomally mediated multiple antibiotic resistance: the mar regulon. Antimicrob Agents Chemother 41:2067-75.

284. Wang X, Wood TK. 2011. IS5 inserts upstream of the master motility operon flhDC in a quasi-Lamarckian way. ISME J 5:1517-25.

285. Mobley HL, Green DM, Trifillis AL, Johnson DE, Chippendale GR, Lockatell CV, Jones BD, Warren JW. 1990. Pyelonephritogenic Escherichia coli and killing of cultured human renal proximal tubular epithelial cells: role of hemolysin in some strains. Infect Immun 58:1281-9.

286. Datsenko KA, Wanner BL. 2000. One-step inactivation of chromosomal genes in Escherichia coli K-12 using PCR products. Proc Natl Acad Sci U S A 97:6640-5.

287. Livak KJ, Schmittgen TD. 2001. Analysis of relative gene expression data using real-time quantitative PCR and the 2(-Delta Delta C(T)) Method. Methods 25:402-8.

288. Litwin MS, Saigal CS, Yano EM, Avila C, Geschwind SA, Hanley JM, Joyce GF, Madison R, Pace J, Polich SM, Wang M, Urologic Diseases in America P. 2005. Urologic diseases in America Project: analytical methods and principal findings. J Urol 173:933-7.

289. Al-Hasan MN, Eckel-Passow JE, Baddour LM. 2010. Bacteremia complicating gram-negative urinary tract infections: a population-based study. J Infect 60:278-85.

290. Bien J, Sokolova O, Bozko P. 2012. Role of Uropathogenic Escherichia coli Virulence Factors in Development of Urinary Tract Infection and Kidney Damage. Int J Nephrol 2012:681473.

291. Brzuszkiewicz E, Bruggemann H, Liesegang H, Emmerth M, Olschlager T, Nagy G, Albermann K, Wagner C, Buchrieser C, Emody L, Gottschalk G, Hacker J, Dobrindt U. 2006. How to become a uropathogen: comparative genomic analysis of extraintestinal pathogenic Escherichia coli strains. Proc Natl Acad Sci U S A 103:12879-84.

292. Subashchandrabose S, Mobley HL. 2015. Virulence and Fitness Determinants of Uropathogenic Escherichia coli. Microbiol Spectr 3.

293. Oelschlaeger TA, Dobrindt U, Hacker J. 2002. Pathogenicity islands of uropathogenic E. coli and the evolution of virulence. Int J Antimicrob Agents 19:517-21.

294. Hacker J, Kaper JB. 2000. Pathogenicity islands and the evolution of microbes. Annu Rev Microbiol 54:641-79.

295. Luo C, Hu GQ, Zhu H. 2009. Genome reannotation of Escherichia coli CFT073 with new insights into virulence. BMC Genomics 10:552.

296. Knapp S, Then I, Wels W, Michel G, Tschape H, Hacker J, Goebel W. 1985. Analysis of the flanking regions from different haemolysin determinants of Escherichia coli. Mol Gen Genet 200:385-92.

297. Syed KA, Beyhan S, Correa N, Queen J, Liu J, Peng F, Satchell KJ, Yildiz F, Klose KE. 2009. The Vibrio cholerae flagellar regulatory hierarchy controls expression of virulence factors. J Bacteriol 191:6555-70.

298. Dhakal BK, Mulvey MA. 2012. The UPEC pore-forming toxin alpha-hemolysin triggers proteolysis of host proteins to disrupt cell adhesion, inflammatory, and survival pathways. Cell Host Microbe 11:58-69.

299. Xia Y, Forsman K, Jass J, Uhlin BE. 1998. Oligomeric interaction of the PapB transcriptional regulator with the upstream activating region of pili adhesin gene promoters in Escherichia coli. Mol Microbiol 30:513-23.

300. Holden NJ, Uhlin BE, Gally DL. 2001. PapB paralogues and their effect on the phase variation of type 1 fimbriae in Escherichia coli. Mol Microbiol 42:319-30.

301. Lindberg S, Xia Y, Sonden B, Goransson M, Hacker J, Uhlin BE. 2007. Regulatory Interactions among Adhesin Gene Systems of Uropathogenic Escherichia coli. Infection and Immunity 76:771-780.

302. Lane MC, Mobley HL. 2007. Role of P-fimbrial-mediated adherence in pyelonephritis and persistence of uropathogenic Escherichia coli (UPEC) in the mammalian kidney. Kidney Int 72:19-25.

303. Lund B, Lindberg F, Marklund BI, Normark S. 1987. The PapG protein is the alpha-D-galactopyranosyl-(1----4)-beta-D-galactopyranose-binding adhesin of uropathogenic Escherichia coli. Proc Natl Acad Sci U S A 84:5898-902.

304. Schaeffer AJ. 2003. Identification of target tissue glycosphingolipid receptors for uropathogenic, F1C-fimbriated Escherichia coli and its role in mucosal inflammation. J Urol 169:1613-4.

305. Lindberg S, Xia Y, Sonden B, Goransson M, Hacker J, Uhlin BE. 2008. Regulatory Interactions among adhesin gene systems of uropathogenic Escherichia coli. Infect Immun 76:771-80.

306. Forsman K, Goransson M, Uhlin BE. 1989. Autoregulation and multiple DNA interactions by a transcriptional regulatory protein in E. coli pili biogenesis. EMBO J 8:1271-7.

307. Soto SM, Smithson A, Horcajada JP, Martinez JA, Mensa JP, Vila J. 2006. Implication of biofilm formation in the persistence of urinary tract infection caused by uropathogenic Escherichia coli. Clin Microbiol Infect 12:1034-6.

308. Juhas M, van der Meer JR, Gaillard M, Harding RM, Hood DW, Crook DW. 2009. Genomic islands: tools of bacterial horizontal gene transfer and evolution. FEMS Microbiol Rev 33:376-93.

309. Yan H, Huang W, Yan C, Gong X, Jiang S, Zhao Y, Wang J, Shi Y. 2013. Structure and mechanism of a nitrate transporter. Cell Rep 3:716-23.

310. DeMoss JA, Hsu PY. 1991. NarK enhances nitrate uptake and nitrite excretion in Escherichia coli. J Bacteriol 173:3303-10.

311. Fukuda M, Takeda H, Kato HE, Doki S, Ito K, Maturana AD, Ishitani R, Nureki O. 2015. Structural basis for dynamic mechanism of nitrate/nitrite antiport by NarK. Nat Commun 6:7097.

312. Li S, Rabi T, DeMoss JA. 1985. Delineation of two distinct regulatory domains in the 5' region of the nar operon of Escherichia coli. J Bacteriol 164:25-32.

313. Noriega CE, Lin HY, Chen LL, Williams SB, Stewart V. 2010. Asymmetric cross-regulation between the nitrate-responsive NarX-NarL and NarQ-NarP two-component regulatory systems from Escherichia coli K-12. Mol Microbiol 75:394-412.

314. Mettert EL, Kiley PJ. 2017. Reassessing the Structure and Function Relationship of the O2 Sensing Transcription Factor FNR. Antioxid Redox Signal doi:10.1089/ars.2017.7365.

315. Azpiroz MF, Bascuas T, Lavina M. 2011. Microcin H47 system: an Escherichia coli small genomic island with novel features. PLoS One 6:e26179.

316. Poey ME, Azpiroz MF, Lavina M. 2006. Comparative analysis of chromosome-encoded microcins. Antimicrob Agents Chemother 50:1411-8.

317. Rodriguez E, Lavina M. 2003. The proton channel is the minimal structure of ATP synthase necessary and sufficient for microcin h47 antibiotic action. Antimicrob Agents Chemother 47:181-7.

318. Trujillo M, Rodriguez E, Lavina M. 2001. ATP synthase is necessary for microcin H47 antibiotic action. Antimicrob Agents Chemother 45:3128-31.

319. Smajs D, Micenkova L, Smarda J, Vrba M, Sevcikova A, Valisova Z, Woznicova V. 2010. Bacteriocin synthesis in uropathogenic and commensal Escherichia coli: colicin E1 is a potential virulence factor. BMC Microbiol 10:288.

320. Sassone-Corsi M, Nuccio SP, Liu H, Hernandez D, Vu CT, Takahashi AA, Edwards RA, Raffatellu M. 2016. Microcins mediate competition among Enterobacteriaceae in the inflamed gut. Nature 540:280-283.

321. Ofek I, Beachey EH. 1978. Mannose binding and epithelial cell adherence of Escherichia coli. Infect Immun 22:247-54.

322. Old DC, Duguid JP. 1970. Selective outgrowth of fimbriate bacteria in static liquid medium. J Bacteriol 103:447-56.

323. Maccacaro GA, Hayes W. 2009. The genetics of fimbriation in Escherichia coli. Genetical Research 2:394.

324. Kikuchi T, Mizunoe Y, Takade A, Naito S, Yoshida S. 2005. Curli fibers are required for development of biofilm architecture in Escherichia coli K-12 and enhance bacterial adherence to human uroepithelial cells. Microbiol Immunol 49:875-84.

325. Cordeiro MA, Werle CH, Milanez GP, Yano T. 2016. Curli fimbria: an Escherichia coli adhesin associated with human cystitis. Braz J Microbiol 47:414-6.

326. Olsen A, Jonsson A, Normark S. 1989. Fibronectin binding mediated by a novel class of surface organelles on Escherichia coli. Nature 338:652-5.

327. Hammar M, Arnqvist A, Bian Z, Olsen A, Normark S. 1995. Expression of two csg operons is required for production of fibronectin- and congo red-binding curli polymers in Escherichia coli K-12. Mol Microbiol 18:661-70.

328. Barnhart MM, Chapman MR. 2006. Curli biogenesis and function. Annu Rev Microbiol 60:131-47.

329. Bian Z, Normark S. 1997. Nucleator function of CsgB for the assembly of adhesive surface organelles in Escherichia coli. EMBO J 16:5827-36.

330. Romling U, Rohde M, Olsen A, Normark S, Reinkoster J. 2000. AgfD, the checkpoint of multicellular and aggregative behaviour in Salmonella typhimurium regulates at least two independent pathways. Mol Microbiol 36:10-23.

331. Taylor JD, Hawthorne WJ, Lo J, Dear A, Jain N, Meisl G, Andreasen M, Fletcher C, Koch M, Darvill N, Scull N, Escalera-Maurer A, Sefer L, Wenman R, Lambert S, Jean J, Xu Y, Turner B, Kazarian SG, Chapman MR, Bubeck D, de Simone A, Knowles TP, Matthews SJ. 2016. Electrostatically-guided inhibition of Curli amyloid nucleation by the CsgC-like family of chaperones. Sci Rep 6:24656.

332. Evans ML, Chorell E, Taylor JD, Aden J, Gotheson A, Li F, Koch M, Sefer L, Matthews SJ, Wittung-Stafshede P, Almqvist F, Chapman MR. 2015. The bacterial curli system possesses a potent and selective inhibitor of amyloid formation. Mol Cell 57:445-55.

333. Romling U, Sierralta WD, Eriksson K, Normark S. 1998. Multicellular and aggregative behaviour of Salmonella typhimurium strains is controlled by mutations in the agfD promoter. Mol Microbiol 28:249-64.

334. Zogaj X, Nimtz M, Rohde M, Bokranz W, Romling U. 2001. The multicellular morphotypes of Salmonella typhimurium and Escherichia coli produce cellulose as the second component of the extracellular matrix. Mol Microbiol 39:1452-63.

335. Hancock V, Klemm P. 2007. Global gene expression profiling of asymptomatic bacteriuria Escherichia coli during biofilm growth in human urine. Infect Immun 75:966-76.

336. Serra DO, Richter AM, Hengge R. 2013. Cellulose as an architectural element in spatially structured Escherichia coli biofilms. J Bacteriol 195:5540-54.

337. Costerton JW. 1995. Overview of microbial biofilms. J Ind Microbiol 15:137-40.

338. Costerton JW, Stewart PS, Greenberg EP. 1999. Bacterial biofilms: a common cause of persistent infections. Science 284:1318-22.

339. Costerton JW, Lewandowski Z, Caldwell DE, Korber DR, Lappin-Scott HM. 1995. Microbial biofilms. Annu Rev Microbiol 49:711-45.

340. Navarre WW, Porwollik S, Wang Y, McClelland M, Rosen H, Libby SJ, Fang FC. 2006. Selective silencing of foreign DNA with low GC content by the H-NS protein in Salmonella. Science 313:236-8.

341. White-Ziegler CA, Villapakkam A, Ronaszeki K, Young S. 2000. H-NS controls pap and daa fimbrial transcription in Escherichia coli in response to multiple environmental cues. J Bacteriol 182:6391-400.

342. van der Woude MW, Kaltenbach LS, Low DA. 1995. Leucine-responsive regulatory protein plays dual roles as both an activator and a repressor of the Escherichia coli pap fimbrial operon. Mol Microbiol 17:303-12.

343. Forsman K, Sonden B, Goransson M, Uhlin BE. 1992. Antirepression function in Escherichia coli for the cAMP-cAMP receptor protein transcriptional activator. Proc Natl Acad Sci U S A 89:9880-4.

344. Guggenbichler JP, Assadian O, Boeswald M, Kramer A. 2011. Incidence and clinical implication of nosocomial infections associated with implantable biomaterials - catheters, ventilator-associated pneumonia, urinary tract infections. GMS Krankenhhyg Interdiszip 6:Doc18.

345. Bailey TL, Gribskov M. 1998. Combining evidence using p-values: application to sequence homology searches. Bioinformatics 14:48-54.

346. Bailey TL, Elkan C. 1994. Fitting a mixture model by expectation maximization to discover motifs in biopolymers. Proc Int Conf Intell Syst Mol Biol 2:28-36.

347. Bailey TL, Boden M, Buske FA, Frith M, Grant CE, Clementi L, Ren J, Li WW, Noble WS. 2009. MEME SUITE: tools for motif discovery and searching. Nucleic Acids Res 37:W202-8.

348. Morgan JL, Strumillo J, Zimmer J. 2013. Crystallographic snapshot of cellulose synthesis and membrane translocation. Nature 493:181-6.

349. Schembri MA, Ussery DW, Workman C, Hasman H, Klemm P. 2002. DNA microarray analysis of fim mutations in Escherichia coli. Mol Genet Genomics 267:721-9.

350. Hasman H, Chakraborty T, Klemm P. 1999. Antigen-43-mediated autoaggregation of Escherichia coli is blocked by fimbriation. J Bacteriol 181:4834-41.

351. Hufnagel DA, Depas WH, Chapman MR. 2015. The Biology of the Escherichia coli Extracellular Matrix. Microbiol Spectr 3.

352. Beloin C, Roux A, Ghigo JM. 2008. Escherichia coli biofilms. Curr Top Microbiol Immunol 322:249-89.

353. Pratt LA, Kolter R. 1998. Genetic analysis of Escherichia coli biofilm formation: roles of flagella, motility, chemotaxis and type I pili. Mol Microbiol 30:285-93.

354. Danese PN, Pratt LA, Kolter R. 2000. Exopolysaccharide production is required for development of Escherichia coli K-12 biofilm architecture. J Bacteriol 182:3593-6.

355. Johnson BK, Scholz MB, Teal TK, Abramovitch RB. 2016. SPARTA: Simple Program for Automated reference-based bacterial RNA-seq Transcriptome Analysis. BMC Bioinformatics 17:66.

356. Wang X, Hammer ND, Chapman MR. 2008. The molecular basis of functional bacterial amyloid polymerization and nucleation. J Biol Chem 283:21530-9.

357. Cimdins A, Simm R. 2017. Semiquantitative Analysis of the Red, Dry, and Rough Colony Morphology of Salmonella enterica Serovar Typhimurium and Escherichia coli Using Congo Red. Methods Mol Biol 1657:225-241.

358. O'Toole GA, Kolter R. 1998. Initiation of biofilm formation in Pseudomonas fluorescens WCS365 proceeds via multiple, convergent signalling pathways: a genetic analysis. Mol Microbiol 28:449-61.

359. Holden NJ, Gally DL. 2004. Switches, cross-talk and memory in Escherichia coli adherence. J Med Microbiol 53:585-93.

360. Sjostrom AE, Balsalobre C, Emody L, Westerlund-Wikstrom B, Hacker J, Uhlin BE. 2009. The SfaXII protein from newborn meningitis E. coli is involved in regulation of motility and type 1 fimbriae expression. Microb Pathog 46:243-52.

361. Praillet T, Nasser W, Robert-Baudouy J, Reverchon S. 1996. Purification and functional characterization of PecS, a regulator of virulence-factor synthesis in Erwinia chrysanthemi. Mol Microbiol 20:391-402.

362. Rouanet C, Nomura K, Tsuyumu S, Nasser W. 1999. Regulation of pelD and pelE, encoding major alkaline pectate lyases in Erwinia chrysanthemi: involvement of the main transcriptional factors. J Bacteriol 181:5948-57.

363. Birukou I, Seo SM, Schindler BD, Kaatz GW, Brennan RG. 2014. Structural mechanism of transcription regulation of the Staphylococcus aureus multidrug efflux operon mepRA by the MarR family repressor MepR. Nucleic Acids Res 42:2774-88.

364. Barnich N, Boudeau J, Claret L, Darfeuille-Michaud A. 2003. Regulatory and functional co-operation of flagella and type 1 pili in adhesive and invasive abilities of AIEC strain LF82 isolated from a patient with Crohn's disease. Mol Microbiol 48:781-94.

365. Tuson HH, Weibel DB. 2013. Bacteria-surface interactions. Soft Matter 9:4368-4380.

366. Norden CW, Green GM, Kass EH. 1968. Antibacterial mechanisms of the urinary bladder. J Clin Invest 47:2689-700.

367. Walters MS, Lane MC, Vigil PD, Smith SN, Walk ST, Mobley HL. 2012. Kinetics of uropathogenic Escherichia coli metapopulation movement during urinary tract infection. MBio 3.

368. Withman B, Gunasekera TS, Beesetty P, Agans R, Paliy O. 2013. Transcriptional responses of uropathogenic Escherichia coli to increased environmental osmolality caused by salt or urea. Infect Immun 81:80-9.

369. Clegg S, Wilson J, Johnson J. 2011. More than one way to control hair growth: regulatory mechanisms in enterobacteria that affect fimbriae assembled by the chaperone/usher pathway. J Bacteriol 193:2081-8.

370. Sands JM, Layton HE. 2009. The physiology of urinary concentration: an update. Semin Nephrol 29:178-95.

371. Wullt B, Bergsten G, Samuelsson M, Svanborg C. 2002. The role of P fimbriae for Escherichia coli establishment and mucosal inflammation in the human urinary tract. Int J Antimicrob Agents 19:522-38.

372. Gluba A, Banach M, Hannam S, Mikhailidis DP, Sakowicz A, Rysz J. 2010. The role of Toll-like receptors in renal diseases. Nat Rev Nephrol 6:224-35.

373. Stromberg N, Marklund BI, Lund B, Ilver D, Hamers A, Gaastra W, Karlsson KA, Normark S. 1990. Host-specificity of uropathogenic Escherichia coli depends on differences in binding specificity to Gal alpha 1-4Gal-containing isoreceptors. EMBO J 9:2001-10.

374. Bowen SE, Watt CL, Murawski IJ, Gupta IR, Abraham SN. 2013. Interplay between vesicoureteric reflux and kidney infection in the development of reflux nephropathy in mice. Dis Model Mech 6:934-41.

375. Choi YD, Yang WJ, Do SH, Kim DS, Lee HY, Kim JH. 2005. Vesicoureteral reflux in adult women with uncomplicated acute pyelonephritis. Urology 66:55-8.

376. Bahrani FK, Massad G, Lockatell CV, Johnson DE, Russell RG, Warren JW, Mobley HL. 1994. Construction of an MR/P fimbrial mutant of Proteus mirabilis: role in virulence in a mouse model of ascending urinary tract infection. Infect Immun 62:3363-71.

377. Bode NJ, Debnath I, Kuan L, Schulfer A, Ty M, Pearson MM. 2015. Transcriptional analysis of the MrpJ network: modulation of diverse virulence-associated genes and direct regulation of mrp fimbrial and flhDC flagellar operons in Proteus mirabilis. Infect Immun 83:2542-56.

378. Pearson MM, Mobley HL. 2008. Repression of motility during fimbrial expression: identification of 14 mrpJ gene paralogues in Proteus mirabilis. Mol Microbiol 69:548-58.

379. Ooka T, Ogura Y, Asadulghani M, Ohnishi M, Nakayama K, Terajima J, Watanabe H, Hayashi T. 2009. Inference of the impact of insertion sequence (IS) elements on bacterial genome diversification through analysis of small-size structural polymorphisms in Escherichia coli O157 genomes. Genome Res 19:1809-16.

380. Casjens S. 2003. Prophages and bacterial genomics: what have we learned so far? Mol Microbiol 49:277-300.

381. Asadulghani M, Ogura Y, Ooka T, Itoh T, Sawaguchi A, Iguchi A, Nakayama K, Hayashi T. 2009. The defective prophage pool of Escherichia coli O157: prophage-prophage interactions potentiate horizontal transfer of virulence determinants. PLoS Pathog 5:e1000408.

382. Lee C, Park C. 2013. Mutations upregulating the flhDC operon of Escherichia coli K-12. J Microbiol 51:140-4.

383. Eshaghi M, Mehershahi KS, Chen SL. 2016. Brighter Fluorescent Derivatives of UTI89 Utilizing a Monomeric vGFP. Pathogens 5.

384. Wilkinson SP, Grove A. 2006. Ligand-responsive transcriptional regulation by members of the MarR family of winged helix proteins. Curr Issues Mol Biol 8:51-62.

385. Perera IC, Grove A. 2010. Molecular mechanisms of ligand-mediated attenuation of DNA binding by MarR family transcriptional regulators. J Mol Cell Biol 2:243-54.

386. Cohen SP, Hachler H, Levy SB. 1993. Genetic and functional analysis of the multiple antibiotic resistance (mar) locus in Escherichia coli. J Bacteriol 175:1484-92.

387. George AM, Levy SB. 1983. Gene in the major cotransduction gap of the Escherichia coli K-12 linkage map required for the expression of chromosomal resistance to tetracycline and other antibiotics. J Bacteriol 155:541-8.

388. Martin RG, Rosner JL. 1995. Binding of purified multiple antibiotic-resistance repressor protein (MarR) to mar operator sequences. Proc Natl Acad Sci U S A 92:5456-60.

389. Hao Z, Lou H, Zhu R, Zhu J, Zhang D, Zhao BS, Zeng S, Chen X, Chan J, He C, Chen PR. 2014. The multiple antibiotic resistance regulator MarR is a copper sensor in Escherichia coli. Nat Chem Biol 10:21-8.

390. Paracuellos P, Ohman A, Sauer-Eriksson AE, Uhlin BE. 2012. Expression and purification of SfaX(II), a protein involved in regulating adhesion and motility genes in extraintestinal pathogenic Escherichia coli. Protein Expr Purif 86:127-34.